Chapter 1 Background and general introduction

1.1 Introduction to Nasal Drug delivery

The nasal route of drug administration is used for either topical or systemic delivery and has recently become a focus of interest as an alternative to oral administration. This has prompted further studies on the bioavailability and absorption of many drugs via this route (Kushwaha *et al.*, 2011). This growing interest is attributed to the relatively thin porous epithelial membrane of the nose, the high vascularity of the endothelial layer, improved bioavailability of many drugs from the nasal mucosa to systemic circulation and avoidance of first-pass metabolism via the gastrointestinal tract (Kushwaha *et al.*, 2011; Wadell, 2002).

Studying the factors affecting the absorption and permeation of drugs through the nasal mucosa is important to determine the suitability of dosage forms, drug absorption and bioavailability. Drug movement across the nasal epithelial layer occurs by transcellular passive diffusion, paracellular passive diffusion, carrier-mediated absorption and secretion or absorption through transcytosis (Figure 1-1). The main factors affecting drug permeation include: 1) the physiochemical properties of the drug, 2) physiological factors in the nose, and 3) formulation factors (Kublik and Vidgren, 1998).

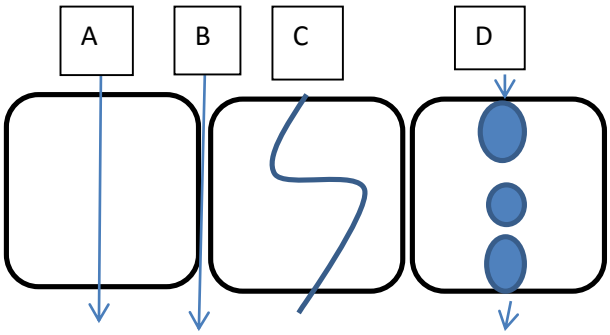

Figure 1-1 Mechanisms of drug permeation through the nasal epithelial membrane: A) transcellular passive diffusion, B) paracellular passive diffusion, C) carrier-mediated transport, and D) absorption through transcytosis.

1) The main physiochemical factors that help to predict absorption rate and hence drug bioavailability are: molecular weight, solubility, ionisation, and partition coefficient. Hussain *et.al*. (1990) found that absorption of a series of barbituric acids improves with increasing the partition coefficient rather than with increasing the molecular weight. On the other hand, Kimura *et al*., (1991) studied nasal absorption of ten aliphatic quaternary ammonium compounds in rats, and the relationship of their physiochemical properties, to conclude that absorption is inversely related to the partition coefficient and directly related to the molecular weight. Different researchers have studied the effect of physicochemical properties of a particular drug on nasal absorption and permeation and found that the absorption of small molecules (below 1000 Da) is a result of interaction between the degree of hydrophobicity, the partition coefficient and molecular weight, while large molecule absorption rate is controlled by molecular weight (Chugh *et al.*, 2009; Donovan and Huang, 1998; Hussain *et al.*, 1985; Kimura *et al.*, 1991; Ozsoy *et al.*, 2009). Generally, compounds

of molecular weight above 1000 Da have a bioavailability of 10% (Donovan and Huang, 1998). Donovan and Huang (1998) studied the different factors effecting nasal drug absorption of polyethylene glycols (PEG) ranging in weight from 600 to 2000 Da, on rats with surgical excised nasal cavities and measuring the amount of PEG excreted in the urine. The amount of nasal drug absorption was normalised with the same dose administered intra-arterially. They found that PEG with a molecular weight below 1000 Da, excretion increased with increasing molecular weight while PEG with a molecular weight over 1500 Da to 2300 Da exhibited low molecular dependency and the physicochemical properties was not affected by increasing molecular weight (Donovan and Huang, 1998).

2) The physiological factors affecting nasal drug absorption are linked to mucociliary clearance. Mucociliary clearance refers to the action of cilia and the mucus layer in the nose, which clears the nose of particles that are trapped in the mucus as a defence mechanism (Türker *et al.*, 2004). It is reported that the normal nasal mucociliary transit time is 12-15 min and the normal mucociliary clearance rate is around 8mm min^{-1} (Marttin *et al.*, 1998). Mucociliary clearance is dependent on several factors such as the beating frequency of the cilia together with their length and density; the rheological properties of mucus and amount of mucus (Pires *et al.*, 2009). Any changes to the clearance rate caused by pathological factors affects drug absorption, e.g., during viral and bacterial infections, nasal clearance is reduced due to the changed rheology of the mucus and lack of cilia (Lindberg, 1994). It is also reported that patients with primary ciliary dyskinesia, a pathological condition in which there are no beating cilia, have a decreased clearance rate from the nose and

this increases the absorption amount (Marttin *et al.*, 1998). Moreover, diabetic patients have a higher clearance rate than non-diabetics due to their high susceptibility for nasal infections, whereas cystic fibrosis patients have impaired clearance due to the thickness of the mucus (Lindberg, 1994; Marttin *et al.*, 1998). It is also reported that physiological factors such as posture and exercise can affect the clearance rate (Türker *et al.*, 2004).

3) Formulation factors are other factors that can affect the absorption rate from the nose. Nasal absorption enhancers are one of these factors which require consideration to achieve a successful nasal drug delivery. They are divided into two main groups: either membrane conditioners, or physicochemical modifiers (Hagesaether, 2011). It is noted that the former act at the nasal mucosal surface, while the latter affect the physicochemical properties of the drug in the dosage form (Na *et al.*, 2010). There are many groups of enhancers including: surfactants such as sodium dodecyl sulphate, chelating agents such as ethylene diamine tetraacetic acid (EDTA), cyclodextrines (e.g. β-cyclodextrin), bile salts (e.g. sodium taurocholate), dry microspheres (e.g. dextran microspheres and degradable starch microspheres) (Hagesaether, 2011; Türker *et al.*, 2004; Wadell, 2002).

1.2 Nasal dosage forms

Drugs delivered to the nose can be in the form of a solution, suspension, emulsion or dry powder.

1.2.1 Liquid nasal solutions

Solutions are widely used for their humidifying effect, which make them convenient and useful for conditions such as allergic rhinitis and the common cold (Kublik and Vidgren, 1998). However, their major disadvantages are microbial contamination and chemical instability (Allen *et al.*, 2011). Different delivery systems are found in solution form e.g. drops (Ephedrine®, a nasal decongestant), rhinyle catheter (Desmopressin for diabetes insipidus), unit-dose containers (Flixonase Nasule® nasal drops), nasal sprays (Avamys® for nasal polyps) (BNF, 2015; Djupesland, 2013; Harris *et al.*, 1986).

1.2.2 Powder dosage forms

Powder is frequently used for improved chemical stability and freedom from preservatives (Watts and Smith, 2011). Powders have many advantages over liquid dosage forms; one of which is to enable prolonged contact with the nasal mucosa (Kushwaha *et al.*, 2011). Furthermore, adding bioadhesive excipients such as Carpopol® polymer has been found to improve contact time and thus reduce the clearance rate (Kublik and Vidgren, 1998). The powder form is preferred over liquid forms when administering large doses where the nasal volume capacity for each nostril is 7.5 ml (Kushwaha *et al.*, 2011). Yet, drawbacks of powder use include solubility, particle size of the active ingredient, and the potential irritability of the dosage form. An example of a powder nasal dosage form used for a spray powder device is Zolmitriptan (Alhalaweh *et al.*, 2009).

1.2.3 Pressurised Metered-Dose Inhaler (MDI)

These systems contain micronised particles suspended in a liquid propellant, facilitated by surfactants e.g. Norisodrine aerotrol (PDR, 1987). They are primarily intended for pulmonary delivery. However, a slight adaptation to the inhaler device shape has enabled them to be used for nasal administration (Righton, 2011). Considerable evaluation needs to be performed, as combining propellants affects vapour pressure, and physical stability of the system such as phase separation, precipitation, and crystal growth (Allen *et al.*, 2011). The new generation pressurised MDI for topical nasal drug delivery contain hydrofluoroalkane (HFA) propellant instead of the ozone-depleting chlorofluorocarbon (CFC). A recently marketed pressurised MDI is beclomethasone dipropionate for sinusitis (Berger *et al.*, 2015).

1.2.4 Nasal gels

Nasal gels have been extensively studied to deliver drugs into the systemic circulation. The first nasal gel for systemic delivery on the market contained vitamin B12 in Nascobal® gel (MedlinePlus, 2010). With regard to their viscosity, gels are poorly deposited and it is difficult to measure the correct dose. This necessitates the use of special pumps for dispensing the doses.

1.3 Anatomy and physiology of the nose

Studying the anatomy and physiology of the nose is important in understanding drug absorption, bioavailability drug disposition, and mucociliary clearance (Donovan and Huang, 1998). There are two major disposition areas in the nose; one near the *ostium internum* and the other in the interior region of the middle turbinate (Figure 1.2). The main nasal passage, which is 3-8 cm behind the opening of the nostril, is the main absorption site for drugs because it is highly vascularised and ciliated. Usually the mucus flow is 8-100 mm min^{-1} for healthy people, while the surface area of the nose from the nostril to the naso-pharynx is 110-140 cm^2 (Gonda, 1998).

Deposition in the nose occurs by different methods including gravitational sedimentation, inertial impaction and Brownian diffusion (Kublik and Vidgren, 1998). Gravitational sedimentation is precipitation of the particles when contacting solid surface due to gravity. Gravitational sedimentation occurs only in small airways, where particles tend to settle under gravity, balanced by air resistance. While inertial impaction is the impaction of large particles with a water droplet which does not let the particles to follow the streamline of the flow and tend to change the direction (Gonda, 1998). This impaction is important for particles with a diameter of larger than 1 µm, and deposition in the nose is enhanced by the obstruction of the airflow and the inspiratory airflow (Kublik and Vidgren, 1998). Furthermore, Brownian diffusion is the random movement of small particles colliding with gas molecules and it is very common in aerosols (Kublik and Vidgren, 1998; Pires *et al.*, 2009). However, Brownian diffusion occurs very rarely and only when particles are below 0.5 µm in diameter and it is not considered when studying

nasal drug delivery because drugs intended for nasal use are usually larger than 0.5µm in diameter. In this mechanism the particles are pushed by collision of gas to the surface and therefore both particle diffusion and deposition increases. Large particles which are generally between 0.5µm diameter and 1µm diameter have more deposition due to inertial forces and turbulent diffusion (Djupesland, 2013; Jaafari *et al.*, 2005). The large particles' nasal deposition increases with increasing the flow rate; however small particles' nasal deposition increases with decreasing the flow rate (Djupesland, 2013). A nasal drug deposition study found that inspiratory nasal deposition is higher than expiratory deposition (Kublik and Vidgren, 1998). On the other hand, particles that do not deposit in the nose will travel with the inspiration airflow. This situation occurs for particles with diameters over 5 µm, and under increasing flow rate (Labiris and Dolovich, 2003) . Moreover the mucociliary clearance in the nose can cause translocation of deposited particles to the lung. Subsequently these particles deposit in the lung and their absorption and efficacy will be affected. Drug deposition is affected by the particle size, the air flow rate, the type of delivery system, and the formulation (Djupesland, 2013).

After drug is deposited in the nose, it is believed that absorption through the mucosa to the systemic circulation occurs by two methods. The first method is paracellular in which water soluble drug particles diffuse passively between the tight junctions of adjacent cells and are inversely related to molecular weight. The second method applies to lipophilic compounds and is transcellular (Allen *et al.*, 2011). Drug particles also transport through cell membranes either actively by carrier-mediated mechanisms or through the tight junction (Kushwaha *et al.*, 2011).

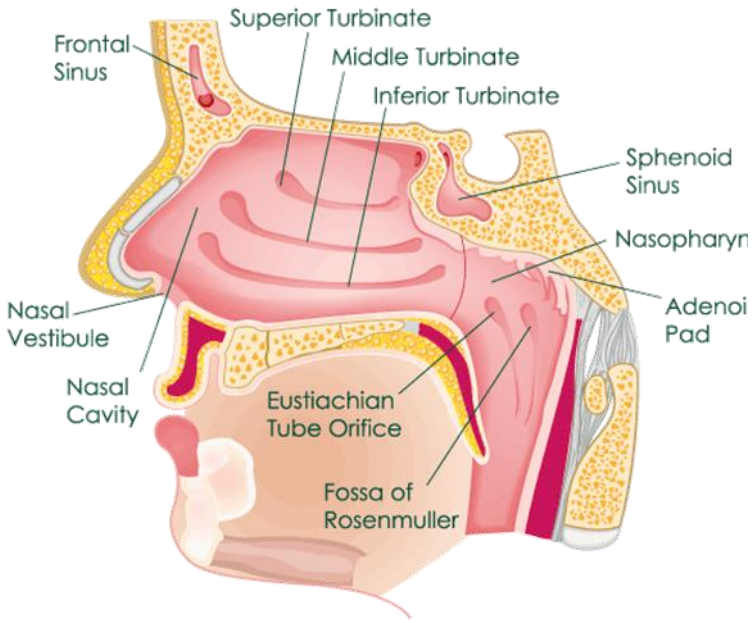

Figure 1-2 Labelled nasal parts.

1.4 Bioadhesion

Bioadhesion describes the attachment of synthetic or natural macromolecules to a biological tissue. Adhesion can occur in epithelial tissue where it is called cytoadhesion or in mucosal tissue and is called mucoadhesion (Gurny and Lenaerts, 1990; Vasir *et al.*, 2003).

Novel mucoadhesive dosage forms have received considerable interest, during the last twenty years (Dubolazov *et al.*, 2006). This type of dosage form has significant potential these days for the following reasons. The first one is prolonged residence time at the site of administration, which means improved absorption, reduced dosing frequency and hence improved bioavailability. The second is increased contact with the mucosal layer which improves the transepithelial transport of poorly soluble drugs and thereby increases their bioavailability (Roy and Prabhakar, 2010).

Vasir *et al*. (2003) described four different mechanisms by which bioadhesive material is attracted to the mucus layer. The first is the *electronic theory,* in which electrons are transferred between the mucosal layer and the bioadhesive material resulting in the formation of electrostatic forces between the two (Vasir *et al.*, 2003). The second is the *adsorption theory* that involves adsorption by surface forces. In this theory either strong or weak forces cause the binding, depending on the type of chemical bond involved; covalent bonds produce strong interaction, whereas hydrogen bonds, ionic bonds or Van de Waal's forces result in weak interactions. The *wetting theory,* expresses the ability of the polymer to spread and form close contact with the mucus membrane. In this case the contact angle between the polymer and mucus needs to be zero and the spreading coefficient of the polymer is positive. The last theory is the *diffusion theory* when physical entanglement between mucin and the polymer is followed by the penetration of mucin strands into the polymer's porous structure (Khutoryanskiy, 2011).

1.5 Polymers in drug delivery

Polymers have a diverse range of structures and properties and therefore are widely used for the temporal and spatial control of drug delivery. However, the theories described by Vasir *et al*. (2003) above cannot explain the mucoadhesion of some polymer formulations and greater understanding of the structural characteristics of the polymers is necessary. Some of these characteristics of polymers involve strong hydrogen bonding groups such as carboxyl, and sulphate, strong anionic or cationic

charge, high molecular weight, chain flexibility, and spread on the mucus surface by surface energy (Dubolazov *et al.*, 2006).

The characteristics of a drug delivery system are derived from the characteristics of polymers used and their interaction with the drug, therefore the characterisation of polymers is the primary target for a successful drug delivery system (Brar and Kaur, 2014). Classification of available polymers also helps in understanding the behaviour of different systems. Generally, polymers can be divided into different groups depending on the functional groups present and the main backbone structure.

Water-soluble polymers, which include poly (acrylic acid), are used in immobilisation of cationic drugs – examples include carbopol and PEG used as plasticisers (Pillai and Panchagnula, 2001).

Cellulose-based polymers comprise a large group that include ethyl cellulose that is insoluble, but dispersible in water for sustained release applications such as aqueous coating systems (Kadajji and Betageri, 2011). This group also incorporates hydroxyethyl and hydroxypropyl celluloses, which are soluble in water and in alcohol and used for tablet coating (Illum, 2003).

Another group of polymers are hydrocolloids, such as alginic acid, which is used as a thickening and suspending agent in a variety of pastes, and chitosan used for preparation of controlled drug delivery applications and mucoadhesive dosage forms (Khutoryanskaya *et al.*, 2010).

Water-insoluble biodegradable polymers include mainly lactide-co-glycolide polymers, which are used in microparticle–nanoparticle delivery of proteins (Patil and Sawant, 2011).

Starch-based polymers are known for binding and disintegration properties and used for tablet manufacturing. The best known in the family is sodium starch glycolate (Wondimu *et al.*, 2014).

Natural polymers are attracting more attention for their biological properties and compatibility with drugs and safety and non-irritating properties to tissue in contrast to synthetic polymers (Basu *et al.*, 2009; Datta and Bandyopadhyay, 2005; Kuotsu and Bandyopadhyay, 2007). The focus of this thesis is to examine the potential of a natural fibre from a common weed, Shepherd's purse, as a nasal drug delivery system.

1.6 *Capsella bursa-pastoris*

Capsella bursa-pastoris L. Medik. (Shepherd's purse), has seeds that are myxospermous, or become surrounded by mucilage on imbibition (Iannetta, 2011). Myxospermy consists of a large quantity of pectinaceous, complex polysaccharide substance in the epidermal cells of the seed coat (Navarro *et al.*, 2009). The gelatin-like substance expands from the surface of the testa (seed coat), and provides a polymer with novel physicochemical properties which has the potential to form a new drug delivery agent. Often the pectin may be further complexed with cellulosic

fibrils (Grubert, 1974). Mucilage from seeds of other plants has been used in this way, whereas Shepherd's purse mucilage has not previously been assessed (Basu *et al.*, 2009; Datta and Bandyopadhyay, 2005; Gaba *et al.*, 2011; Guo *et al.*, 2011; Kuotsu and Bandyopadhyay, 2007).

Shepherd's purse is described as an annual or biennial tetraploid herb (Aksoy *et al.*, 1999; Hurka *et al.*, 2003; Knezevic *et al.*, 2010). Even though it is native to Europe, it is widely distributed all over the world. It is mainly found in arable lands, gardens and rubbish grounds (Byfield, 2005), yet, it has an ability to grow in rural and urban areas. It grows in a soil range from clay to sandy loam and with a pH in the range 5.0 - 8.0 (Andreasen and Skovgaard, 2009). Compared with other arable plants, Shepherd's purse has a wide range of phenotypes and is capable of self-pollinating (Hawes *et al.*, 2005; Hurka and Neuffer, 1997; Iannetta *et al.*, 2007b; Karley *et al.*, 2008).

The Brassicaceae family to which the genus *Capsella* belongs contains members of considerable importance for food such as rapeseed/canola (*Brassica napus* L.), broccoli (*Brassica oleracea italica*), Brussel sprouts (*Brassica oleracea gemmifera*), cabbage (*Brassica oleracea capitata*), radish (*Raphanussativus* L.), and turnip (*B. rapa* L.), as well as the genetic model plant mouse-ear-cress (*Arabidopsis thaliana* L.) (Moser *et al.*, 2010).

1.6.1 Taxonomic Hierarchy

In the past, there has been significant controversy surrounding the classification of species within the genus *Capsella*; a few scientists refer to it as belonging to the Cruciferae family (Kahuthia-Gathu *et al.*, 2009; Newall *et al.*, 1996; Zhang *et al.*, 2008). As the plant has many phenotypes there are huge differences in the morphological characteristics of the plant leaves and fruits; this has led to many taxonomical classifications and therefore, there is no clear concept to define the exact family group (Hurka and Neuffer, 1997). These days, after considerable research, scientists have agreed to classify *Capsella* as belonging to the Brassicaceae family, which is also known as the cabbage family (Moser *et al.*, 2010).

Additionally, Shepherd's purse can be compared to *Arabidopsis thaliana*, since both plants have many similar characteristics (Vaughan, 1955). Furthermore, genomic data from Arabidopsis is mimicked by other members of the Brassicaceae family, and most commonly Shepherd's purse (Hawes *et al.*, 2005). Since Arabidopsis also belongs to the Brassicaceae family, Shepherd's purse is most likely to belong to the same family and the two plants are likely to be close relatives of each other (Hintz *et al.*, 2006). The hierarchy is described in Table 1 as recognised by the United States National Plant Data Centre (USDA, 2010).

Table 1.1 Taxonomic Hierarchy of *Capsella bursa-pastoris* L. *Medikus*.

Kingdom: *Plantea*
Subkingdom: *Tracheobionta* - vascular plants
Division: *Magnoliophyta-angiospermers*
Class: *Magnoliopsida* – dicots
Subclass: *Dileniidae*
Order: *Capparales*
Family: *Brassicaceae* – mustards
Genus: *Capsella Medikus-Capsella*
Species: *Capsella bursa-pastoris (L) Medikus*
Common Name: shepherd's purse

1.6.2 Plant Description

1.6.2.1 Leaf Morphology

The leaves are arranged tightly near the ground forming a thick rosette shape around the stem (Figure 1.3). *Capsella* leaves are identified as complex not simple, and they have a lobe shape that narrows at the stalk and flattens at the terminal end (Iannetta *et al.*, 2007b).

Figure 1-3 Shepherd's purse plant showing stem, basal leaves, inflorescence and flowers. Photographed by Abusriwil, A. (2015).

1.6.2.2 Stem Morphology

The stem can be either simple or branched with pale green to yellow colour ranges from 3 to 103 cm in height (Figure 1.4). The stems can be smooth or covered with fine, short hairs (Wichtl and Bisset, 2001).

Figure 1-4 Branched stem of Shepherd’s purse. Photographed by Abusriwil, A. (2015).

1.6.2.3 Flowers Morphology

The flowers are arranged on a long inflorescence with four green sepals, four white petals, six stamens and a singular pistil (Figure 1.5) (Wichtl and Bisset, 2001).

Figure 1-5 Inflorescence and seed pods on branched Shepherd's purse stem. Photographed by Abusriwil, A. (2015).

1.6.2.4 Seed Morphology

The seeds are enclosed in two-valved triangular or obcordate pods (silicula), which are yellowish green in colour and tend to be reddish when the seeds are ripening (Figure 1.5). From the purse-like shape of the pod, the plant gets the name of Shepherd's purse. These pods are considered the fruit of the plant and each pod usually contains 20 to 40 orange coloured seeds (Toorop *et al.*, 2012). As the seeds ripen they range in colour from dark reddish to yellowish brown shown in Figure 1.6. The seeds are oblong and flat with a longitudinal groove on both sides. The mean dark seed dry weight is 0.150mg (Aksoy *et al.*, 1998).

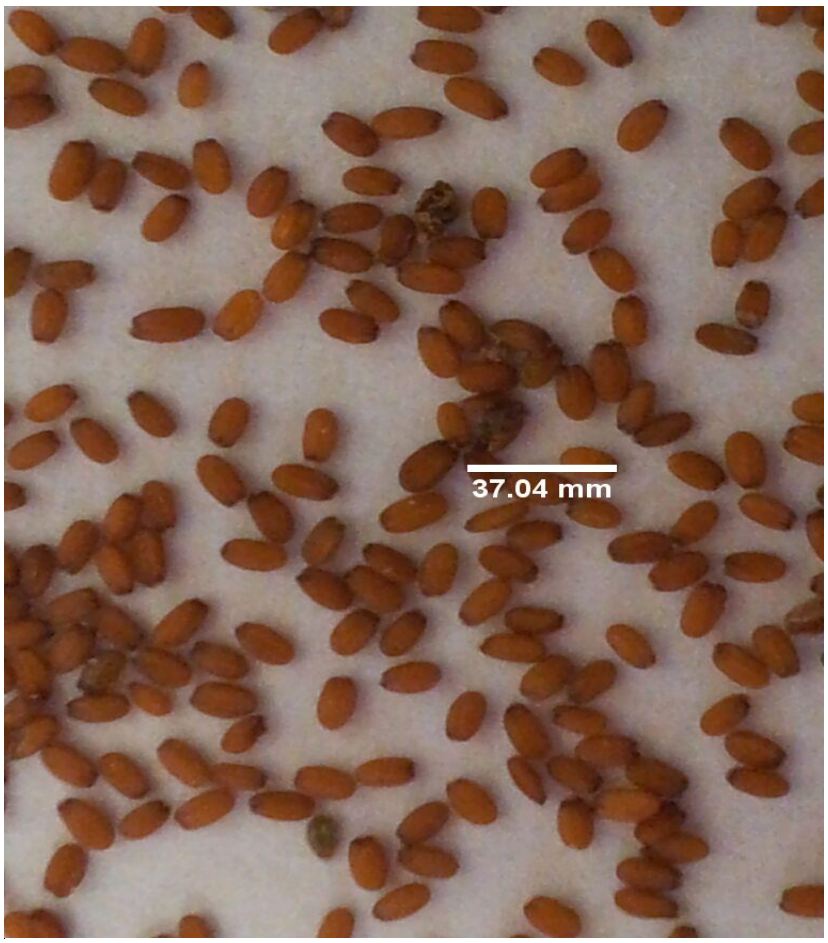

Figure 1-6 Shepherd's purse seeds. Photographed by Abusriwil A. (2012)

Phenotypic variation is genetically determined (Clements *et al.*, 2004). Phenotypes of *Capsella bursa-pastoris* are generally different in many facets, the fruit shape and colour, the leaf shape, the flowering time and geographical distribution (Iannetta *et al.*, 2007a; Karley *et al.*, 2008). Iannetta *et al.* (2011) described two different phenotypes depending on the colour of the seeds, which underlies the difference in mucilage secretion. They reported that the difference in intensity of the colour of the seed coat is a result of morphotypic differences. Dark seeds originating from the silicula located in the upper part of the plant are not mature, while light brown seeds produced from the lower located silicula are mature enough to produce mucilage. It is believed that the immature seeds have enough time to deposit the necessary

carbohydrates for the formation of mucilage needed by the seeds for germination and imbibition (Windsor *et al.*, 2000). Scanning electron microscopy (SEM) of both light and dark dry seeds of Shepherd's purse show that they differ in the structure of the outer surface of the testa, where the dark-brown seeds appear less swollen and more wrinkled than the light brown seeds (Iannetta *et al.*, 2010; Toorop *et al.*, 2012). When the dark seeds are placed in water, initially they appear hydrophobic, floating on the water surface; while light-brown seeds are hydrophilic as they imbibe and sink rapidly. In addition, the light brown seeds increase by 20-25% of their size when immersed in water than the dark seeds which appears to be caused by mucilage expansion (Iannetta, 2011). Furthermore, when calcoflour stain is used to stain the light brown seeds, the mucus fluoresces strongly and appears as a bright-blue halo around the seeds, which indicates a high density of polysaccharide. In contrast, the dark seeds show no staining, indicating the absence of mucus (Iannetta, 2011).

1.6.2.5 Root Morphology

Shepherd's purse has a white tap-root (Figure 1.7) that branches in a forked shape just after 10 cm into a few secondary roots (Aksoy *et al.*, 1998).

Figure 1-7 Shepherd's purse roots. Image by Abusriwil A. (2015)

1.7 Phytochemical composition of Shepherd's purse seeds

The seed mucilage is mainly composed of pectin, which is a hydrophilic polysaccharide (North *et al.*, 2010), of which galacturonic acid and rhamnose are the major sugars (Aksoy *et al.*, 1998; Willats *et al.*, 2001). In addition, there are minor sugars such as arabinose, galactose, xylose and glucose present. In Arabidopsis, pectin is organised in two layers both containing rhamnogalacturonan I (RGI), as well as galactan, homogalacturonan (HG), and xylocan (North *et al.*, 2010). Additionally, the inner layers contain cellulose while the outer contain arabinan (Verhertbruggen *et al.*, 2009). Pectin is synthesised by methyl-esterification of galacturonosyl residues, which are 1,4-linked to form the three main backbones of pectin which are RGI, rhamnogalacturonan-II (RGII), and HG with diverse side chains (Caffall *et al.*, 2009). It is believed that the high water holding capacity of pectin from Shepherd's purse seeds is due to the presence of arabinan, a highly

branched sugar side chain. It is still unclear how these polymers link together and integrate towards the nature of the polymer, but it is believed that the pectic polysaccharides integrate with hemicelluloses, wall proteins, and phenolic compounds to form the complex structure of the seed coat (Caffall *et al.*, 2009).

Cellulose microfibrils are present in the inner and outer cell walls and are mainly β-(1,4)-D-glucan chains associated with hydrogen bonds to xyloglucan and xylan to form a cellulose-hemicellulose network (Caffall *et al.*, 2009). Hemicellulose is important for microfibril organisation and crystallinity.

In Arabidopsis seeds, proanthocyanidins accumulate in the seed coat and flavonols in the seed coat, embryo and endosperm (Haughn and Chaudhury, 2005; North *et al.*, 2010). Quercetin is the commonly found flavonoid in *Capsella bursa-pastoris* (Song, 2007).

Environmental factors and geographical location affects the seed weight and lipid content. It has been found in general, that seeds from warm regions are light in weight and higher in lipid content compared with those from colder regions (Mukherjee *et al.*, 1984). Shepherd's purse lipid content is specifically, polyunsaturated fatty acids. The main fatty acids are linolenic, linoleic acids, oleic, and gondoic acids (Moser *et al.*, 2010). All *Capsella* species contain palmitic, stearic, and oleic acids. Cutin and suberin are two types of polymers derived from lipid polyesters and are responsible for permeability barriers (North *et al.*, 2010).

Generally the amount of tannins that have been found is not abundant and the only one to date is gallic acid (Aksoy *et al.*, 1998; HMPC, 2010).

The proteins which are present are wall glycosyl hydrolases, extensins, expansins, arabinogalactan proteins, hydroxyproline-rich glycoproteins, proline-rich proteins and wall-associated kinases (Caffall *et al.*, 2009). Oil body-associated proteins are structural proteinsoleosins, and caleosins, enzymes (e.g. lipase) and minor proteins (e.g. aquaporins). They prevent oil body coalescence and electrostatic repulsion (North *et al.*, 2010). In Arabidopsis seeds, storage proteins include 12S (cruciferins) and 2S (arabins) (North *et al.*, 2010).

1.8 Seed coat development and mucilage release

The seed coat is composed of multiple layers of tissues protecting the embryo and assisting in germination. The seed coat is derived from the ovule integument during differentiation after fertilisation (North *et al.*, 2010). It is found that there is no cell division during the process of seed coat differentiation (Windsor *et al.*, 2000).

The seed coat is composed of an outer and inner integument, which is composed of two and three cell layers, respectively. The outer integument is the origin of the seed coat and the place where mucilage is deposited (Penfield *et al.*, 2001). In early development of the seed coat, a large vacuole is formed that fills most of the cell volume of the outer integument. In the next stage of differentiation, starch granules are formed in the two cell layers and appear proximal to the embryo in the outer cells of the outer integument and distal to the embryo of the inner cells of the integument

(Francoz *et al.*, 2015; Windsor *et al.*, 2000). At this stage, starch continues to accumulate in both layers and the outer cells secret mucilage between the cell wall and the protoplasm and around the starch granules in a doughnut ring form (Western *et al.*, 2001). Furthermore, as mucilage secretion increases it displaces the protoplasm until it forms a column shape and the starch granules increases while the large vacuoles are broken into smaller sized vacuoles and continue to decrease until they vanish. Finally during maturation of the seeds, the starch degrades and the mucilage takes most of the cell volume and squeezes the protoplasm into a column in the centre of the cell (Western *et al.*, 2000). Meanwhile the inner cells of the outer integument are compressed against the outer cells and their walls are reinforced to form a thick secondary wall underneath the outer cells (Windsor *et al.*, 2000). After maturation the mucilage dries into a thin layer under the cell wall, deposited between the plasma membrane and the cell wall (Haughn and Chaudhury, 2005).

When the seed is placed in water, the mucilage is released and envelopes the seed within seconds. Under examination using dyes, the outer-layer of mucilage appears cloudy and diffuse while the inner has dark-staining rays in the form of a halo around the seed (Deng *et al.*, 2012; Willats *et al.*, 2001). When the seeds are soaked in an aqueous solution of Ruthenium red, acidic compounds (such as pectin) are revealed red in colour (Deng *et al.*, 2015). Furthermore, when the seeds are treated with pectinase enzyme, a rhamnogalacturonan hydrolase, no mucilage capsule around the seeds is observed, which confirms that pectin is the main constituent of the mucilage (Macquet *et al.*, 2007).

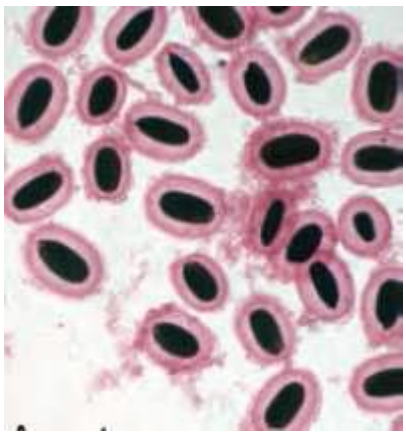

Figure1-8 Shepherd's purse seeds immersed in water containing Ruthenuim red and examined using light microscopy (Deng *et al.*, 2012).

Studies on *A. Thaliana* have shown that the major component of the pectic structures of the mucilage is de-esterified RG I and is only present in the epidermis (Willats *et al.*, 2001). However, the inner layer of the seeds' coat contains mucilage which is highly methyl-esterified HG. In addition, significant quantities of cellulose in the inner layer have been detected by binding with calcoflourin (Macquet *et al.*, 2007).

Willates *et al*. (2001) studied gel formation within the primary cell wall and found it to be formed by calcium cross-linking of de-esterified HG. On the other hand, *in vitro* gel formation was found to be initiated by high methoxyl HG and stabilised by solutes such as sucrose. Determination of the monosaccharide composition of Arabidopsis mucilage, using antibodies for labelling, have indicated the abundance of rhamnose and galacturonic acid, suggesting the occurrence of rhamnogalacturonan components in addition to HG (Willats *et al.*, 2001).

1.9 Project Aims

The main aim of this project was to evaluate whether polymer extracted from Shepherd's purse mucilage could be developed into a mucoadhesive drug delivery system for nasal application. *Capsella bursa-pastoris* seed mucilage has not been studied before for suitability of the development of a delivery system and therefore, this was considered a novel application.

An overview of the experimentation is given below:

Since there is not an established standardised method of extraction of the seeds' polymer, the first task was to develop a suitable procedure. In general, plant mucilage extraction methods vary depending on the type of polymer. A review of the literature showed that Shepherd's purse mucilage is mainly composed of pectinous substances. Identifying the chemical structure of the polymer was a key for understanding the main properties to facilitate drug delivery system development. Studying the physicochemical properties of the mucilage polymer was considered important in order to choose the best drug for use with the polymer. **Chapter two** of this thesis focussed on these aspects.

Chapter three mainly focused on mucoadhesion studies of the polymer and the evaluating the potential of forming mucoadhesive dosage forms for the nasal cavity using extracted Shepherd's purse mucilage.

After choosing the right method of extraction and characterising the polymer, developing the polymer into a system suitable for the route of administration is vital

as different sites have different dosage forms. The dosage form system in this case was designed for the nose as the site of administration. A study of release properties of different drugs are described in **Chapter four**.

Chapter five describes the study of the viscosity properties of the extracted polymer after it had been freeze-dried and properties of the hydrated polymer in the drug delivery system. It also investigated the rheological behaviour of the polymer solution dissolved in simulated nasal fluid in order to understand the polymer behaviour when dissolved in nasal mucus and secretions, and underpins its capacity to form a nasal drug delivery system.

Chapter six concludes the outcome of the research in a brief statement and gives suggestions of future work.

Chapter 2 Extraction and physicochemical characterisation of Shepherd's purse seed mucilage

2.1. Introduction

The development of new drugs and biological therapeutics involves three stages, which include preclinical investigations (investigational new drug 'IND' submission); clinical investigation submission (NDA) and market approval. The preclinical investigation required by FDA involves comprehensive characterisation of physical and chemical properties for all constituents (FDA, 2002). Characterisation is therefore essential to understand the behaviour of the material.

There is a growing interest in the use of natural polymers for novel drug delivery systems. The use of such polymers require detailed characterisation of the physicochemical properties of the polymers (Malviya *et al.*, 2011). In the present study, finding the best extraction method was considered a priority in order to obtain an extract with the minimum substances from the deeper layers of the seed coat.

Pectin is believed to be the main constituent in the Shepherd's purse seed mucilage (Aksoy *et al.*, 1998). Pectin is a complex polysaccharide and a major compound in the structure of the cell wall of many plants. It is always present either as a single compound or cross linked with proteins and fatty acids (Urias-Orona *et al.*, 2010). Generally the pectin backbone consists of (1→4)-linked α-D-galacturonic acid units. However, it is found that the structure and composition of pectin can change during extraction and isolation depending on the method used (Novosel'skaya *et al.*, 2000).

Pectin is thought to consist mainly of D-galacturonic acid (GalA) units (Mukhiddinov *et al.*, 2000), joined in chains by means of α-(1-4) linkages and called HG. These units are intercepted with (1→2)-linked α-L-rhamnopyranosil residues, called RG. The carboxyl group on galacturonic acid residues can be partially esterified by methanol; additionally, the secondary hydroxyl can be acetylated (Sriamornsak, 2003). However, rhamnosyl units can be substituted by side chains containing arabinose and galactose sugars (Harholt *et al.*, 2010). These structures of pectin are illustrated schematically in Figure 2.1 (Harholt *et al.*, 2010).

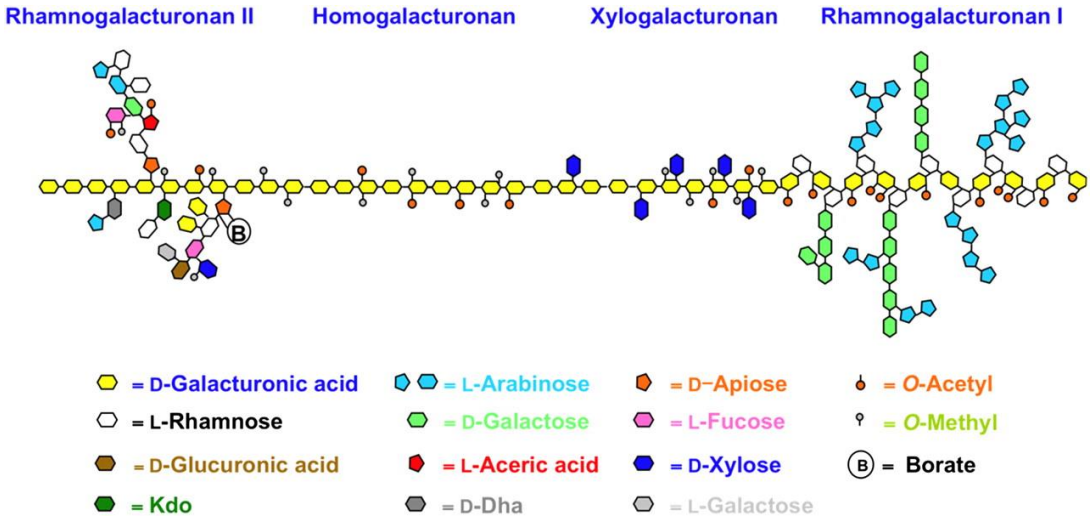

Figure 2-1 Schematic diagram showing different pectin structures.

Pectin is viscoelastic and gels under certain circumstances, depending mainly on the degree of methoxylation (DM). Pectin forms gels in the presence of a high sugar concentration, usually sucrose or fructose and at low pH when the DM is less than 50%; in contrast pectin with a DM of more than 50% forms gels in the presence of divalent ions, e.g. calcium (Urias-Orona *et al.*, 2010).

Studies on Shepherd's purse seed mucilage have shown that galacturonic acid and rhamnose are the major sugars of pectin (Aksoy *et al.*, 1998; Willats *et al.*, 2001). It is believed that the pectic polysaccharides integrate with hemicelluloses, wall proteins, and phenolic compounds to form the complex structure of the seed coat (Caffall *et al.*, 2009). Cellulose microfibrils are present in the inner and outer cell walls (Caffall *et al.*, 2009).

2.1.1 Physicochemical properties characterisation

In this chapter, it was important to establish that pectin had been extracted. There are different tests to identify carbohydrate components of a mixture. Extensive study of the sugar components also helped in identifying the polymer in the seeds' mucilage (Ngwuluka *et al.*, 2014).

A. Colorimetric assays

Colorimetric assays are easy and reliable. Two colorimetric assays were employed in this chapter. One test was to identify the different sugars and another assay to identify the presence of uronic acid which is an indicator of pectin. The colorimetric assay of sugars is a reaction based on the colour produced by sugars upon reaction with phenols in the presence of hydrochloric acid or sulphuric acid (Browne and Zerban, 1941). The colour is generated due to the formation of condensation products between the phenol and the decomposition products from the sugar by the effect of sulphuric acid (Browne, 1912).

The uronic acid detection assay depends on the reaction of uronic acids with carbazole in sulphuric acid, forming a crystalline precipitant that is pink in colour. This assay is better as a qualitative rather than as quantitative assay due to difficulty in measuring UV absorbance of the precipitate and the positive reaction of interfering substances such as other carbohydrates (e.g. glucose).

B. Degree of Esterification

In order to determine the suitability of the extracted polymer for further studies with regard to drug delivery, knowledge of the degree of esterification (DE) of the major component, pectin, in the Shepherd's purse mucilage was important (Ngwuluka *et al.*, 2014). The degree of esterification has been found to affect the gelling properties of pectin in addition to having an impact on stability (Urias-Orona *et al.*, 2010; Voragen *et al.,* 2009). There are four major methods cited in the literature for the calculation of DE: titration, quantification of methanol, High Performance Liquid Chromatography-Nuclear magnetic Resonance (HPLC-NMR), and Fourier Transform Infra-Red (FTIR).

Recently, a new method has been developed using the FTIR technique that does not involve chemical changes to the pectin to determine the DE. This methodology is based on the difference in the carboxyl group absorption compared with that of the ester carbonyl. The DE is estimated by measuring the absorption intensity, frequency, and band area of esterified carbonyl group relative to the carboxyl group (Barros *et al.*, 2002; Kačuráková *et al.*, 2000; Kačuráková and Wilson, 2001).

An estimate of DE is calculated using the following equation:

DE= band area of ester carbonyl / (carboxyl band area + ester band area)

In terms of pectin analysis, the region of interest for the evaluation of DE is between 1800 and 1500 cm^{-1} as it allows the observation of infrared absorption of the carbonyl group of the carboxylic acid and the carboxylic ester functionalities of the pectin molecules (Stewart and Morrison, 1992).

C. Dynamic Vapour Sorption (DVS)

Different materials behave differently when exposed to atmospheric water vapour. The adsorbed water has an effect on physical properties such as stability and dissolution rate (Nokhodchi *et al.*, 1997). The absorbed water can be of three different types depending on location: monomolecular layer, externally adsorbed layer and internally absorbed layer. When a dry molecule is exposed to water vapour, the adsorbed water forms a monomolecular layer that may produce adhesion forces onto the surface or it can be transferred into the inside of the particle. The monomolecular adsorbed layer is known for its ability to form capillary forces between particles at low moisture content due to formation of discrete liquid bridges between particles at the contact points on their surfaces. This layer increases cohesive forces because of formation of surface tension and negative capillary pressure (Nokhodchi *et al.*, 1997). As the liquid content on the surface increases, several bridges may merge, and the void surfaces are demolished and surface

bonding is then affected by negative capillary surface tension from the interior absorbed water.

The Dynamic Vapour Sorption (DVS) apparatus provides a controlled environment with regard to atmospheric moisture content and temperature in order to measure any changes in the weight of material due to adsorption or absorption of water vapour. The apparatus is supplied with a Cahn microbalance, which is very sensitive to any changes in the weight of the sample and able to record changes as small as 0.002 mg. It also consists of a chamber within which humidity and temperature are closely regulated. The relative humidity inside the chamber is increased by a constant rate in each step and the changes in sample weight are recorded until it reaches a stable weight and no more changes are recorded before moving into the next step of higher relative humidity.

The DVS data is helpful in estimating the wettability of mucilage inside the nasal cavity by measuring the vapour adsorption and sorption rates (Agrawal *et al.*, 2004). It is also a tool for predicting the shelf life and possible changes to the material during storage (Nokhodchi *et al.*, 1997).

D. Thermal analysis

Thermogravimetry (TGA) and Differential scanning calorimetry (DSC) are very useful tools for the characterisation of physiochemical properties such as melting point, and glass-transitions under precisely controlled atmosphere. They measure sample mass and the heat flow of the sample to detect thermal events that are not

accompanied by a change in mass, such as melting, glass transitions, and solid-solid transitions (Riesen, 2008). Thermal analysis is a versatile quantitative tool for measurements of phase transitions and chemical reaction of material in controlled conditions.

TGA is the method of choice to measure sorption and desorption of gases and moisture; sublimation, evaporation, vaporisation; kinetics of decomposition process; quantitative content analysis; thermal stability; identification of decomposition products; pseudo polymorphism; determination of Curie temperatures. While DSC is useful for the analysis of melting behaviour, crystallisation, polymorphism, glass transition, heat capacity, and reaction and transition enthalpy (Hammer, 2010).

According to Schubnell (2005), method development depends on the information required or needed. The main questions that thermal analysis is looking to answer are: Is there glass transition and at what temperature? Is it a polymorphic polymer? Does crystallisation occur and at what temperature? Is the polymer heat stable and to what temperature? What is the moisture content in the polymer?

Therefore, the material needs to be checked by TGA for heat stability first. Then DSC analysis is used for other properties and measurements.

Heating-cooling-heating experiments for polymer screening are practically used to eliminate the thermal history and to check samples. The first heating run shows all transition with regard to the sample's history from melting, glass transition

temperature (Tg), crystallisation and relaxation enthalpy while the second run shows smaller Tg due to less amorphous material left and more crystal content formed (Hammer, 2010). It is believed that in quench cooling a larger glass transition step occurs due to the high availability of amorphous content (Schawe *et al.*, 2000). On the other hand, cold crystallisation occurs when the samples are cooled rapidly without leaving time to crystallise (Hammer, 2010).

E. Nuclear Magnetic Resonance spectroscopy

Nuclear Magnetic Resonance (NMR) spectroscopy is a powerful analytical tool that is widely used in identifying compound structure elucidation. Since each nuclei has its own resonance frequency in the magnetic field depending on the atom properties, NMR provides information about the surrounding atoms and the type of chemical bonding between the atoms (Lampman, 2010).

^{1}H NMR spectroscopy is used to indicate the chemical shifts, coupling constant and relative abundance of compounds. ^{13}C NMR is used to find the carbon atoms order and J-modulated ^{13}C NMR is useful to distinguish between primary, secondary and tertiary carbon peaks. 1H-1H correlation spectroscopy (COSY) is utilised to correlate neighbouring protons. Total correlation spectroscopy (TOCSY) is similar to COSY in relating the sequence of protons but it further shows the networks correlation (spin systems) within a polymer and is extensively used for sugars. Heteronuclear single-quantum correlation spectroscopy (HSQC) shows the correlation between two different nuclei by showing the chemical shift of the coupling between the proton and the attached one bond to the Carbon. Multi Bond Coherent Spectroscopy

(HMBC) usually shows the long range correlation between ^{1}H and ^{13}C nuclei of 2-4 bonds distance. These different NMR experiments are used to elucidate the chemical structure of the compound by identifying the different links of each atom and the types of bonds in the structure (Ning, 2011).

2.2. Aims

The aim of this chapter was to extract the polymer from Shepherd's purse seeds with minimum interfering compounds coming from the other seed coat layers and, the seed embryo and to characterise the physical and chemical properties (Ngwuluka *et al.*, 2014).

Different extraction methods were used to extract the polysaccharide polymer from the Shepherd's purse seed, and carbohydrates were identified by colorimetric assay. The DE of Shepherd's purse extracted pectin was measured using FTIR. Furthermore, the water content within the polymer structure was examined using DSC and the ability to absorb atmospheric vapour was evaluated by dynamic vapour sorption to calculate the amount taken up. Importantly, the effects of heat on stability, and the possibility of any phase changes using TGA which is a characteristic for many polymers was also evaluated. Finally, NMR spectroscopy was employed to detect the purity of the extracts and to elucidate the chemical structure of the pectic polymer extracted.

2.3. Materials and methods

2.3.1. Material and Equipment

- *Capsella Bursa-pastoris* seeds were purchased from Herbiseeds, Twyford UK.
- Methanol, (analytical reagent grade) purchased from VWR, UK.
- Ethyl acetate (analytical standard grade), hexane (HPLC grade), mucin from porcine stomach (type III bound sialic acid 0.5-1.5%), sulphuric acid (99.9%), propanol-2 (HPLC grade), pectin standards with a known degree of esterification (31%, 68% and 93%), apple pectin (meets USP xxiii) lot number 67H16351, deuterium oxide (99.9%)(lot number STBD15150), and sodium chloride (analytical reagent grade; lot number 10370); were all purchased from Sigma-Aldrich, UK.
- Hydroxypropyl methylcellulose (HPMC) powder K100 LV[1] grade (lot number KK08012N21) was obtained from Dow Chemicals, USA.
- Phenol (analytical standard grade) lot number S4970896842 was procured from Merck, UK.
- D-(+)-glucose monohydrate (99%) lot number 10163267; D-(+)-galactose (98%) lot number 10134490; D-(-)-fructose (99%) lot number 10159807; D-(+)-mannose (99%) lot number 10161809; D-(-)-arabinose (99%) lot number 10158778; L-(+) - rhamnose 99% lot number 10158772 ; D-(+)-xylose (98%) lot number 10159466; Carbazole (99%) lot number 10164487 were procured from Alfa Aesar, UK.

[1] The letter K represents hydroxypropyl molar substitution of 0.21 and a methoxyl degree of substitution of 1.4. The number 100 indicates the viscosity in millipascal-seconds of 2% aqueous solution at 20ºC. The suffix LV refers to special low viscosity product.

- De-ionised distilled water was prepared in the laboratory.
- Alumina pan and Aluminium crucibles were procured from Mettler Toledo, UK.
- Christ™ Epsilon 2-4 LSC freeze dryer (Martin Christ, Germany).
- Fourier Transform Infra-Red (JASCO™ model FT/IR 4200 Type A) spectrophotometer, with TGS detector.
- The Dynamic Vapour Sorption (DVS 1000™, Surface measurement systems) Apparatus (Cheshire, UK).
- Thermogravimetric Analyser TGA/STDA 851e, operating with TS0801 RO Sample Robot (Mettler Toledo™, Leicester, UK).
- Differential Scanning Calorimeter DSC/SDTA 822e, (Mettler Toledo, Leicester, UK).
- Bruker AVANCE NMR spectrometer at 400.03 and 600.13 MHz frequency working with Topspin version 2.1 software and equipped with (^{1}H, ^{13}C) probe heads (Bruker Biospin, Germany). All spectra were recorded in D_2O at temperature 343.0 ± $0.1^{0}K$ number of scans 32 at relaxation delay 2s, acquisition time 0.12s.

2.3.2. Methods

The schematic diagram in Figure 2-2 describes the different extraction methods used with Shepherd's purse mucilage. It also illustrates the experiments employed in order to study and compare the physicochemical properties of the extracted mucilage using different extraction methods.

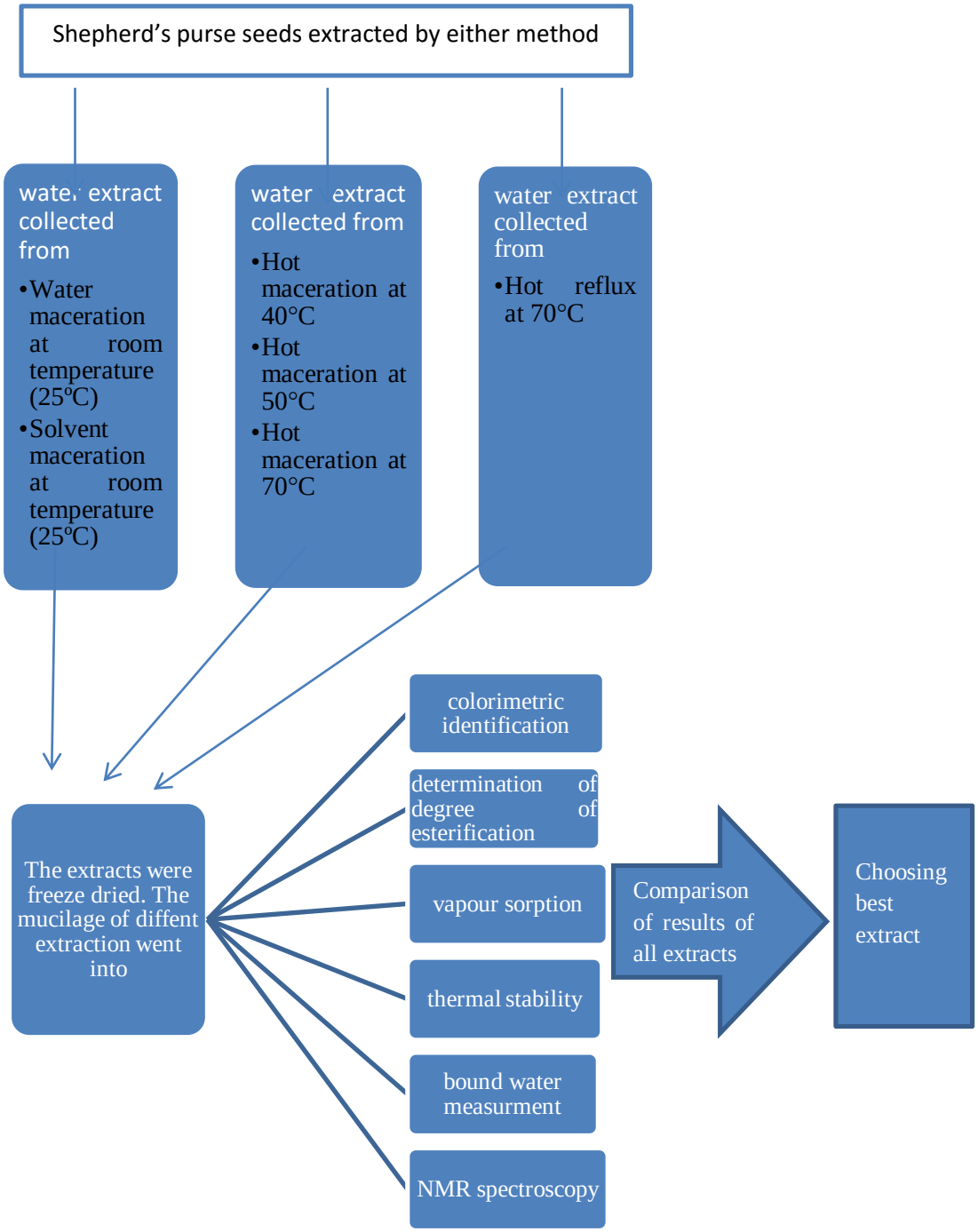

Figure 2-2 Summary of experiments carried out in this chapter.

2.3.2.1. Extraction

Four different extraction methods were used to obtain the mucilage from the Shepherd's purse seed coat, using different solvents with variations in temperature.

2.3.2.1.1. Water maceration

This method involved soaking the seeds in water at 25 ºC in which 100 ml of deionised water was added to a beaker containing 10 g of Shepherd's purse seeds and stirred for 12 h. The extract was then centrifuged at 4000 rpm (1252 g) for 30 min, and the supernatant decanted and collected for subsequent freeze-drying.

2.3.2.1.2. Solvent maceration

In this method the seeds were macerated with hexane at 25 ºC by placing 10 g of ground Shepherd's purse seeds in a stoppable flask with 25 ml of hexane over a magnetic stirrer for 12 h. The extract was decanted, filtered and left in a fume cupboard to dry. The process was repeated until the extract was clear and showed no signs of fatty acids when examined by proton NMR. This process was repeated six times.

After the last hexane maceration, the seed powder was left to dry and any residual hexane was evaporated off in a fume cupboard for 24 h. The dry seed powder was returned to a stoppable flask and 50 ml deionised distilled water was added and stirred for 12 h. The mixture was centrifuged at 4000 rpm (1252 g) for 30 min. The supernatant was then dialysed for 8 h against 1 L distilled water with stirring. This

process was repeated three times before the dialysed extract was collected for subsequent freeze-drying.

2.3.2.1.3. Hot reflux

This method used gentle heating to protect sensitive compounds from the damaging effect of heat. In a Soxhlet maintained at 40ºC for 24 h, 30 g of whole seeds were refluxed with 450 ml of hexane. Subsequently 450 ml of ethyl acetate was used for extraction for 24 h at 40ºC; followed by 450 ml methanol for 24h at 35ºC; then proceeded with 450 ml of methanol: water (1:1) for another 24h at 35ºC. Each time before adding the subsequent solvent the seeds were allowed to dry in a fume cupboard to evaporate any residual solvent and at the end of each extraction the extract was collected and the solvent evaporated by rotary evaporation at 40ºC. Finally 450 ml water was added at 35ºC for 24 h then the extract was collected for subsequent freeze-drying.

2.3.2.1.4. Hot maceration

Five beakers were each filled with 10 g of Shepherd's purse seeds and 100 ml of deionised water. One beaker was kept at 50ºC while the second at 40ºC and the third at 70ºC and stirred for 1 h; while the forth and the fifth were kept at 40ºC and 50ºC respectively for 2 h. The extracts were collected separately then centrifuged, and the decanted supernatant collected for subsequent freeze-drying.

2.3.2.2. Freeze drying extracted mucilage

The final water extracts of mucilage following solvent maceration, water maceration, hot maceration and hot reflux were collected and placed in a Christ™ freeze-drier. The freeze-drying method included 10 phases and 30 h in total as shown in Table 2-1. The first phase was the loading of the samples at the set temperature of -70ºC so that samples were frozen for 24 h in advance. Then the following four phases were freezing the samples at -70ºC for 2 h each within atmospheric pressure. From the sixth phase the main drying lasted for 5 h in each phase for four phases with the shelf temperature increased from 10ºC to 15ºC, 20ºC, and 22ºC in the 6^{th}, 7^{th}, 8^{th}, and 9^{th} phases, respectively to allow gradual sublimation. Also the applied vacuum changed from 0.140 in the 6^{th} phase to 0.055 in the 7^{th}, 8^{th} and 9^{th} phases. The last phase which is the finishing stage lasted for 2 h where the sample was kept at 25°C under vacuum. When the process finished the sample was collected.

Table 2-1. Steps of Christ Freeze dryer cycle to lyophilise the mucilage.

Step	**1**	**2**	**3**	**4**	**5**	**6**	**7**	**8**	**9**	**10**
Phase	Load	Freeze	Freeze	Freeze	Freeze	Main drying	Main drying	Main drying	Main drying	End
Section (h:min)	00:0	1:00	2:00	2:00	2:00	5:00	5:00	5:00	5:00	00:10
Shelf temp (˚C)	-70	-70	-70	-70	-70	+10	+15	+20	+22	+25
Vacuum mbar	Atm	Atm	Atm	Atm	Atm	0.14	0.055	0.055	0.055	0.055

2.3.2.3. Characterisation tests

2.3.2.3.1. Galacturonic acid and carbohydrate identification

The phenol sulphuric acid assay is based on the colour of carbohydrates produced when they react with phenol. Samples of 200µl freeze dried mucilage solution (1mg/ml) were prepared and mixed with 200 µl of 5% (w/v) phenol in water. Then 1.0ml of concentrated sulphuric acid was added to the sample tube and left to stand for 10 min before shaking gently to allow mixing of all substances and promote the reaction. Standards were prepared for comparison using D-glucose solution

(20mg/ml), D-galactose solution (20 mg/ml), D-fructose solution (1.0 mg/ml), D-mannose solution (20mg/ml), D-arabinose solution (1.0 mg/ml), L-rhamnose solution (1.0 mg/ml), D-xylose solution (1.0 mg/ml).

The carbazole assay was based on carbazole reagent which was prepared by dissolving 0.15 g of carbazole (95% pure) in 100 ml ethanol under slow and continuously stirring. Samples (200µl) were placed in borosilicate tubes then 3ml sulphuric acid was added before adding 100µl carbazole reagent and mixed. The pink coloured crystals were observed when cooling the sample tubes after they had been heated for 1 h at 60°C.

2.3.2.3.2. Degree of Esterification using Fourier Transform Infra-Red (FTIR)

FTIR spectroscopy was used to determine the DE of pectin content of Shepherd's purse seed mucilage.

Pectin standards with 20-34%, 55-71% DE were mixed in deionised distilled water and freeze dried as for the mucilage extracts (section 2.3.2.2) to prepare pectin of DE 35-46%, 46-66%, and 56-66% DE.

Pectin samples were prepared by mixing a 1:100 mg ratio, pectin: KBr, the mixture was ground and then hydraulically pressed into even surface discs of 5 mm diameter using flat faced punch die set. The discs were placed in a sampling holder for transmission analysis. The measurements of FTIR spectral parameters including band area and peak heights were obtained using spectra management software

preinstalled in the JASCO spectrometer. The spectra values were average values from 50 scans at a resolution of $2cm^{-1}$ scanned at a rate of 1mm/sec. From each standard or mucilage extract, 10 independent samples were analysed and their FTIR spectra were recorded and the area of interest measured. The mucilage extracts were prepared in the same way as the standards. The ratio of the areas of the bands A1749/ (A1749+A1630) was calculated from the FTIR spectrum of every sample and using the calibration curve.

2.3.2.3.3. Dynamic Vapour Sorption (DVS) analysis

The DVS apparatus allowed controlled relative atmospheric humidity, temperature and sensitive measurement of any weight changes during sorption and desorption cycles using a Cahn microbalance.

The method employed was adopted from McInnes *et al*. (2007) in which RH increased by 10% each step. The DVS method consisted of two cycles of sorption and desorption phases each, where the RH was increased in 10 stepwise increments to 95% RH in the sorption phase and decreased in a reverse order during the desorption phase. Then the cycle was repeated in the same order, maintaining the temperature at 25ºC throughout all the cycles. Samples of 10 mg were loaded each time. The change in sample weight was measured every 10 seconds while data was saved every 15 min. The increase in RH for the next step in the cycle was only induced when the sample weight remained constant over 20 min, i.e., the change in sample weight was less than 0.002 mg/min (McInnes *et al.*, 2007).

Data was processed with DVS 1/1000 software version 2.16 to get an isotherm analysis report of the samples and isotherm plot (relationship between the target RH percentage and percentage of change in mass), in addition to change in mass plot (relationship between the percentage target humidity and percentage mass change with time).

Moisture sorption and desorption isotherms data were used to detect the moisture uptake and content for the extracted mucilage.

2.3.2.3.4. Thermal screening

A. Thermogravimetric Analysis

Dry mucilage samples were carefully weighed; 5-10 mg of the dry sample was loaded in Alumina open crucible pan and lightly pressed to ensure heat transmission. The pans were then placed in the TGA apparatus and heated from 25°C TO 300°C at 10°C/min (283.15K/min) in nitrogen atmosphere. HPMC K100 sample was carefully weighed and 5-10 mg placed in alumina open pan and heated from 25ºC to 240ºC at 10ºC /min in nitrogen atmosphere. TGA is used for screening of the mucilage sample to detect any decomposition, evaporation, vaporisation, sublimation and heat stability. The obtained data were analysed using STAR® software supplied with the instrument.

B. Differential Scanning Calorimetry analysis

Samples were carefully weighed and ~3-5 mg placed into a 40 µl aluminium pan, which was then hermetically sealed with a pin-holed lid. An empty standard

aluminium pan with a pin-hole was used as a reference. With existence of the enthalpy relaxation, there is a need to undergo a quench-cool step to remove thermal history for the material (Schubnell, 2005). Quench cool method was followed where samples were heated from 25°C to 200°C at 10° C/min, then from 200°C to -25°C in 200°C/min, followed by -25°C to 25°C at 10°C/min under nitrogen.

The accuracy of the DSC sensor is 0.1°C. The measurements were performed in triplicate and spectra were inspected for any changes in the heat transfer. Any changes in enthalpy were calculated using STAR® software. DSC 822e was used to determine the midpoint of the Tg, and ΔC_p.

2.3.2.3.5. Determination of bound water

Samples of 10 mg were carefully weighed and compressed hydraulically into 5 mm diameter flat faced discs using a manual press and then placed into 40 µl aluminium crucibles and hydrated with 10 µl deionised distilled water. The hermetically sealed pans with a pin-hole lid were held at 25ºC for 30 min before freezing to -30ºC at 20ºC/min then heating from -30ºC to 20ºC at 10ºC/min.

The enthalpy of fusion of ice was measured and corresponded to the quantity of unbound water. Then the quantity of bound water was calculated by subtracting the enthalpy of fusion of ice in the sample from the standard water enthalpy of fusion. All measurements were conducted in a DSC 822e instrument.

2.3.2.3.6. Chemical structure elucidation using Nuclear Magnetic Resonance

Extensive 1D and 2D experiments were carried out using a Bruker NMR spectrometer (400 MHz and 600 MHz) to elucidate the structure of the compounds extracted in the mucilage to understand the behaviour of mucilage and its interactions with other compounds. Deuterium oxide was used for dissolving samples to study the aqueous extracts of Shepherd's purse mucilage.

^{1}H NMR, J-modulated ^{13}C NMR, COSY, HMBC, HSQC, TOCSY experiments were performed to get all relevant information to elucidate the structure of the compounds. NMR spectra analysis was performed using the MestReNova™ software for NMR analysis (Mestrelab, Santiago de Compostela, Spain).

2.3.3. Statistical analysis

All measured data were subjected to statistical analysis using Minitab 16 software. ANOVA was conducted to compare the different extracts.

2.4. Results

2.4.1. Carbohydrate identification and galacturonic acid content determination

A phenol-sulphuric acid test identified that the main carbohydrates were rhamnose and arabinose sugars by comparing the colour of the standards with the colours in the samples tubes.

The pectin test showed that all the samples produced a pink colour solution, which is an indicator of the presence of uronic acid or pectin.

2.4.2. Degree of Esterification (DE)

The FTIR spectra baselines were corrected automatically with the 'automatic baseline correct' function in the Spectra Management™ software.

The area of the carbonyl group was the main area of interest and was used to predict the DE. From the literature, the ester carbonyl group usually appears in the region of 1700-1780 cm^{-1}, and the carboxylic acid group absorbs at 1600 and 1414 cm^{-1}, while amides stretch at both bands 1650 or 1550 cm^{-1} (McCann *et al.*, 1994). Additionally, the region below 1500cm^{-1} is the fingerprint of the compound and noticeably aliphatic C-H and aromatic rings usually appear between 3150 and 3000cm^{-1}. Table 2-2 shows all the absorption bands of standard pectin, examined by Gnanasambandam and Proctor (2000), which were used as a reference for naturally extracted pectin.

The carbonyl group absorption and carboxylic acid group absorption of standard pectin examined by FTIR are illustrated in Figure 2-3. The FTIR spectrum of all standard pectin samples were analysed and peaks heights and area under curve for corresponding bands were measured and displayed in Table 2-3.

Table 2-2. Frequencies and intensities of functional groups on commercial pectin samples analysed by FTIR Spectroscopy (Gnanasambandam and Proctor, 2000)

Frequency (wave number, cm^{-1})	**Functional groups**	**Intensity**
3600-2500	O-H stretching Broad	Strong
3000-2800	C-H stretching, symmetric, asymmetric	Sharp, occasionally double overlapping with O-H
1760-1745	C=O, esterified	Strong
1640-1620	COO^{-2} asymmetric stretching	Strong
1400	COO^{-2} symmetric stretching	Weak
1380	C-H bending	Weak
1300-1000	C-O Stretching	Weak

Table 2-3. Standard calibration curve table for standard pectin DE along with the absorption bands of interest and peak height (H) and Area under the curve (AUC) of the sample peaks (n=10)

Standard pectin %DE*	**Peak ester carboxyl group cm^{-1}**	**Peak free carboxyl group cm^{-1}**	**Peak height of ester carboxyl (a) cm**	**Peak height of free carboxyl cm**	**AUC of ester carboxyl group (b) cm^2**	**AUC of free carboxyl group cm^2**
30	1745.29 ±0.03	1615.18 ±4.29	0.13 ±0	0.39 ±0.01	7.67 ±0.65	43.37 ±2.30
40	1745.30 ±0	1612.20 ±0	0.25 ±0	0.35 ±0	14.82 ±0.22	41.97 ±0.44
50	1745.30 ±0	1615.32±0	0.29 ±0	0.29 ±0	15.69 ±0.49	31.21 ±0.96
60	1742.56 ±2.9	1621.86 ±2.02	0.34 ±0.01	0.26 ±0.01	17.41 ±0.78	21.54 ±1.53
70	1745.30 ±0	1637.91 ±0.91	0.47 ±0	0.20 ±0	27.06 ±0.64	20.89 ±0.58

(a) P=0.003; (b) P=0.017; *DE illustrated is the midpoint of the range of DE of the standard pectin.

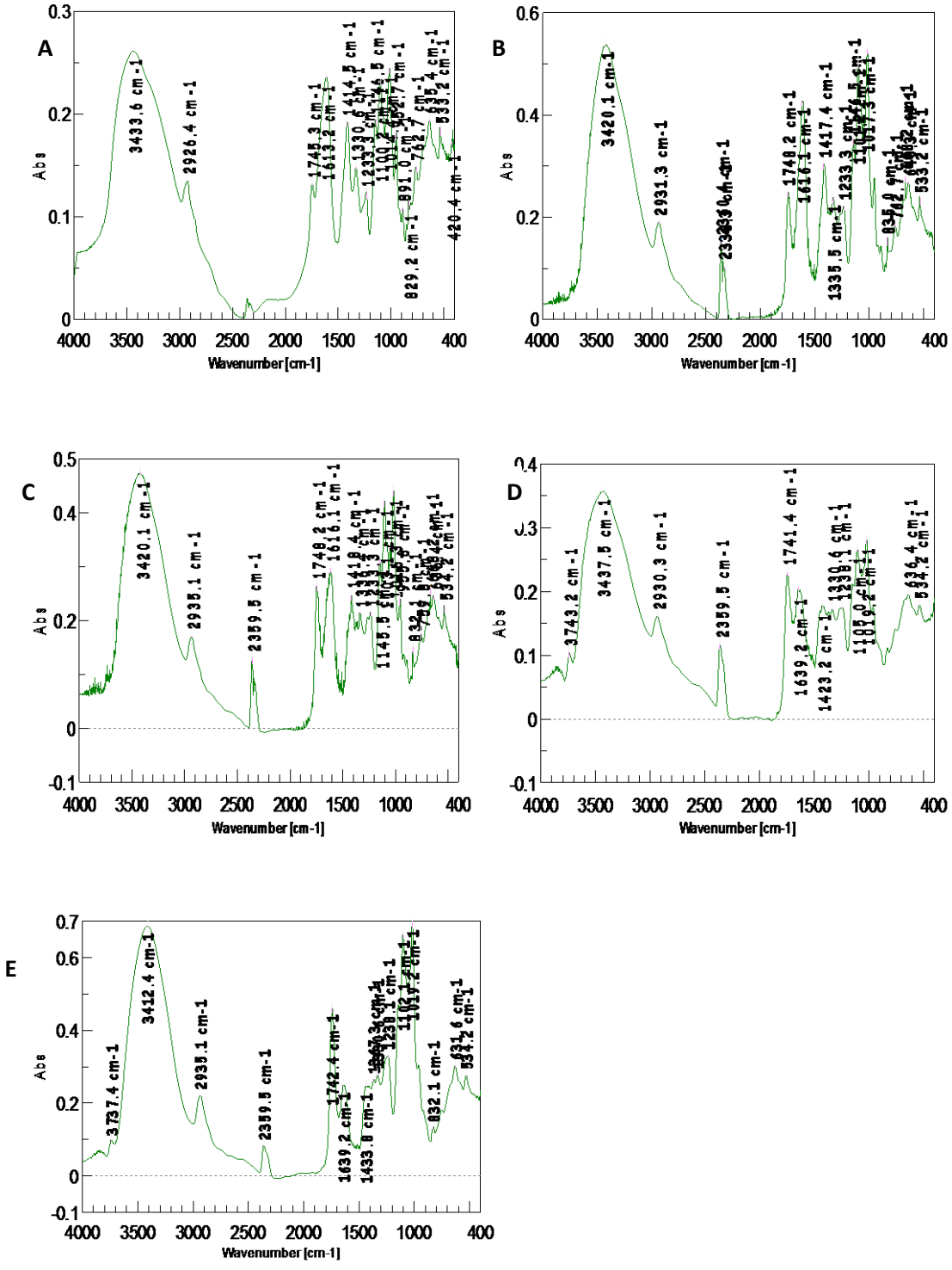

Figure 2-3. FTIR Spectra of standard pectin with known DE (A) 20-34% DE, (B) 34-46% DE, (C) 46-55% DE, (D) 55-65% DE, (E) 61-70% DE.

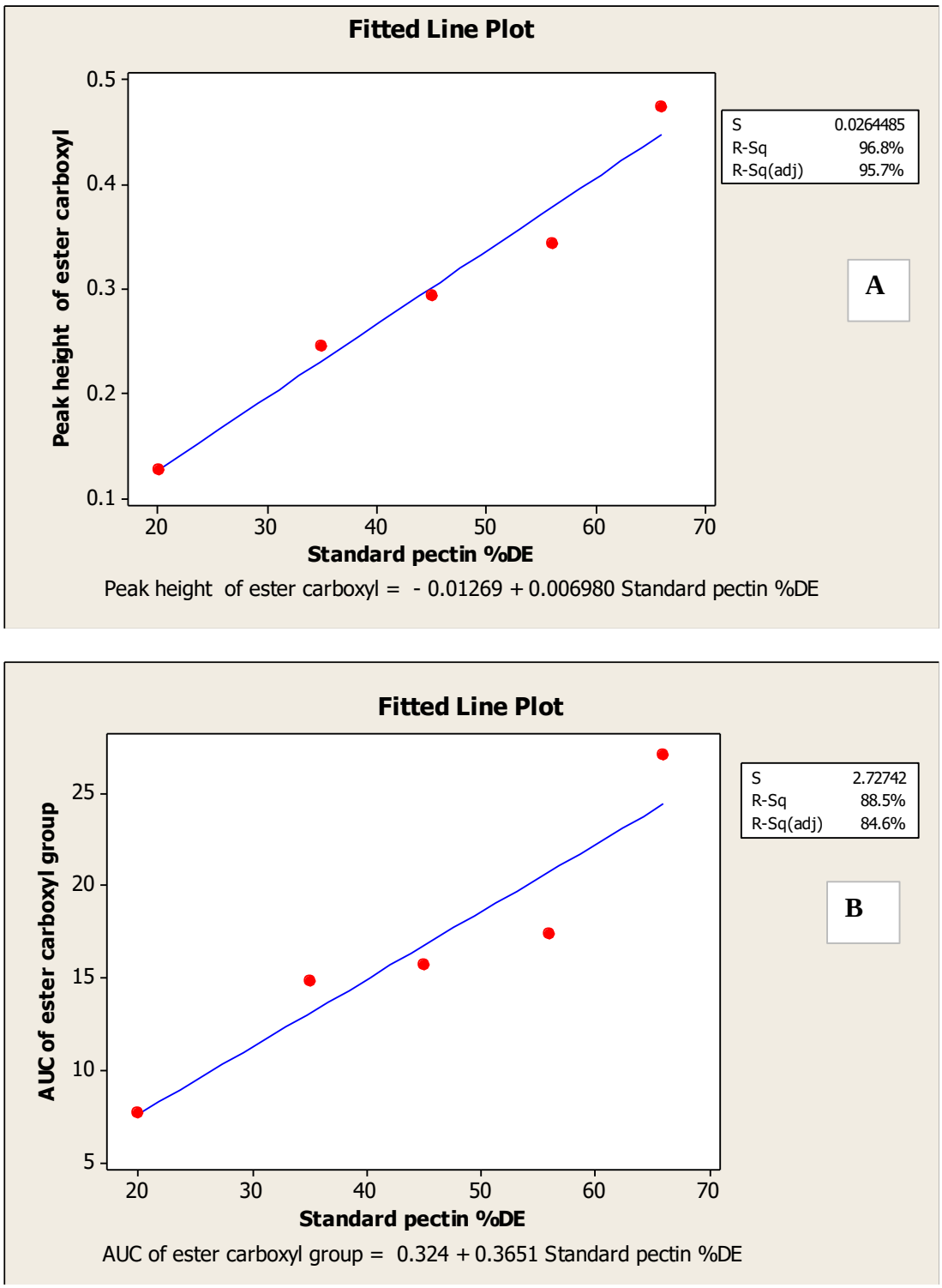

Figure 2-4 The best fit line (A) Peak height against % DE for standard pectin, (B) AUC against % DE of standard pectin.

The best fit line was extracted by regression of the height of the ester carboxyl group peak against standards and the straight line equation was concluded as shown in Figure 2-4 (A).

The AUC was also used to measure the DE of pectin and the best fit line was concluded using the regression of data of AUC of the ester carboxyl group peak against standards and the line equation extracted in Figure 2-4 (B). The straight line equation extracted from using the peak height of the ester carboxyl group and AUC were both used to measure the DE of the extracted mucilage pectin.

Depending on the literature reviewed the area of interest that shows carboxylic groups and carboxylic esters are between 1800 and 1500 cm^{-1} (Barros *et al.*, 2002; Chatjigakis *et al.*, 1998; Lampman, 2010).

The spectra analysis of all samples in Table 2-4 showed peaks at the same region of 1610-1620 cm^{-1} and in the band range of 1415-1420 cm^{-1}, except for the solvent maceration and mucilage hot maceration 70^{o}C samples which had peaks at 1655 cm^{-1} and 1627 cm^{-1} respectively. The esterified carboxylic group band had disappeared from all extracts spectra and the data displayed in Table 2-4 showing peaks at the bands from 1400 cm^{-1} to 1550 cm^{-1} and was referred to as peak 2 in the table. All FTIR spectra obtained for Shepherd's purse mucilage extracts were displayed in Figure 2-5.

Table 2-4.The peaks bands, peaks heights (H) and Area Under the Curve (AUC) of the same peaks of all samples from different mucilage extracts (mean ± SD, n=10)

Sample	**Peak of 1 cm^{-1}**	**Peak of 2 cm^{-1}**	**H of peak 1 cm**	**H of peak 2 cm**	**AUC of peak 1 cm^2**	**AUC of peak 2 cm^2**
Water maceration	1622.8 ±0	1418.4 ±0	1.03 ±0.01	0.60 ±0	438.16 ±11.89	78.25 ±29.27
Solvent maceration	1655.75 ±1.36	1541.73 ±2.11	0.96 ±0	0.66 ±0	103.60 ±32.34	51.78 ±0.24
Hot reflux	1608.67 ±2.19	1419.53 ±1.21	0.73 ±0.01	0.43 ±0	82.12 ±0.07	41.77 ±4.40
Hot maceration 40º C-1h	1616.1 ±0	1417.03 ±1.97	0.55 ±0	0.38 ±0	109.02 ±13.80	93.63 ±20.26
Hot maceration 40ºC-2h	1621.47 ±1.22	1518.5 ±0.42	0.87 ±0	0.41 ±0	124.73 ±1.22	12.78 ±0.77
Hot maceration 50ºC-1h	1615.3 ±0	1420.3 ±0	0.94 ±0	0.66 ±0	118.90 ±3.55	126.96 ±3.06
Hot maceration 50ºC-2h	1620.9 ±0	1514.8 ±0	0.62 ±0	0.28 ±0	81.63 ±2.11	9.61 ±0.36
Hot maceration 70ºC	1626.36 ±3.85	1514.76 ±0.1	0.181 ±0	0.12 ±0	37.24 ±11.97	5.60 ±2.03

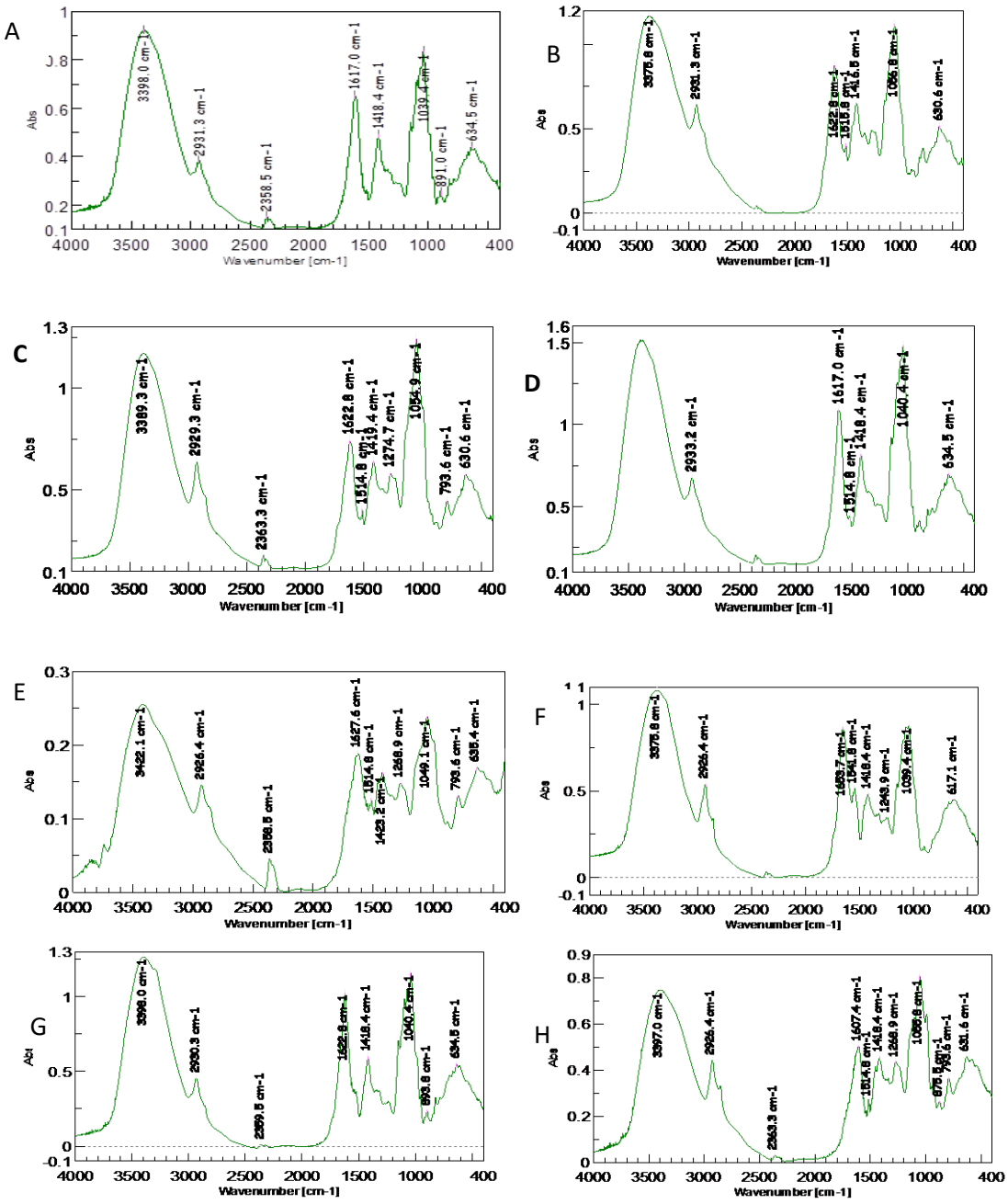

Figure 2-5. FTIR Spectra of mucilage extract, (A) hot maceration 40ºC-1h, (B) hot maceration 40ºC-2h, (C) hot maceration50ºC-2h, (D) hot maceartion50ºC-1h, (E) hot maceartion70°C, (F) solvent maceration, (G) water maceration 25ºC, (H) hot reflux.

Both hot maceration 40ºC mucilage extracts in Figure 2-5 (A and B), showed peaks at 1612-1620 cm^{-1} and 1415- 1418cm^{-1}. The expected esterified ester carboxyl group did not appear in the region of 1700-1780cm^{-1} as stated in literature (Stewart and Morrison, 1992).

Comparing mucilage from hot maceration 40ºC-2h with hot maceration 50ºC-2h, showed a small peak at 1515.8 cm^{-1} and 1514cm^{-1} respectively that were totally masked by an adjacent peak at 1622.8cm^{-1}. Since amides are usually found to have an absorbance at the 1550-1500 cm^{-1} band, it was expected that a small amount of amide was present in these extracts (Manrique and Lajolo, 2002).

The band of wavenumbers 1200-900 cm^{-1} in Figure 2-5 was the substance fingerprint of hot maceration at 40°C extracts. This area had peaks at 1039, 893, 635 cm^{-1} revealed the same material was extracted in Figure 2-5 A and B.

The mucilage extracted at 50ºC shows peaks at 1620 and 1418 cm^{-1} without any peaks at range of 1740-1780cm^{-1}. The fingerprint in Figure 2-5 C and D showed similarity in the spectra between the two different extracts.

The spectrum of mucilage extracted at 70ºC in Figure 2-5 E showed absorbance at wavenumbers 3422 cm^{-1}, 2926 cm^{-1}, 1627 cm^{-1}, and 1423 cm^{-1}. The peak at 3422 cm^{-1} was for -OH stretching, while 2926 cm^{-1} was denoted as C-H stretching.

The solvent maceration extract spectrum in Figure 2-5 (F) showed absorbance at 3375 cm^{-1}, 2926 cm^{-1}, 1653cm^{-1}, 1514 cm^{-1}, and 1418 cm^{-1}.

The water maceration mucilage 25ºC spectrum in Figure 2-5 (G) had 4 peaks at 3398 $cm^{-1}$for -OH, 2930 cm^{-1} for C-H, 1622 cm^{-1} and 1418 cm^{-1} for -OOC.

The spectrum of mucilage extracted by hot reflux shown in Figure 2-5 (H) was similar to spectra of mucilage 70º C and maceration samples.

It was important to note that the peak which appeared at wavenumber 2360cm^{-1} did not belong to any sample and was attributed to atmospheric carbon dioxide.

2.4.3. Dynamic Vapour Sorption (DVS)

DVS studies provided a means of characterising polymer stability in different humidity conditions. The change in mass of mucilage upon exposure to different levels of humidity was related to the stability and helped to estimate the storage conditions.

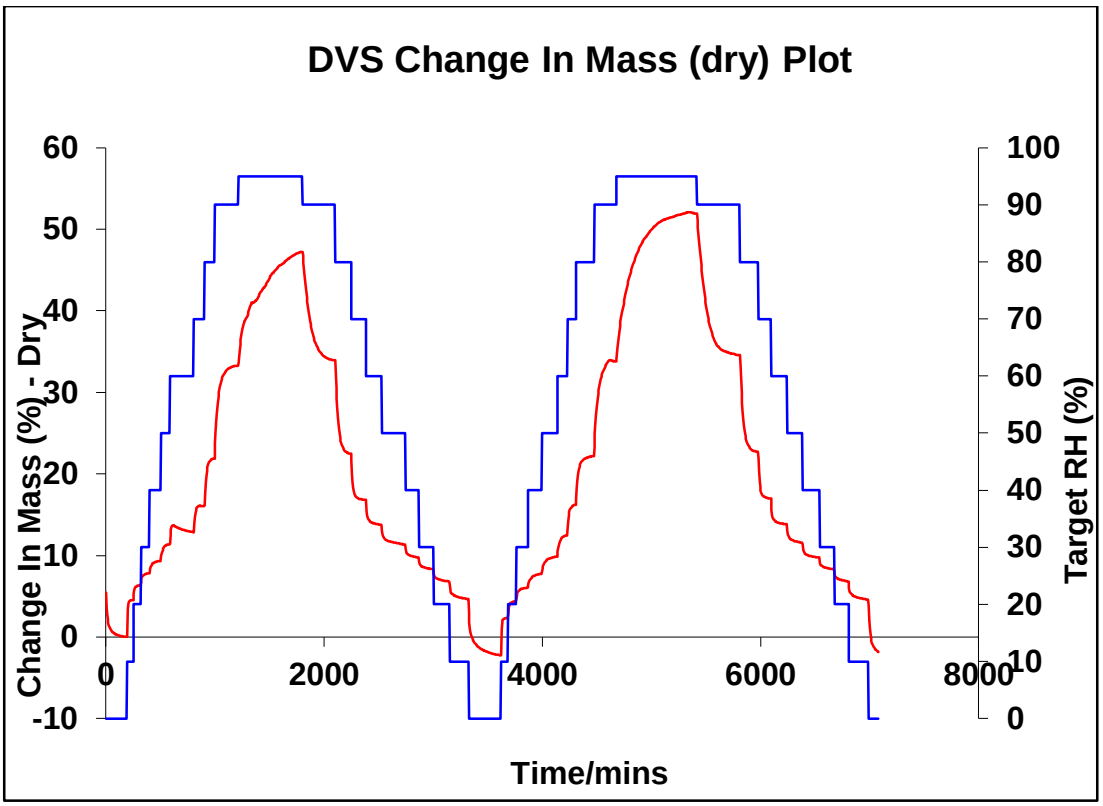

Figure 2-6 DVS Chart of changes in the mass with changes in target RH% against time for water maceration mucilage 25ºC (n=1)

Crystallisation occurred for water extracted mucilage 25ºC in the beginning of the first cycle as illustrated in the change in the dry mass chart when the target RH reached 10% (Figure 2-6).

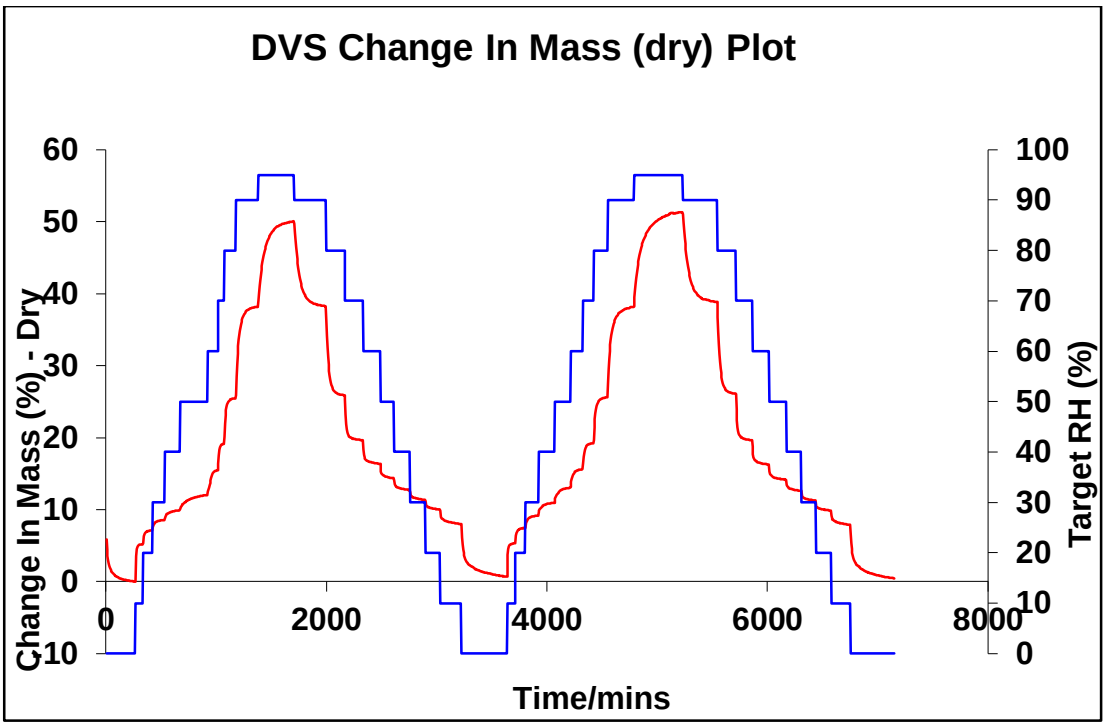

Figure 2-7 DVS chart of change in mass with change in target RH% against time for hot maceration 40°C-1h (n=1)

The DVS chart for 40°C-1h in Figure 2-7 showed that the mucilage mass changed by 50% from dry weight when exposed to a RH of 90%. It also showed that the mucilage had undergone the same change in weight in the second cycle while it retained 0.72% of the RH taken up in the sorption phase.

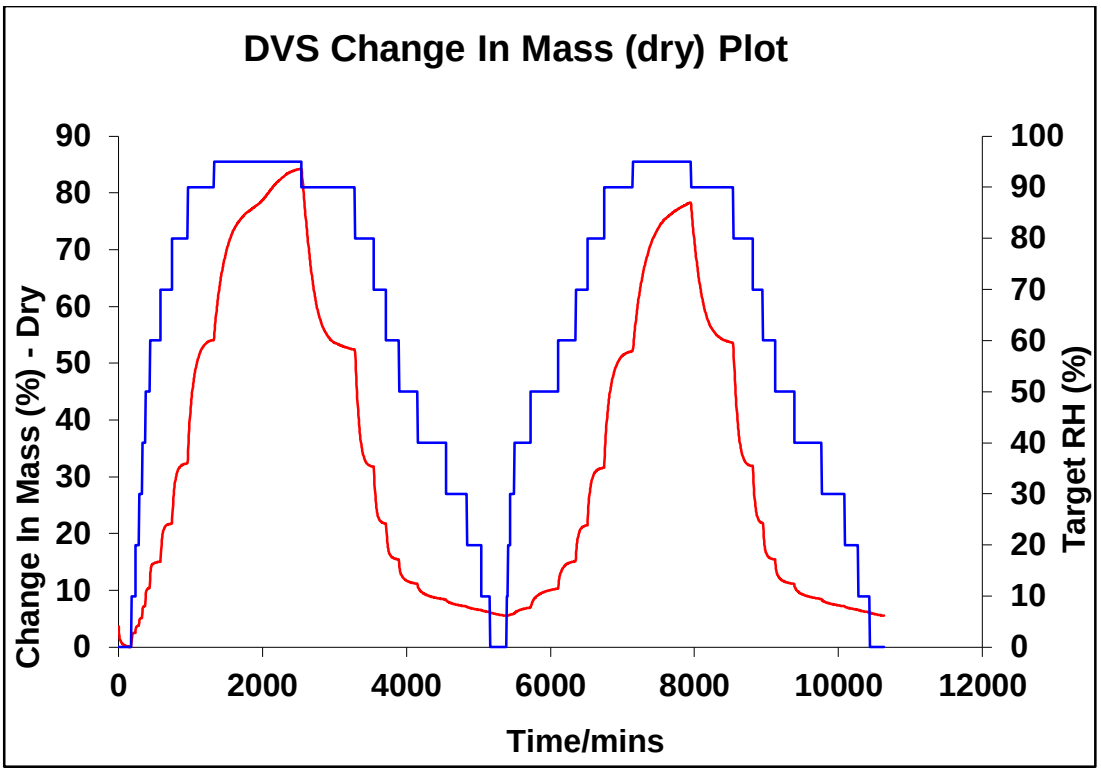

Figure 2-8 DVS chart of change in mass with change in target RH % against time for hot maceration 40°C-2h (n=1)

The hot maceration mucilage obtained by extraction at 40ºC-2h in Figure 2-8 took up moisture as 80% of its dry weight during 2542 min (42h). Though 10% of the absorbed vapour was retained in the mucilage after the desorption phase, the mucilage continued to take up moisture vapour up to 77% of its dry mass. Interestingly, the mucilage lost some of its own water content during the desorption phase from 80% to 50% RH.

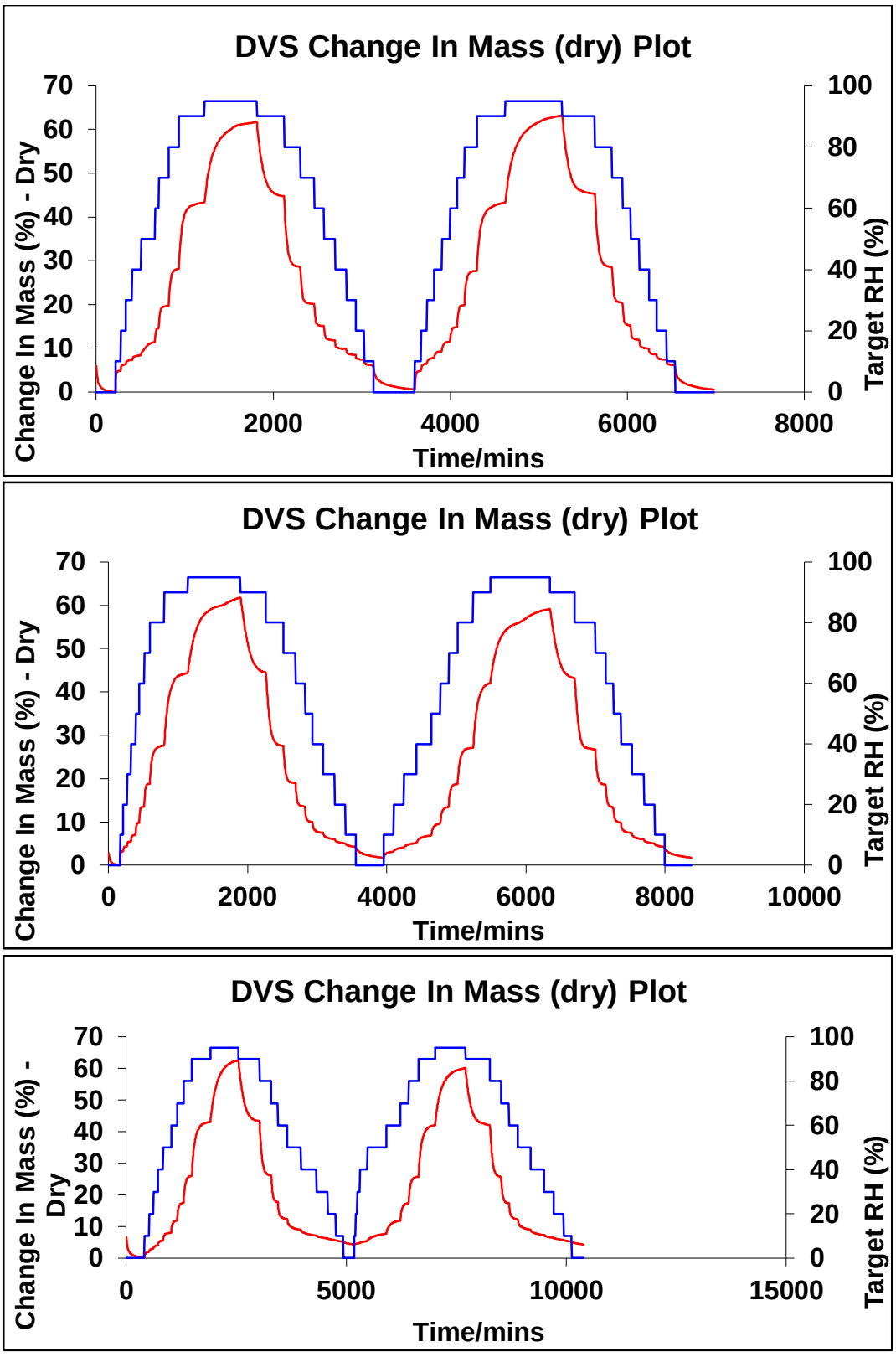

Figure 2-9. DVS chart of change in mass with change in target RH% against time for hot maceration mucilage (n=1) (A) 50°C-1h, (B) 50°C-2h, (C) 70°C.

Hot maceration mucilage obtained at 50ºC-1h and 50ºC-2h in Figures 2-9A and B showed similar behaviour in vapour uptake and changes in dry mass to each other. They both reached 60% change of their dry mass when exposed to 90% RH at almost the same time (1780 min=29.5 h). The 50ºC-2h mucilage in Figure 2-9B tended to retain 2% of the absorbed vapour from the first vapour sorption phase during the first desorption phase.

The hot maceration mucilage 70°C illustrated in DVS chart Figure 2-9C revealed that this mucilage took only vapour moisture from the atmosphere equal to 60% of its dry mass during 2549 min (42.5 h). The amount of retained moisture into the mucilage did not affect its moisture uptake ability where it took up the same mass and lost it in the same speed of uptake. This mucilage underwent the same condition as the HM mucilage 40ºC-2h during the desorption phase when it lost its own water content from 90% RH to 60% RH.

Hot reflux mucilage (DVS chart Figure 2-10) displayed the mucilage as a very slow moisture uptake where the first sorption phase took 3900 min (65h) to reach the maximum mass taken from the surrounding which was 67% its dry mass. There was no difference between the two cycles of sorption and desorption of vapour. The whole cycle took 6780 min (113h) to complete, which was double the time taken by other cycles to finish the whole experiment.

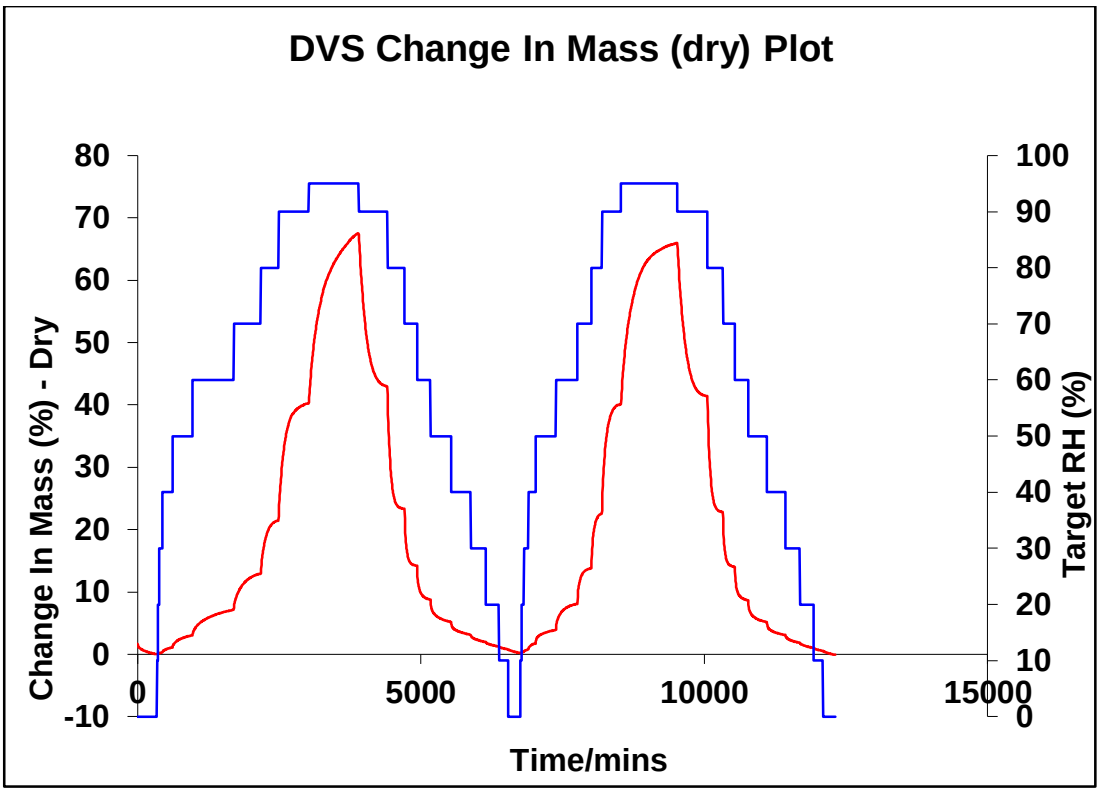

Figure 2-10 DVS chart of change in mass with change in target hot reflux mucilage % against time for hot reflux mucilage extract (n=1).

In comparison to the other extracts, solvent maceration mucilage exhibited in Figure 2-11 the least vapour sorption % which was just above 32% of the dry mass and lost 0.55% of its starting dry mass upon the end of the first desorption phase of cycle 1. This weight loss was believed to be loss in the water content that was captured inside the structure of mucilage upon storage.

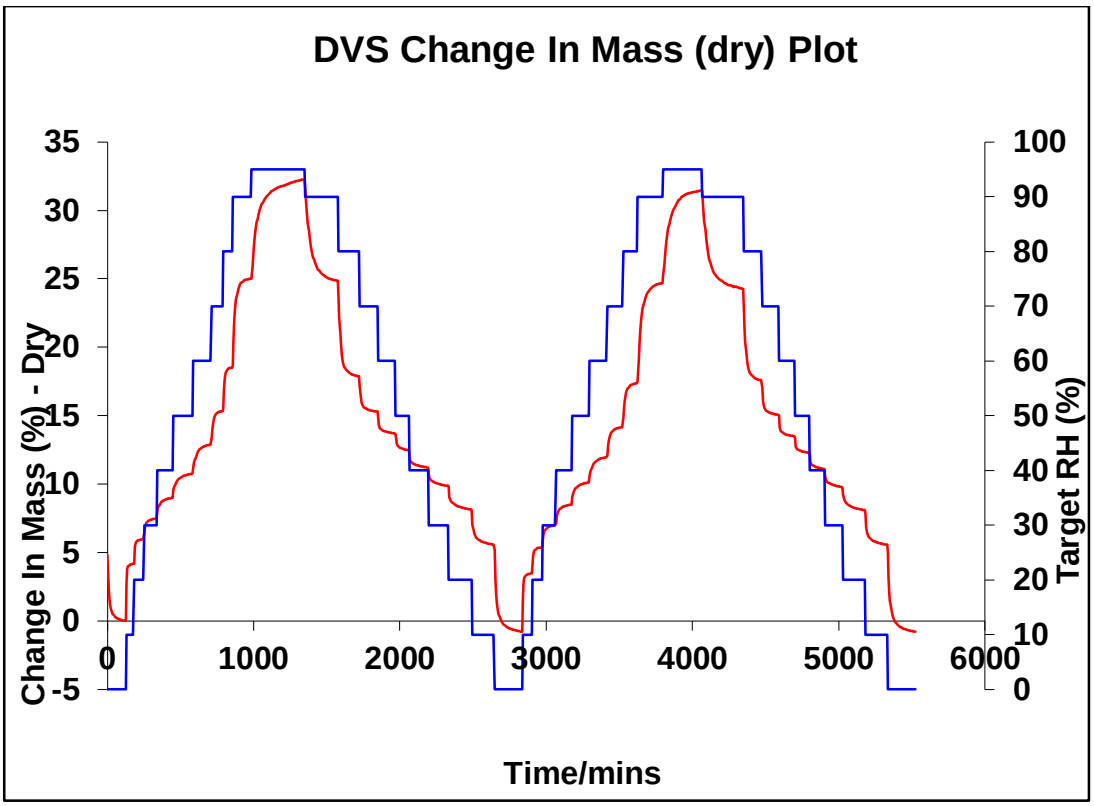

Figure 2-11 DVS chart of change in mass with change in target solvent maceration mucilage % against time for Solvent maceration (n=1).

2.4.4. Thermal analysis

2.4.4.1. Thermal Gravimetric Analysis (TGA)

The TGA curve of water maceration extracted mucilage in Figure 2-12 showed a 44.7 % weight loss in a form of a huge moisture loss and evaporation from room temperature to 300°C (Hammer *et al.*, 2013). The drying and slow gradient moisture loss occurred from room temperature to 140ºC followed by gradual decomposition with formation of gaseous products after 240ºC with the formation of a black charred residue forming 55.3% of starting mass (Widmann, 2001).

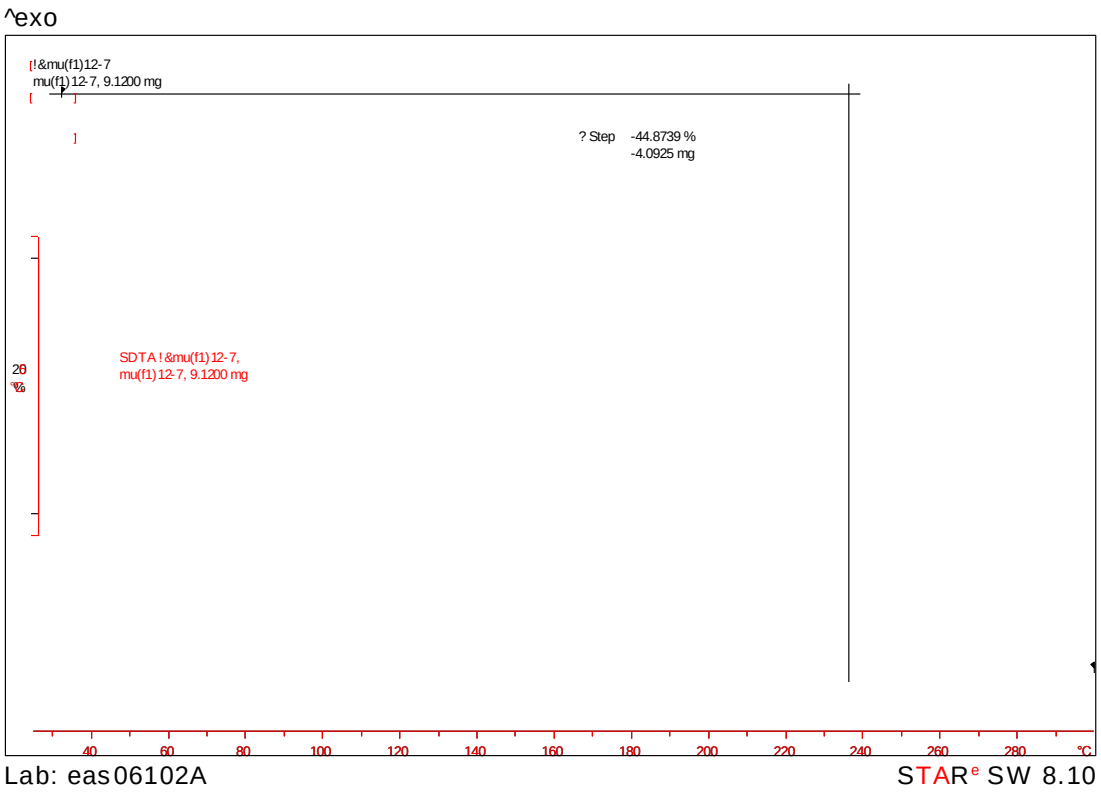

Figure 2-12 TGA thermogram of Shepherd's purse mucilage by water maceration 25ºC heated from 25°C to 300°C at 10°C/min.

Heating water maceration 25º C mucilage from 25ºC to 150ºC at a rate of 10ºC/min illustrated in Figure 2-13 showed that mucilage lost just over 4% of its weight. It shows that mucilage can be studied for any changes below 200ºC.

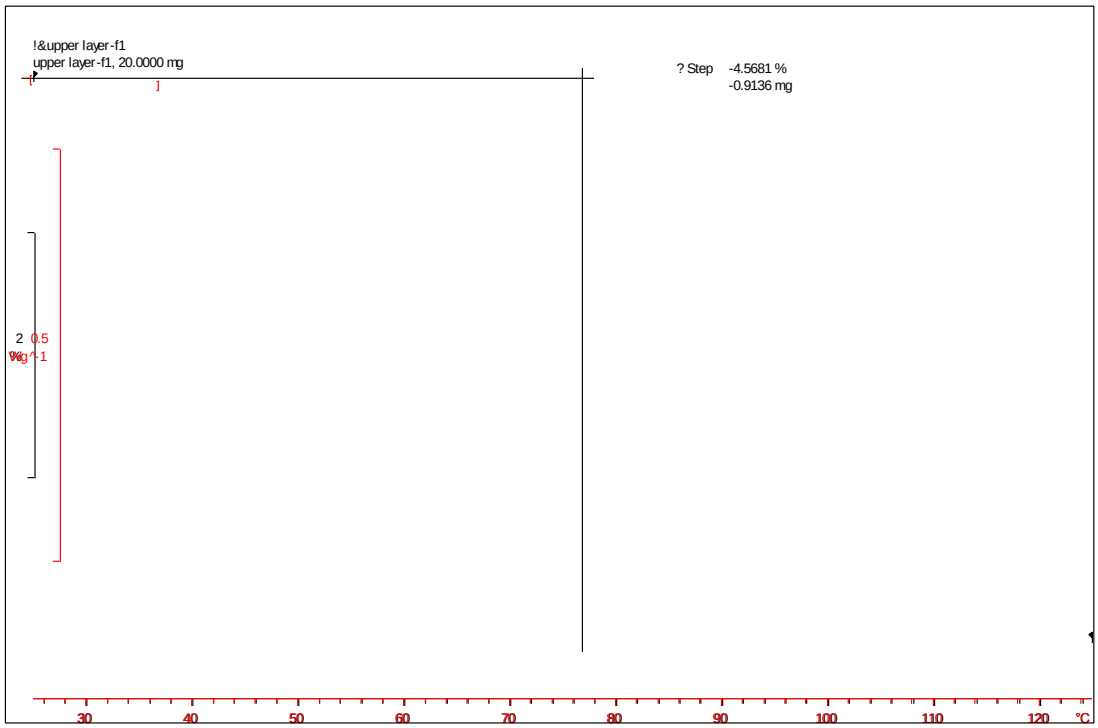

Figure 2-13 TGA thermogram of Shepherd's purse mucilage by water maceration 25ºC heated from 25°C to 150°C at 10°C/min.

2.4.4.2. Differential Scanning Calorimetry (DSC) analysis

A DSC spectrum of the first heating run of water maceration 25ºC mucilage shown in Figure 2-14 revealed a large enthalpy relaxation. All mucilage extracts showed a wide relaxation enthalpy and only water maceration spectrum was chosen to display as an example. All DSC spectra from first heating of different mucilage extracts were displayed in Appendix 2.

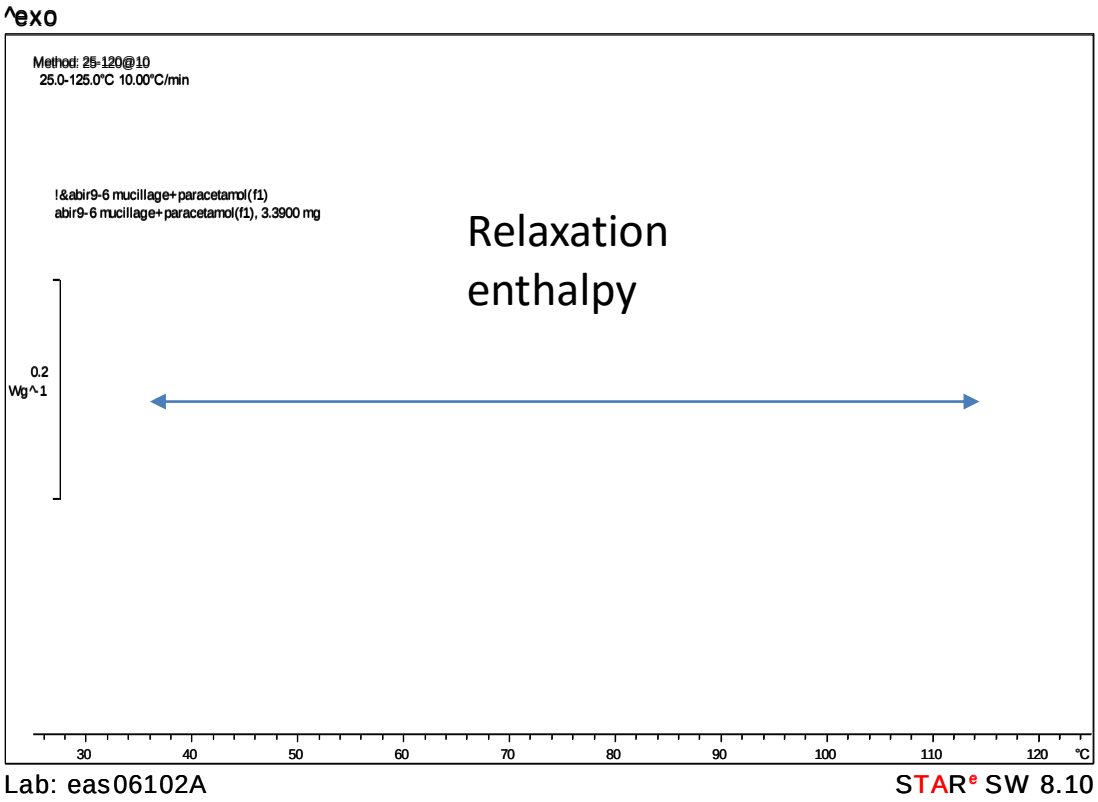

Figure 2-14. DSC thermogram of water maceration 25ºC mucilage.

DSC spectrum of water maceration 25ºC mucilage under gone quench-cool shown in Figure 2-15 had an endothermic peak starts at around 50°C and its extrapolated peak at 100°C. The drying peak for solvent maceration mucilage had an extrapolated peak at 76°C and the onset at which the adsorbed moisture was easily released and vaporised was 37°C. The occurrence of moisture evaporation at 37°C indicated the thermo-instability of the mucilage at low temperature (Einhorn-Stoll *et al.*, 2007).

Also there was an exothermic peak on the second reheating of the mucilage after the quench cool step which was referred to as cold crystallisation. The cold crystallisation peak had an onset at almost 17ºC for the majority of the extracted

mucilage. Table 2-5 below shows the cold crystallisation onset temperature and the heat of crystallisation measured for all extracts.

Table 2-5 The cold crystallisation onset temperature and heat of crystallisation for all mucilage extracts (n=3). Results represented mean ± SD.

Sample	**Crystallisation temp ºC**	**Heat of crystallisation Jg^{-1} ***
Water Maceration 25ºC	16.67±0.15	1.42±1.50
Solvent Maceration	16.85±0.19	5.5±1.80
Hot Reflux	17.04±0.25	2.5±2.30
Hot Maceration 40°C-2h	17.02±0.15	5.3±1.70
Hot Maceration 50°C-2h	17.18±0.15	3.22±1.72
Mean	16.96±0.18	3.87±1.73

- # P> 0.05 cold crystallisation temp mean was NOT significantly different from the standard mean
- * Displayed the mean of crystallisation temp and heat of crystallisation of the different extracts at the same temperature.

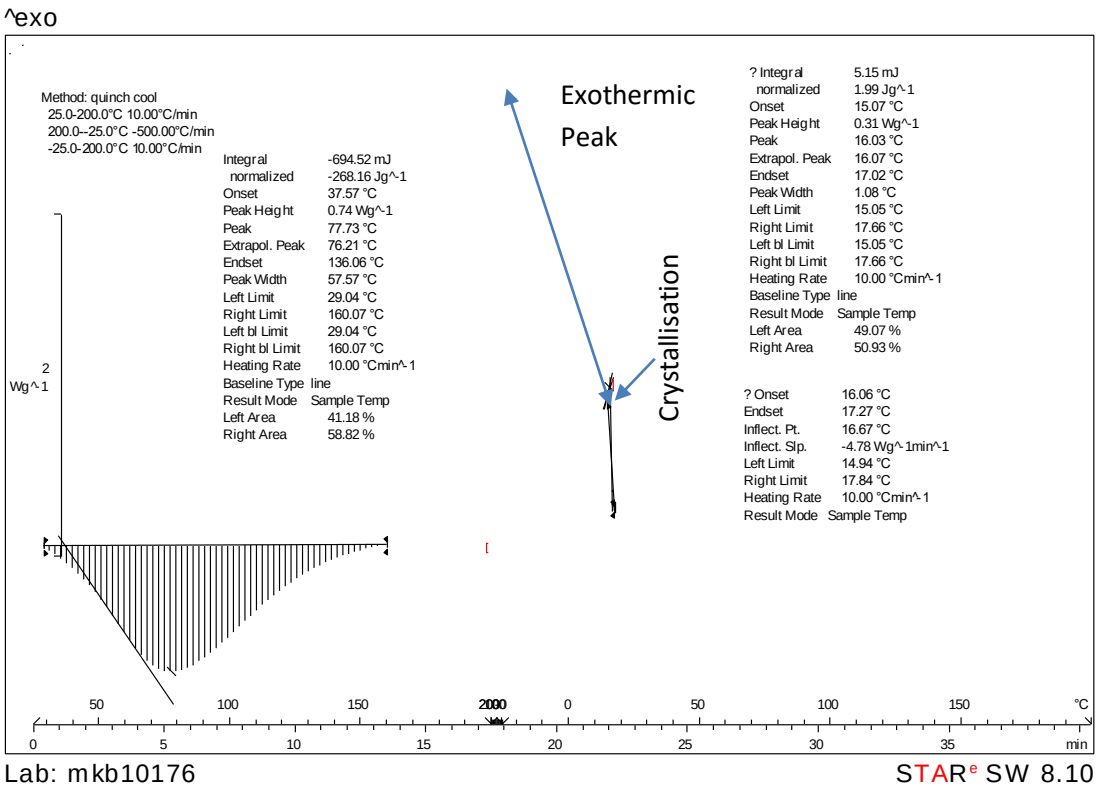

Figure 2-15 DSC thermogram of water maceration 25º C mucilage by the quench-cool method.

2.4.5. Bound water measurement

Measuring the enthalpy of fusion of ice correspondence to the unbound water and subtracting it from the fusion enthalpy of blank water resulted in calculating the amount of bound water. All measurements and calculations were shown in Table 2-6 below.

Table 2-6. The amount of water absorbed by mucilage from different extracts

Sample	**Measured heat of fusion of ice (unbound water) J/g**	**Calculated heat of fusion of bound water J/g**	**% Water bound**
10µl water	-330.67±4.46	0	0
Standard pectin	-211.41±24.31	-122.09	36.60
HPMCK100	-245.79±30.18	-87.71	26.30
Hot maceration 40°C-1h mucilage	-206.77±27.62	-126.73	38
Hot maceration 40°C-2h mucilage	-217.81±33.89	-115.69	34.69
Hot maceration 50°C-2h mucilage	-183.6±36.23	-149.9	44.95
Hot maceration 50°C-1 h mucilage	-204.12±25.41	-129.38	38.79
Hot maceration 70°C mucilage	-195.18±35.72	-138.32	41.47
Solvent maceration mucilage	-172.08±32.33	-161.42	48.40
Water maceration mucilage	-151.40±37.16	-182.1	54.60
Hot reflux mucilage	-164.55±29.51	-168.95	50.65

2.4.6. Chemical structure elucidation

The proton spectra of all extracts were assessed to determine the nature of extracted compounds and identify their purity. The primary outcome showed similarity between mucilage 70°C (Figure 2-16) and the hot reflux extracts (Appendix 4) which were different from mucilage 40°C-1h (Appendix 4), cold maceration (Appendix 4) and 50°C-1h (Figure 2-22). Furthermore 40°C-1h and 50°C-1h were similar to each other. It was also clear from the proton spectra there was a mixture of water soluble compounds overlapping each other. Depending on this comparison, hot maceration 70°C and hot maceration 50°C -1h were chosen for analysis. Additionally these two compounds showed better quality NMR spectra suitable for analysis.

2.4.6.1. NMR spectra analysis for mucilage 70°C

The ^{1}H spectrum of mucilage 70°C (Figure 2-16) showed two compounds of interest; a para-substituted aromatic region and a glycosidic aliphatic region. ^{13}C-jmod NMR shown in Figure 2-17 revealed a mixture of compounds. The aromatic compound seemed to be a separate compound from the glycosidic compound.

The aromatic region (Figure 2-16) appeared as proton signals at 8.07ppm and 6.87 ppm in a form of complex doublets typical for P-substituted benzene (Lampman, 2010).

The HMBC NMR spectrum (Figure 2-21) showed that H at 7.40ppm was linked to carbons at 107.5 ppm, 138.2 ppm and 147.8 ppm. On the other hand the aromatic ring proton at 6.85 ppm was found coupled to C at 126.2 ppm while the other

aromatic ring H at 8.05 ppm was coupled to a carbonyl group C at 168.5 ppm and 107.5ppm. The rest of the aromatic ring was not clear in any of mucilage 70°C spectra.

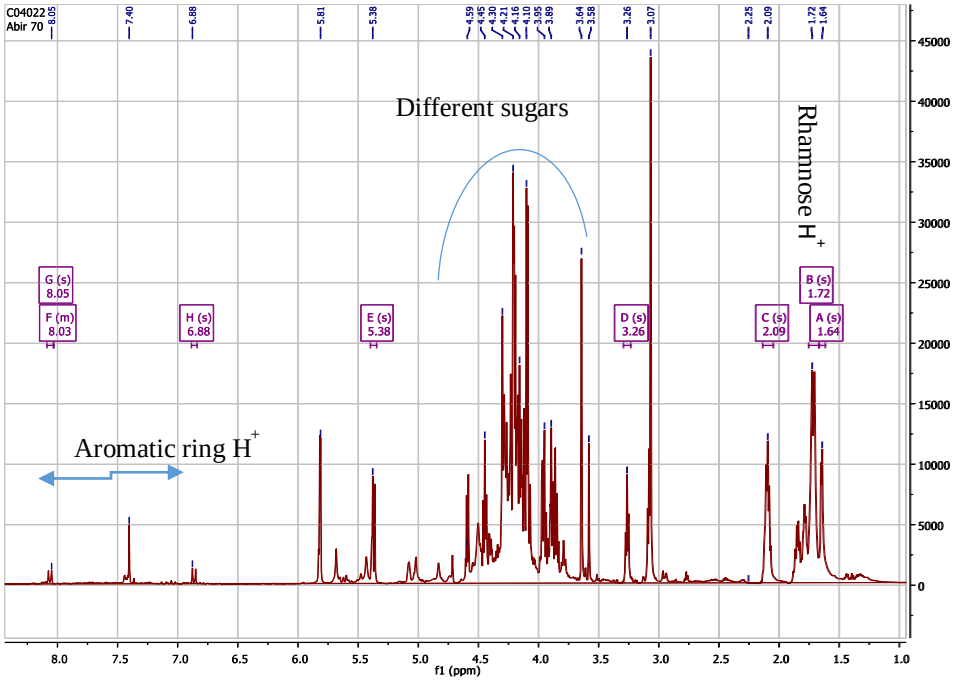

Figure 2-16 ^{1}H NMR spectrum of Shepherd's purse mucilage extract 70°C in D_2O at 400MHz with water suppression at 4.8 ppm.

Examination of the ^{1}H NMR (Figure 2-16) clarified that the glyosidic side of the spectrum was composed of few different sugars, though rhamnose was the major one. The presence of rhamnose was shown by carbon at 17.05 ppm on the ^{13}C spectra (Figure 2-17) and the doublet ^{1}H centred at 1.64 (d, *J*=4 Hz) in the ^{1}H NMR spectrum (Figure 2-16) (O'Neill *et al.*, 2004). These findings were confirmed with the HSQC spectrum (Figure 2-20), which showed that the methyl carbon of rhamnose that appeared at 17.2 ppm was directly linked to a proton at 1.65 ppm (Ramos *et al.*, 1996).

The TOCSY spectra which correlate H-6 of the rhamnose at 1.64 ppm with the other rhamnose sugar protons showed that H-6 of the rhamnose was related to H-5 of rhamnose at 4.19ppm and H-4 at 3.78ppm (Figure 2-19). The HMBC spectrum in Figure 2-21 showed rhamnose sugar carbon (C-5) at 69.02 ppm coupled with proton at 1.65 ppm (H-6). H-5 was at 4.20 ppm, and H-3 was 4.18 ppm, which is directly attached to C73.7 ppm in the HSQC spectrum. Furthermore the methyl proton at 1.65ppm was directly attached to H at 4.18 ppm in the COSY NMR spectra (Figure 2-18).

The anomeric carbon at 92.7 ppm seen in the HSQC spectrum (Figure 2-20) was for C-1 of another major hexose glycoside compound, and linked to a H-1 that appeared at 5.83 ppm (d, J=4Hz). However, ^{1}H-^{1}H COSY NMR (Figure 2-20) showed that H-2 and H-1 of a sugar (3.97 ppm, 5.83pmm respectively) are coupled. Also H-2 appeared at 3.97ppm coupled to H-3 at 4.15 ppm.

The TOCSY spectrum (Figure 2-19) showed connections between H-1, H-2, H-3 (at 5.83 ppm, 3.96 ppm, 4.17 ppm) of the major glycoside compound. The HSQC spectrum (Figure 2-20) the H-1 at 5.83 ppm was coupled to C-1 at 92.7ppm, H-3 at 4.17 ppm linked to C at 73.3ppm. Although C-6 seemed to be CH_2-H or CH_2-OR, no linkage to carbons at 75 ppm or 62 ppm nor coupling to protons at 4.43 ppm or 4.45 ppm could be observed. Moreover, 1-6 linkage of sugars to form the expected polymer could not be confirmed due to disappearance of C-6 in this spectrum.

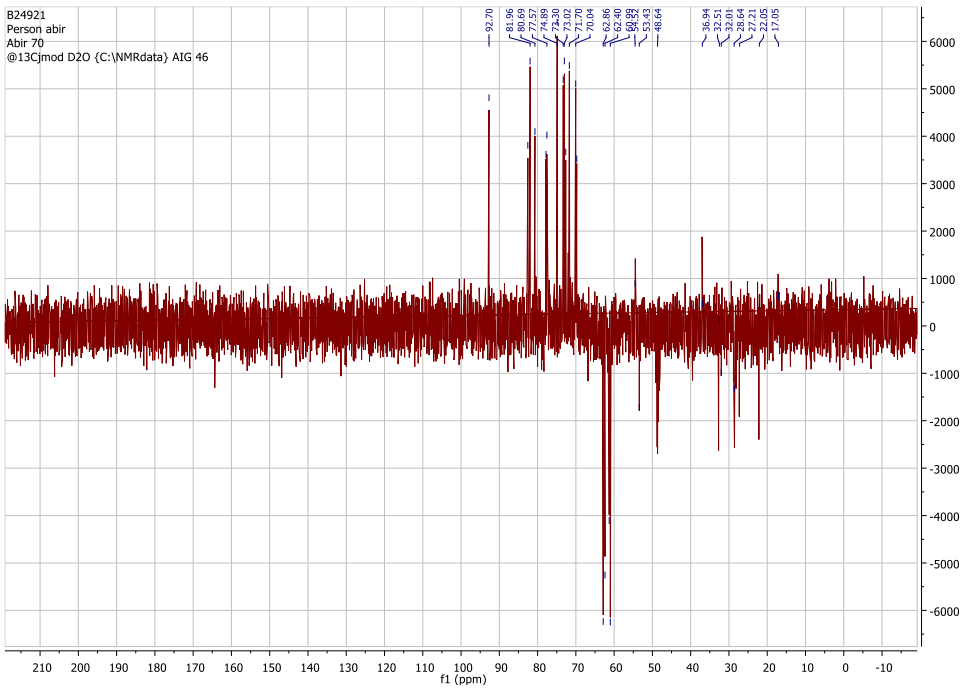

Figure 2-17^{13}C J-mod spectrum of hot maceration mucilage 70°C in D_2O at 400MHz.

Furthermore, the TOCSY spectrum (Figure 2-19) revealed a minor sugar with a doublet H at 5.37ppm and coupled to H-2 at 3.86 ppm linked to another proton at 4.21ppm (H-3) (Roslund *et al.*, 2008).

The HMBC spectrum (Figure 2-21) showed another compound (minor sugar) of which C-1 (82.6 ppm) was linked to two carbons at 73.2 ppm and 77.8 ppm (Omicron, 2014; Roslund *et al.*, 2008). One of these two carbons was the C5 of that sugar. Furthermore, H at 5.36 ppm was H1 and attached to carbons in the range of 69 ppm to 81 ppm and these carbons were not related to C6 of the sugar, but only C-2, 3, 4 of the minor sugar compound. Moreover, C-1 of this compound at 82.6 ppm was coupled to H-2 at 3.85 ppm, and another proton (H-4) at 4.21 ppm. The HSQC

spectrum (Figure 2-20) showed that this compound carbon at 77.6ppm was attached to H at 4.58 ppm directly while C at 74.7 ppm was directly attached to H at 4.43ppm.

The HMBC spectrum (Figure 2-21) showed a carbonyl atom at 146.9 ppm was coupled to an aliphatic chain proton at 3.06 ppm and 2.09 ppm in addition to the C-1 of the minor glycosidic compound at 5.36 ppm.

It was clear in the HMBC spectrum (Figure 2-21) that there was a chain of CH_2 with C-1 at 32.4 ppm, C-2 at 22.1ppm, and C-3 at 28.7 ppm. Additionally, C-3 of this chain ended up attached to CO from the minor sugar at 164.9 ppm. In other words, a sequence of CH_2 groups seemed to be attached in one row forming a side chain, in COSY NMR spectrum in Figure 2-18. This sequence was ended up with a carbonyl group attached via an ester bond to C-1 of a sugar compound. Additionally, the HSQC spectrum (Figure 2-20) revealed this sequence connection of CH_2 where C at 28.7ppm directly linked H at 1.72 ppm, while C at 22.1ppm directly attached to H at 2.09 ppm, and C at 32.5 ppm linked to H at 3.07ppm.

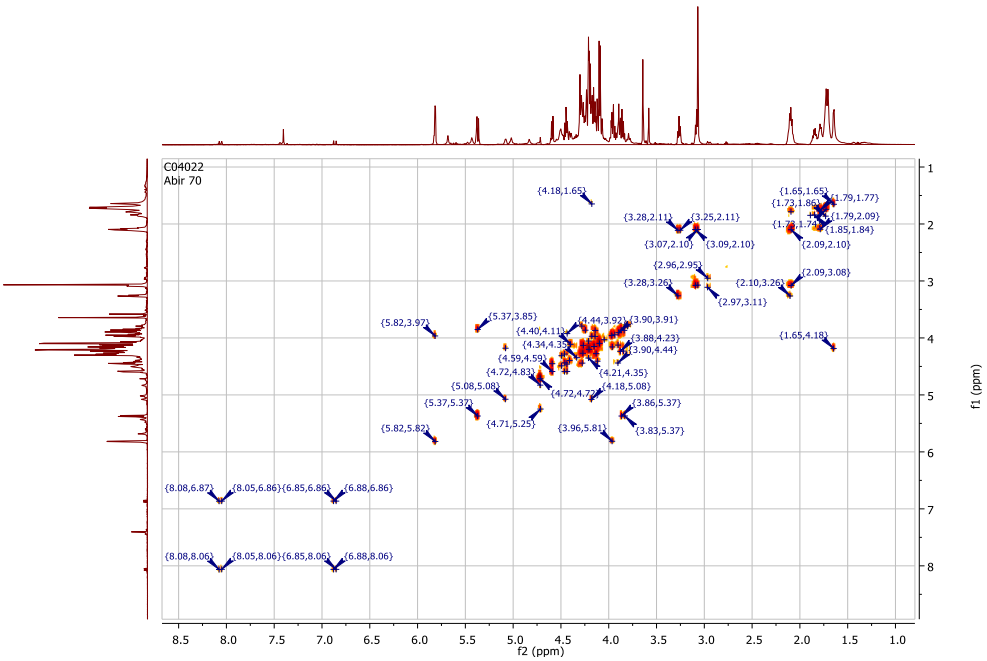

Figure 2-18. ^{1}H-^{1}H COSY NMR spectrum of mucilage of maceration 70°C in D_2O at 600MHz.

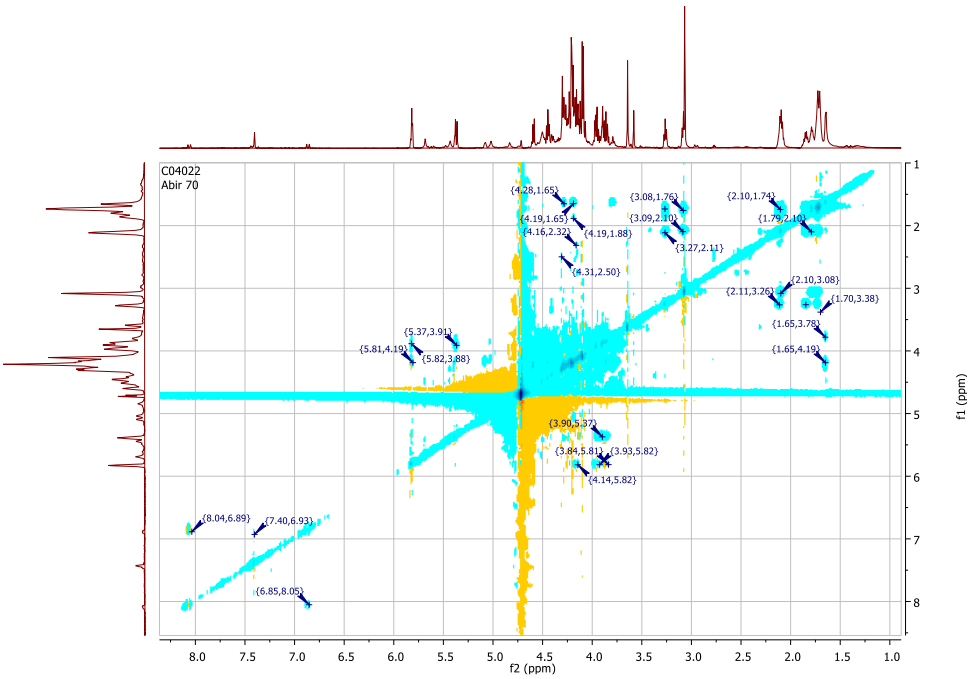

Figure 2-19 2D TOCSY NMR spectrum for mucilage hot maceration 70°C in D_2O at 600 MHz

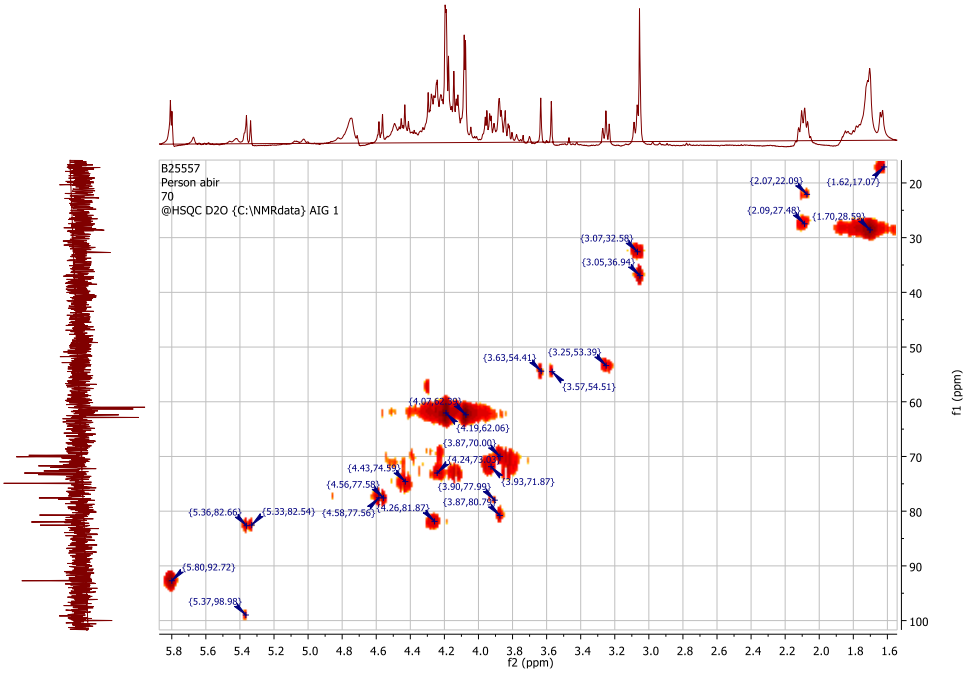

Figure2-20 2D HSQC NMR for hot maceration mucilage 70°C in D_2O at 600 MHz

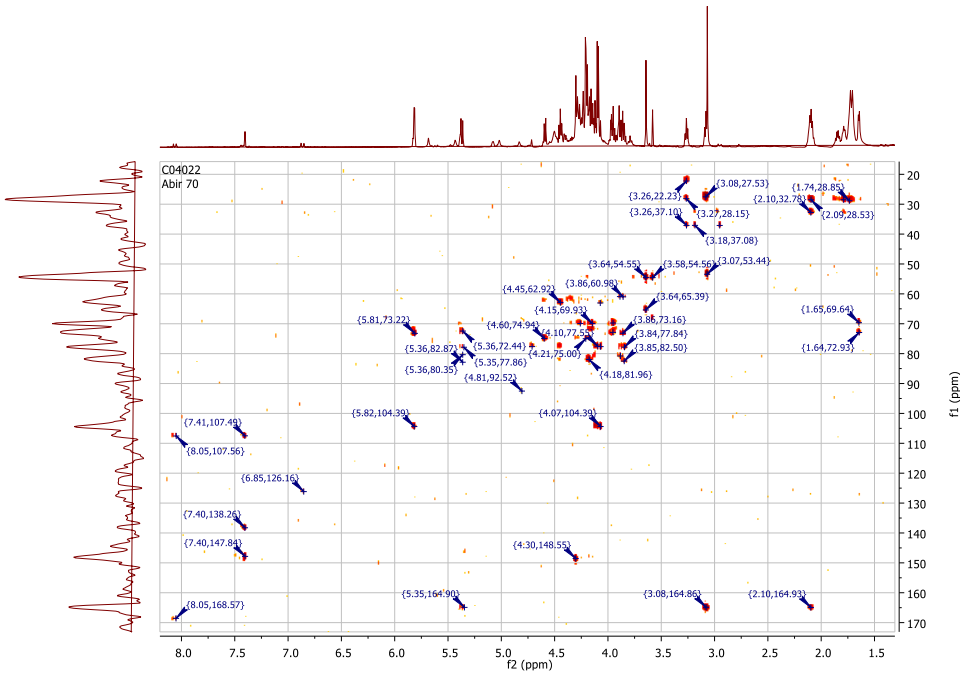

Figure 2-21. 2D HMBC NMR spectrum for hot maceration mucilage 70°C in D_2O at 600 MHz

2.4.6.2. NMR spectra analysis for mucilage 50°C-1h

Analysis of the 50°C-1h spectra helped in identifying rhamnose and uronic acid structures. The aromatic region that appeared in the ^1H NMR spectrum (Figure 2-16) for the mucilage 70°C, did not appear in the ^1H spectrum of mucilage 50°C-1h (Figure 2-22). Moreover, the CH_2 chain that appeared in the hot maceration mucilage 70°C sample did not appear in the hot maceration mucilage 50°C-1h sample.

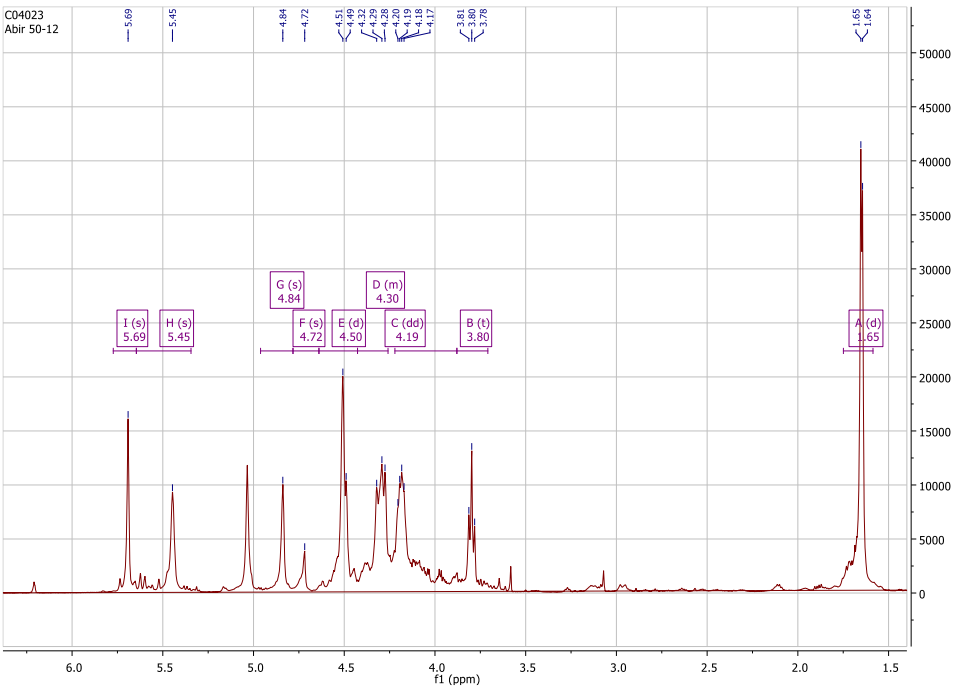

Figure 2-22. ^{1}H NMR spectrum for mucilage 50°C-1h in D_2O at 600 MHz

The ^{1}H-^{1}H COSY spectrum (Figure 2-23) showed protons at 1.65 ppm that could belong to the methyl group of the rhamnose (H-6) and linked to H-5 at 4.20ppm. These (H-6) protons appeared in the form of a doublet in the ^{1}H spectrum of mucilage 50°C-1hr sample in Figure 2-22. Also the 2D HMBC spectrum (Figure 2-24) for mucilage 50°C-1h showed a methyl (C-6) proton that appeared linked to C5 (69.5 ppm), and C4 (72.9 ppm). These findings were confirmed with the ^{1}H-^{1}H COSY spectrum of mucilage 50°C-1h that showed in Figure 2-23 that rhamnose H-5 at 4.20ppm was coupled to H4 of rhamnose at 3.80 ppm (Table2.7).

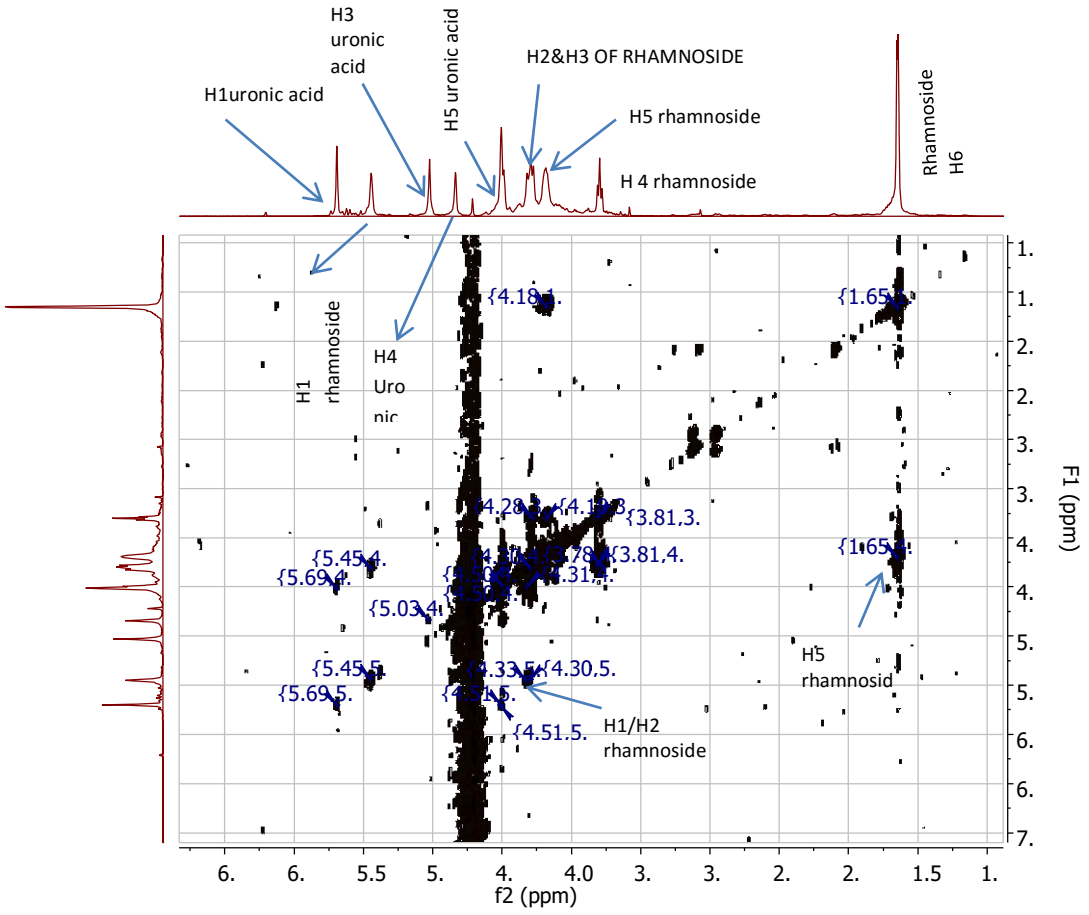

Figure 2-23. ^{1}H-^{1}H COSY NMR spectrum for mucilage 50°C-1h in D_2O at 600 MHz..

The HSQC spectrum (Figure 2-25) analysis showed that C1 was at 92.7ppm directly attached to proton at 5.81 ppm, H2 was at 3.96 ppm while H3 was at 4.15 ppm. Additionally the C6 was attached to CO and appeared for this reason at 164.9 ppm.

The HMBC spectrum in Figure 2-24 of mucilage 50ºC-1h revealed 1→3 glucuronic or galacturonic acid linkage to rhamnose (Ramos *et al.*, 1996). On the other hand,

uronic acid units were linked by 1-4 linkage through the coupling of H1 (5.70 ppm) and H4 (4.88 ppm). However, H3 of uronic acid was most deshielded. The HMBC NMR spectrum in Figure 2-24 revealed a coupling of C3 (72.1PPM) of uronic acid with H at 1.66ppm of a rhamnose. Furthermore, the COSY spectrum in Figure 2-23 showed few uronic acid groups linked to each other. It showed that H2 (4.8 ppm) of uronic acid was at 90° with H3 (5.03 ppm) while H4 (4.84 ppm) coupled with H5 (4.50 ppm). While the carbonyl group of carboxylic acid appeared at 174.9 ppm was with equatorial protons in HMBC spectrum in Figure 2-24.

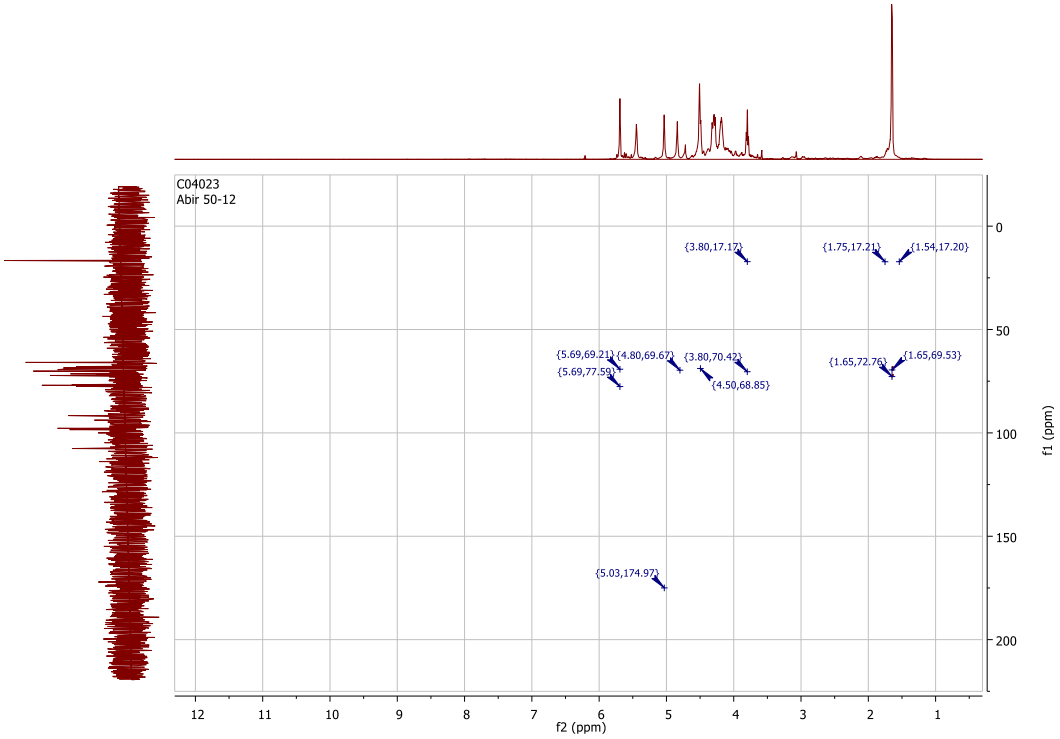

Figure 2-24. 2D HMBC spectrum of hot maceration mucilage 50ºC-1h in D_2O at 600MHz.

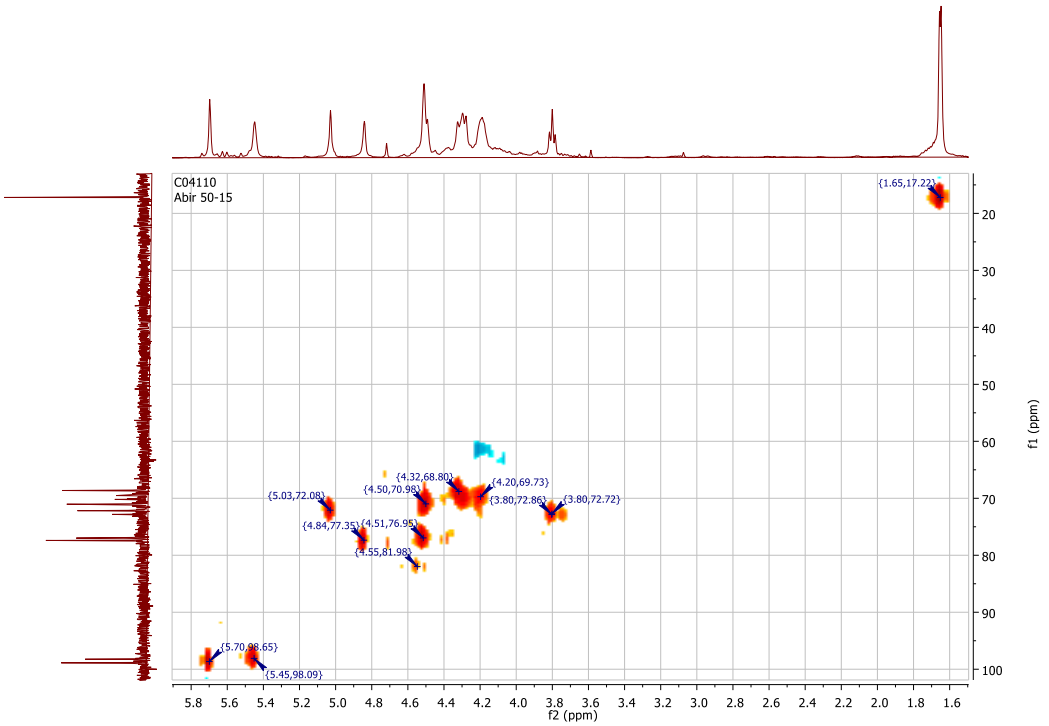

Figure 2-25. 2D HSQC NMR spectrum for mucilage 50°C-1h in D_2O at 600 MHz.

Table 2-7. Rhamnose $^{13}C/^{1}H$ chemical shifts

Position	5	4	3	2	1	6	-OMe
H δ(ppm)	4.20	3.80	4.29	4.32	5.45	1.65	3.30
C δ(ppm)	69.7	72.9	70.2	68.8	98.7	17.7	53.4

The HSQC spectrum (Figure 2-25) revealed that the carbon atoms and their linked protons for uronic acid as illustrated in Table 2-8. The analysis showed that C1 was at 92.7ppm directly attached to proton at 5.81 ppm, H2 was at 3.96 ppm while H3 was at 4.15 ppm. Additionally the C6 was attached to CO and appeared for this reason at 164.9 ppm.

Table 2-8. Glucuronate $^{13}C/^{1}H$ chemical shifts

Position	1	2	3	4	5	6
H δ (ppm)	4.8	4.5	4.84	5.03	4.51	5.7
C δ (ppm)	175.0	70.6	77.4	72.1	77.0	98.7

Using ChemoDraw 15 (PerkinElmer informatics) software to draw the structure of rhamanose, glucuronic acid utilising ^{13}C and ^{1}H assignments of rhamnose and uronic acid displayed in Table 2-7 and Table 2-8; the lactone ring of glucuronic acid was predicted. It was structured by intramolecular esterification of C6 carboxylic acid group with -OH group from C3 of uronic acid structure (Figure 2-26) through analysing HMBC spectra of hot maceration 50C-1h in Figure 24. The formed lactone ring then was found to be linked to the rhamnopyranosyl by 1→3 linkage to suggest the repeating unit of the extracted polymer in Figure 2-27 was rhamnoglucuronolactone units.

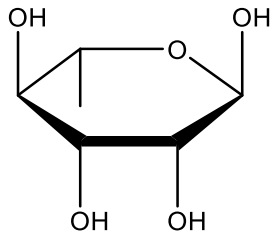

A

(2R,3R,4R,5R,6S)-6-methyltetrahydro-2H-pyran-2,3,4,5-tetraol (rhamnose)

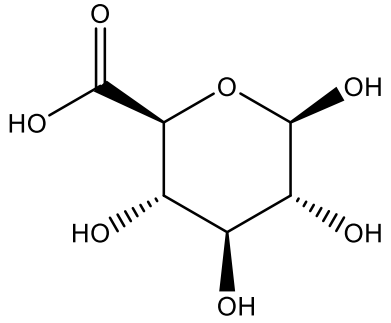

B

(2S,3S,4S,5R,6R)-3,4,5,6-tetrahydroxytetrahydro-2H-pyran-2-carboxylic acid (glucuronic acid)

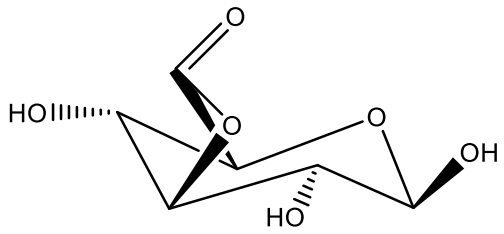

C

(3R,5S)-3,4,8-trihydroxy-2,6-dioxabicyclo[3.2.1]octan-7-one (glucurono-lactone)

Figure 2-26. The chemical structure of (A) rhamnose pyranosyl sugar; (B) glucuronic acid; (C) glucuron-lactone ring

The presence of the lactone ring in NMR would suggest that the mucilage consisted mainly of rhamnoglucuronolactone units shown in Figure 2-27 rather than

rhamnoglucuronic acid units and the appearance of the carbonyl group peak of carboxylic acid in the FTIR was just to confirm the findings.

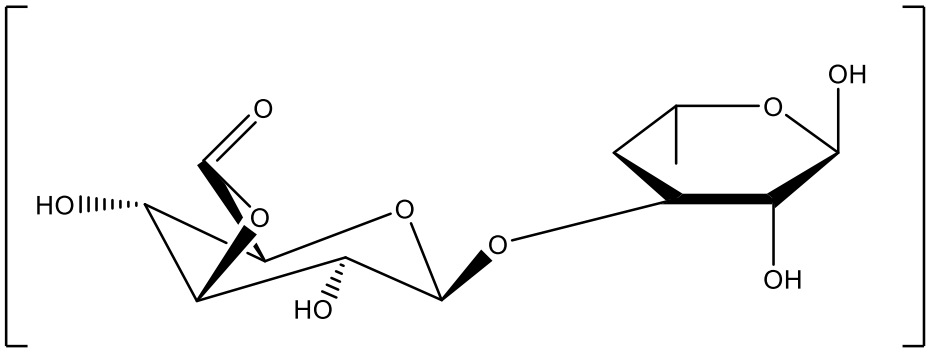

Figure 2-27. (3R, 5S)-3-(((2R, 3S, 6S)-2, 3-dihydroxy-6-methyltetrahydro-2H-pyran-4-yl) oxy)-4, 8-dihydroxy-2, 6-dioxabicyclo [3.2.1] octan-7-one. (Proposed repeating unit of the polymer).

It is the first time the structure of Shepherd's purse mucilage was elucidated and illustrated as shown in Figure 2-27.

2.5. Discussion

The purpose of the work in this chapter was to extract the polysaccharide polymer into the mucilage and to characterise the physicochemical properties of the mucilage polymer and to understand its behaviour and the effects of different conditions on its properties.

Determination of the monosaccharide composition of *A. thaliana* mucilage has indicated an abundance of rhamnose and galacturonic acid, suggesting the occurrence of rhamnogalacturonan components in addition to HG (Willats *et al.*,

2001). The presence of arabinose, and rhamnose in Shepherd's purse mucilage extracts would indicate the similarity between the two plants' mucilage. The findings of the colorimetric assays were in agreement with published literature (Aksoy *et al.*, 1998; Macquet *et al.*, 2007; Moser *et al.*, 2010; Slotte *et al.*, 2007 ; Walter and Taylor, 2012; Willats *et al.*, 2001). It was reported by Windsor and colleagues that *A. thaliana* mucilage is closely related to Shepherd's purse species and that the mucilage component was mainly a pectic polysaccharide, composed of rhamnose and galacturonic acid, confirmed by ruthenium red stain, though the structure and chemical linkage of the units were not determined (North *et al.*, 2014; Windsor *et al.*, 2000). Macquet *et al.* (2007) successfully isolated the sugars from the mucilage of *A. thaliana* using enzyme hydrolysis and identified rhamnose and galacturonic acid which formed >90% of a water extracted mucilage. They also suggested that the presence of unbranched RG1 was due to the powerful degradation effect of rhamnogalacturonan hydrolase enzyme which was present in the cell wall membranes (Macquet *et al.*, 2007). Ruthenium, calcoflour and anti-pectin antibody staining studies suggested that the outer layer of mucilage consisted of water soluble unbranched non-esterified RGI, while the inner mucilage is mainly moderately esterified RG I, cellulose, and less abundant highly esterified HG. Deng *et al*. (2015) indicated that Shepherd's purse mucilage was 25% of the dry mass of seeds and rhamnose and galacturonic was >95% (w/w) of total sugars. Therefore, it was believed that all extracts contained the pectic polysaccharide of Shepherd's purse seeds.

The literature suggested that the Shepherd's purse mucilage was composed mainly of pectic carbohydrate polymer. Different methods were used to extract the mucilage from Shepherd's purse seeds' coat. Depending on the solubility of pectin into water and different studies on water imbibition during seed germination, water was the major solvent to extract the mucilage from the seed coat. The first extraction method was a simple method relying on water absorption into the seeds at room temperature under continuous stirring. Other types of solvents were used to compare their ability to extract the mucilage without extracting other compounds present in the seed. Solvent maceration was believed to extract all the fatty acids in the seed coat by hexane before macerating the seeds with water. Furthermore, hot maceration was believed to inactivate any enzymes such as rhamnogalacturonan hydrolase enzyme which was secreted with the mucilage during extraction. However, heat is known to affect pectin (Novosel'skaya *et al.*, 2000), therefore different temperatures (40°C, 50°C, 70°C) were used to examine the mucilage and any possible effect the temperature would exert. Furthermore, the combined effect of different solvents with temperature was examined through hot reflux, where the seeds were extracted by hexane followed by ethyl acetate, then methanol before methanol-water and finally water at 40°C. The different extracts were collected and underwent comparison studies of the physical and chemical characteristics in order to find the ideal extraction method.

The different extracts were examined by colorimetric assays to detect the presence of carbohydrates and pectin. The phenol-sulphuric acid test for sugars showed that all the extracts contained rhamnose and arabinose sugars, while the carbazole test

indicated the presence of uronic acid. These two compounds present in the mucilage were indicators of pectic polysaccharide. These findings confirm literature review findings. However, the carbazole test is very sensitive to uronic acid and able to detect 1µg of uronic acid; it had a limitation of interference of neutral sugars extracted from the cell wall. These neutral sugars were galactose, arabinose, and rhamnose which were the residues branched from the uronic acid of the pectin backbone. It was cited in the literature that adding potassium sulfamate would reduce the interference considerably (Filisetti-Cozzi and Carpita, 1991). Alternatively M-biphenyl assay could have been used to avoid the interference and to quantify the uronic acid.

Further analysis of the mucilage was aimed at identifying the DE of the pectic polysaccharide with FTIR. The DE was important to understand the viscosity, the gelling properties and the hydrodynamic characteristics (Morris *et al.*, 2000). Examining the FTIR spectra obtained from the extracts compared with standards resulted in defining peaks at different regions. Each FTIR spectrum was divided into three different regions. Lower DE (<50%) pectin would form a weak gel; in contrast, high DE pectin (>50%) would form a strong gel.

The first region between 3500-1800 cm^{-1} which showed the O-H centred at 3370cm^{-1} and C-H of O-CH_3 groups at 2925 cm^{-1} which was masked by the O-H group (Gnanasambandam and Proctor, 2000).

The second region was 1800-1500 cm^{-1} which was of great importance as it allowed the observation and measurement of carboxylic acid and ester group absorption and subsequently identifying the DE of standard pectin. In order to utilise FTIR spectroscopic results to monitor the structural changes in extracted mucilage with respect to carboxylates, all the examined samples of extracts were found that they did not show any absorption in the region of 1700-1780 cm^{-1} which corresponds to the absorption of the ester carboxyl group. On the other hand, the ester carbonyl group would appear solely at the region of 1780-1740 cm^{-1} (Navarro *et al.*, 2009). While the peaks that appeared in the 1620 and 1415 cm^{-1} were thought to belong to the non-esterified carboxylic group (Manrique and Lajolo, 2002). These peaks correspond to the stretching and vibration of aliphatic carboxylic acids in their anionic form (Chatjigakis *et al.*, 1998; Manrique and Lajolo, 2002; Monsoor *et al.*, 2001).

A third region below 1500 cm^{-1} was the 'fingerprint region'. The examination of absorption in this region revealed similarity between different spectra of mucilage samples. This region was believed to be unique for each compound as it represented the different molecules and the structure of the compound (Stewart and Morrison, 1992).

Moreover, an absorption band attributed to amides was believed to be a result of the effect of heat during extraction for an extended time. It appeared in the extracts of hot maceration 50°C-2 h, hot maceration 40°C-2h, hot maceration 70°C, and hot reflux.

The FTIR analysis indicated the same compound was extracted by all the different methods. The inability to detect the ester carbonyl absorption band in the spectra of all the extracts and all peaks appeared to be consistent with the findings of Monsoor *et al.,* (2000) when analysing polygalacturonic acid led to a conclusion that it was a polygalacturonic acid than esterified pectin.

To understand the properties of the extracted mucilage and its suitability for further use in drug delivery and stability, its water adsorption characters were examined by DVS to show water vapour sorption properties and its effect on mucilage structure and behaviour. Basically, Shepherd's purse mucilage showed vapour uptake characteristics that ranged from 50-70 % for most extracts except for solvent maceration which had very low vapour sorbent and absorbed from atmosphere 32% of its dry mass. In contrast the hot maceration 40°C-1h extract absorbed water vapour equal to 80% of its dry mass.

Crystallisation occurred in the water extracted mucilage 25ºC in the beginning of the first cycle of DVS which was a clear sign of instability of the mucilage in a low percentage of RH (Agrawal *et al.*, 2004). The water absorbed from the moisture provoked structural rearrangement and led to crystallisation, especially the compound that was in amorphous form as stated in the literature (McFeeters, 1985; Sebhatu *et al.*, 1997). These changes where similar to changes that occurred with a microcrystalline cellulose studied by Agrawal *et al*., (2004).

The DVS chart for the 40°C-1h extract showed that the sample retained 0.72% of the RH taken up in the sorption phase. It was also clear that the initial weight change from the first cycle was gradual until a conformational change occurred that was permanent and did not appear in the sorption phase of the second cycle (Hammer *et al.*, 2013).

All the extracts were slow in moisture uptake from the atmospheric vapour, though some including hot maceration 40°C-2h, hot maceration 70°C, solvent maceration, hot maceration 50°C-2h underwent permanent changes. Furthermore, only the DVS charts of the water maceration and hot maceration 40°C-1h mucilage showed instability of the polymer matrix which tended to occur at relatively low humidity. These findings indicate that the mucilage would absorb a huge amount of vapour water at the nasal cavity and it would swell. However, this property would dissolve the enclosed drug and would help water soluble drugs diffuse out of the drug delivery system, but would not help other types of drugs similarly.

The findings of vapour sorption led to further studies to examine the thermal stability of the mucilage by TGA and DSC. Importantly, TGA curves allow detection of decomposition, loss of water for crystallisation, combustion, oxidation reactions, vaporisation, evaporation, sublimation desorption and drying as weight loss. However, chemical reaction with gaseous substances in pure gas such as O_2, N_2 with formation of non-volatile or barely volatile, or from physical transition by gas adsorption such as active charcoal are detected as weight gain (Widmann, 2001).

The TGA curve of Shepherd's purse water maceration mucilage 25ºC showed a slow gradient moisture loss occurred in the same sample from room temperature to 140ºC followed by decomposition with formation of gaseous products after 240ºC accompanied with a weight loss of 44.7% at 300°C and a formation of a black charred residue constituted 55.3% of starting mass, these changes were reported in relation to pectin thermal analysis (Einhorn-Stoll *et al.*, 2007). This indicated the thermo-liability of the moisture at low temperatures and the relative instability of the dried polymer as the temperature rose to 240°C (Jörimann *et al.*, 1996). The charred residue was left from decomposition of organic hydrocarbons at moderately high temperature (Widmann, 2001). While heating another mucilage sample of water maceration 25ºC extract from 25ºC to 150ºC at a rate of 10ºC/min showed that mucilage lost 4% of its weight which is a result of moisture release and gas desorption. Heating Shepherd's purse mucilage below 200ºC was more suitable to study phase transitions and changes in the heat capacity before any decomposition (Einhorn-Stoll *et al.*, 2007). The mucilage showed that it lost its moisture at moderate temperature (27°C- 40°C); therefore, the storage of the mucilage needs to be kept away from heat (over 30°C) in order to prevent any changes.

The enthalpy relaxation that occurred in the DSC thermograms of all the mucilage extracts masked any possible glass transition and drying from appearing in the spectra. Hammer (2011) suggested that relaxation enthalpy coexists with glass transition and always looks as an overlapping endothermic peak especially. He also proposed this peak appears as a wider peak when the sample is stored for a long time under temperatures below the glass transition temperature (Tg) (Schawe *et al.*, 1999).

Schubnell (1998) suggested that scanning any new material would essentially involve pre-treatment which means heating the sample to eliminate relaxation (Hammer, 2010). As glass transition is reversible, physical transition for amorphous material and can be removed by quench cooling to eliminate the material thermal history (Hammer, 2011). Therefore the quench-cool method was suitable to scan the extracted mucilage for its physical and thermal properties.

The DSC thermogram of the water maceration mucilage 25ºC undergoing the quench-cool method showed an endothermic peak corresponding to drying which started at around 50°C and its extrapolated peak was at 100°C. The drying peak for solvent maceration mucilage had an extrapolated peak at 70°C and started at 37°C. These findings suggested that the adsorbed moisture was easily released and vaporised at 40°C. This peak accounts for the thermal instability of the mucilage (Einhorn-Stoll *et al.*, 2007).

It was important to note that most extracts showed the same DSC thermograms except hot reflux mucilage. The hot reflux extracted mucilage was the only extract that showed two endothermic peaks at 166°C and 192°C subsequently these were not investigated further. Einhorn-Stoll studied the thermal analysis of chemically and mechanically treated pectin and pointed out that the preparation techniques and use of solvent could cause structural modifications and changes detected by thermal analysis (Einhorn-Stoll *et al.*, 2007). The two peaks were believed to show changes triggered by increased temperature up to 200°C. Therefore, the hot reflux method would not be a suitable method for the extraction of Shepherd's purse mucilage.

Importantly, all mucilage extracts showed crystallisation at 17°C. The crystallisation temperature was counted as low stability of the mucilage at room temperature. Furthermore, the heat needed for crystallisation was 3.60 Jg^{-1} and this indicated that the mucilage was present in amorphous form and changed the form at low temperature and low RH.

As vapour sorption studies found the mucilage was hugely water sorbent and the findings of the DSC studies revealed that mucilage crystallises at low temperature, the measurements of bound water was essential for the development of this potential drug delivery system. Measurement of bound water was used to measure the amount of water absorbed into and bound to the structure of the extracted mucilage. There were different types of water present in the polymer-water systems of the extracted mucilage. They were type I water which was unbound to the polymer and available for freezing, type II was partially bound to the polymer and available for freezing, while type III was tightly bound and not available for freezing (Ford, 1999). Knowing these waters and their interactions with the polymers, unveil the polymers' behaviour and drug release properties. All the kinds of water adsorbed and absorbed into materials were described previously. Any loss of this moisture during scanning would result in different Tg than the original. All the extracted mucilage by different means showed smilarity in adsrobing water from the enivronmnet and behaving as a sponge able to bind over 50% of the available water in direct contact within the mucilage polymer. This measured water counts for type III of water. However DVS measurements showed that Type I of water which is adosrbed on the surface of the

molecules and it reached 70% of the dry weight of mucilage from all extracts. Nokhodchi *et al*., (1997) explained the process of water sorption and binding with HPMC They described the water adsoped from the atmoshpere as the moisture vapour adsrobed onto the surface of the molecules. This water is arranged in monolayer on the surface and contributes to the adhesion properties of the molecules (Nokhodchi *et al*., 1997). This water can be difussed inside the molecule and bind tightly to the molecule structure and cause physical phase changes such as the cystallisation.

In depth understanding of the structure and chemical composition of polymer extracted from the mucilage was conducted by different NMR experiments. The NMR spectra of all extracts were examined and found that all the extracts were a mixture of different sugar compounds, which were overlapping and shielding each other. Tracing the coupling and elucidating the structure of small compounds in a mixture of compounds was quite difficult due to overlapping of the chemical shifts of the similar protons in NMR spectrum. NMR analysis of hot maceration 70°C showed that an aromatic compound was released with the polysaccharides. The aromatic compound detected in the NMR was not part of the polysaccharide. The same compound was seen in the NMR spectra of hot reflux mucilage. It was believed that reaching 70°C and the use of different solvents during extraction triggered the release of the aromatic compound from the inner layers of the seed coat. NMR spectra of hot maceration 70° C could not be analysed further due to the presence of a mixture of compounds with close chemical shift protons and carbons. The NMR analysis of 50C-1h mucilage revealed that the polygalacturonic acid tended to form

lactone ring through ester bonding between C6 and C3 of the same molecule. The rhamnopyranosyl residue was attached to the uronolactone ring by 1→3 linkage to form the repeating units of the polymer.

2.6. Conclusion

Different methods were used to extract the mucilage from Shepherd's purse seeds' coat. They were water maceration, solvent maceration, hot reflux, and hot maceration. In comparison, Shepherd's purse mucilage resembled that of *A. Thaliana* as described in literature in its chemical composition.

The colorimetric assays found the extracted mucilage consisted mainly of rhamnose and uronic acid. All assay and experiments found that the different extraction methods extracted the same polysaccharide. Therefore, the use of solvents or heat for extraction would not change the chemical composition of the pectic polysaccharide in the mucilage.

FTIR analysis also showed that the different extraction methods isolated the same compounds and all the extracts did not resemble standard pectin as they lacked the presence of esterified carbonyl groups and therefore they were not an esterified pectic polysaccharide. In other words, the mucilage was polygalacturonic acid.

The DVS analysis revealed that all the extracts had water sorbent properties and they were able to adsorb vapour moisture from the atmosphere equal to 50-70% of their dry weight. The mucilage would absorb water vapour from the nasal cavity and this

water would penetrate the structure of the mucilage and would cause the mucilage to swell and dissolve incorporated drugs.

The thermal analysis showed that the mucilage polymer was heat sensitive and drying its moisture started from 40°C. The presence of moisture in the structure of the polymer affected the glass transition and crystallisation temperature. The glass transition measured for all mucilage extracts occurred at the same temperature which was 17°C with very small value of heat (3.87 ± 1.73 Jg^{-1}) need for such a change. Furthermore the DVS data revealed that the mucilage is able to crystallise at relative low humidity. This Tg temperature is very low for such change, and thereby Shepherd's purse mucilage is an unstable material that changes from amorphous state to the crystalline state at temperatures below the room temperature even if at low humidity. This property could be a disadvantage and contribute to the instability of drug delivery system at the room temperature.

The water binding affinity of the polymer is very strong. All mucilage extracts, irrespective of method of extraction, were able to bind around 50% of water available from the surrounding atmosphere. Comparing DVS data to the water binding efficiency of Shepherd' purse mucilage showed that the mucilage was capable of adsorbing vapour moisture from 50% to 70 % of the mucilage dry weight.

All the extracts contain a mixture of different sugars and other compounds, which were overlapping and shielding each other in NMR. The major components of the mucilage were believed to be rhamnogluc/galacturonic acid units. Rhamnose was a

major sugar linked to the uronic acid through 1→3 linkage. Furthermore the uronic acid tended to form a lactone ring through intramolecular linkage. The formation of this lactone ring would be the reason of the disappearance of the esterified carboxylic acid peak in the FTIR.

In conclusion, a polysaccharide polymer was successfully extracted from Shepherd's purse seeds' coat that was mainly composed of rhamnose and uronic acid and resembling polygalacturonic acid in composition. It was identified as thermo-unstable with great water binding ability.

Comparing the mucoadhesion properties of different extracts will help in choosing the best extract. Therefore, the next chapter studied the mucoadhesion properties of the different extracts along with their surface properties (including surface roughness).

Chapter 3 Mucoadhesion Study

3.1. Introduction

A variety of polymers have been tested and evaluated for their use as mucoadhesives to different sites e.g. HPMC K4M is used with artemether (antimalarial) nasal *in situ* gel; gelatine-chitosan microspheres have been used to deliver clonazepam (antiepileptic) to the brain via the nasal route; hydroxypropylcellulose mucoadhesive *in situ* gel has been used for nasal delivery of ondansetron (antiemetic) ((Duchêne and Ponchel, 1997; Mahajan *et al.*, 2011; Shaji *et al.*, 2009).

The nasal mucus membrane is a layer of connective tissue covered by an epithelial layer, which is kept moist with mucus secreted from specialised cells or glands present in the connective tissue and called goblet cells (Orahilly *et al.*, 2008). The main constituents of mucus are glycoproteins, lipids, salts and water in which mucus becomes either a gel-like or soluble or suspended form (Marieb, 2003).

The nasal mucosal clearance rate discussed in section 1.3 is a limiting factor when administering drugs to the nasal cavity, especially for controlled release dosage forms or drugs for systemic effect. The nasal cavity is a good site for administering drugs targeting the brain because of its large surface area, bypassing first pass metabolism and rich vascular blood supply.

Scientists have studied and described how mucoadhesion occurs in stages starting between the mucoadhesive surface of the polymer and the mucus with intimate

contact by wetting or swelling of the mucoadhesive surface (Kharenko *et al.*, 2008; Khutoryanskiy, 2011; Ponchel *et al.*, 1987). This is followed by penetration of the polymer chain into the tissue or merging of the polymer and the mucus (Sriamornsak *et al.*, 2010; Tamburic and Craig, 1997). The theories, which were developed to understand and explain the performance of adhesives, have been adapted to gain an understanding of mucoadhesion (Roy and Prabhakar, 2010).

Atomic force microscopy (AFM) is a newly developed technique that is very sensitive to changes on the surface of a material under study (Acton, 2012). As mucoadhesion is a surface force that attaches two materials, it is possible to apply AFM to measure any changes on the surface of mucus due to the adhesion force (Joergensen *et al.*, 2011). Various cantilevers for the AFM enable different measurements of surface properties. SCANASYST-AIR-HR probe with 2° cantilever bend is very sensitive to any changes on the scanned surface and is able to measure every point of that surface. The adhesion force is measured as a function of the force needed to detach the two adherent particles. The stronger the adhesion, the greater the power needed to detach both particles (Le *et al.*, 2013).

3.2. Aims and Objectives

The aims of this study were to scrutinise the suitability of Shepherd's purse mucilage for bioadhesion and to compare it to HPMC K100 and standard pectin in order to develop a suitable bioadhesive drug delivery system. HPMC was chosen as it is widely studied for its mucoadhesive properties and there was abundant literature citing its characteristics.

The objectives of this chapter were to get images of the mucilage-mucin interactions and to study the surface properties of both mucilage and mucin and to compare the adhesion properties of extracted mucilage with standard pectin and HPMC K100.

3.3. Methods and Material

3.3.1. Material and Equipment

- Mucin from porcine stomach (type III bound sialic acid 0.5-1.5%) lot number 020M7011V and sodium chloride (analytical reagent grade) lot number 10370 were purchased from Sigma-Aldrich; apple pectin (meets USP xxiii) lot number 67H16351was purchased from Sigma;
- HPMC K100 LV (lot number KK08012N2) was obtained from the Dow Chemical Company;
- De-ionised distilled water was prepared in-house.
- Mica sheets (G250-1) were obtained from Elektron Technology
- SCANASYST-AIR-HR cantilevers for MultiMode 8 were obtained from Bruker.
- Bruker MultiMode with NanoScope IIID Controller Scanning Probe Microscope (Digital Instruments), USA

3.3.2. Sample preparation

The method was adapted from Joergensen *et al.* (2011) and performed using a Bruker MultiMode with NanoScope IIID Controller Scanning Probe Microscope operated using the new Peak Force QNM mode. Samples were deposited onto mucin

coated freshly cleaved mica. AFM measurements were carried out in air in the contact mode using SCANASYST-AIR-HR cantilevers for MultiMode 8 (v≈130-160 kHz, k≈0.4-0.6 N/m), and the spring constant t (Nominal 0.4 N/m) and deflection sensitivity was calibrated, but not the tip radius (the nominal value has been used; 2 nm). AFM images were collected from two different samples and at random spot surface sampling (at least five areas per sample). Instrument control and image acquisition was performed using the Nanoscope analysis software (v5.3.3). The quantitative mechanical data was obtained by measuring DMT modulus/Pa using Bruker NanoScope software Version 6.14r1 (NanoScope Analysis).

Mucoadhesion of the polymers to mucin coated mica sheets was examined using AFM. Firstly, freshly cut mica sheets (approximate size 100 mm^2) were loaded with 100µL of 2.00 wt% mucin dissolved in 12.5mM NaCl was placed on each of the mica plates and left to dry for 24h at ambient temperature (Joergensen *et al.*, 2011).

To ensure uniformity between all mucin coated mica sheets, a first scan was performed in air 24h after all the solvent had been evaporated off. A second scan with the AFM under wet conditions was performed after rehydration of the pre-coated mica with 500µL of pure water. Subsequently, 100µL of the test polymer was placed on the pre-coated mica sheet for 10 min (incubation period) followed by repetitive washing (10 x 500 µL) with water. The concentrations used were 0.001 wt% for standard pectin, while for the HPMC K100, and mucilage, the concentration was raised to 0.010 wt% in order to maximise the effect. It is important to keep the samples wet therefore there was 100 µL of water left on the coated mica sheet to

keep it hydrated. Instantly the sample surface was scanned again in several places by AFM to detect changes in the sample topology caused by the mucoadhesion of the polymer during the incubation time.

It was impossible to probe the same point and to scan it through the whole experiment. Moreover, adhesion could not be concluded from the images without calculations therefore three different points were chosen for calculations and measurements randomly.

Roughness and adhesion force parameters were taken for all images using Nanoscope software. Arithmetic average roughness (R_a) of the absolute values and peak height upon adhesion towards the surface were considered.

3.3.3. Statistical Analysis

The roughness data were analysed using a Student's unpaired t test (Minitab version 17). A value of $p \leq 0.05$ was considered statistically significant.

3.4. Results

AFM topographic images and images of the slides are shown in Figure 3.1 for all samples and standards.

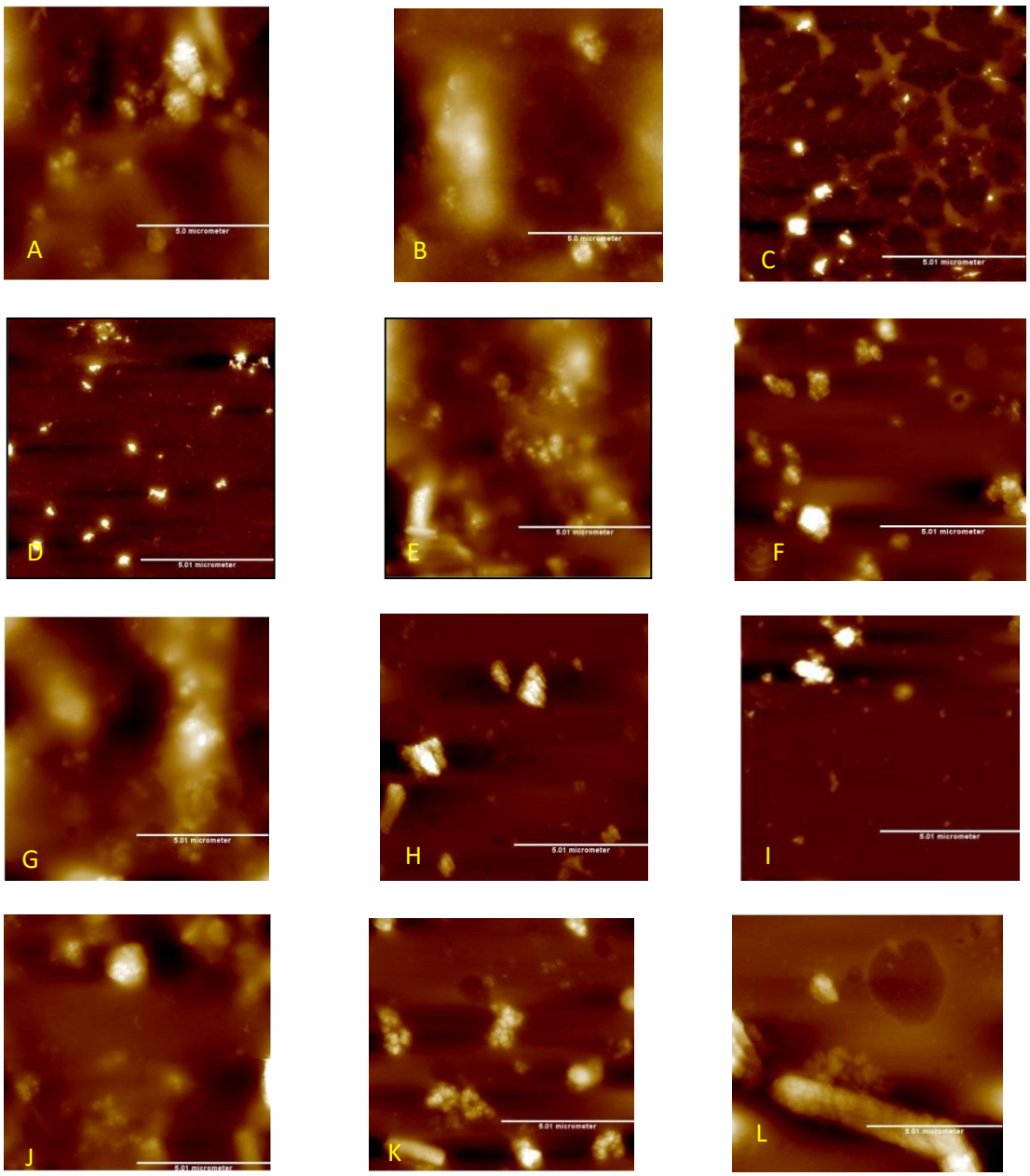

Figure 3-1 AFM topography images (the scale=5.01 µm): A) Control surface of mucin covered mica ; B): rehydration of the mucin covered mica sheets; C) mucilage from hot maceration (50ºC-2h); D) HPMC K100LV; E) Std Pectin; F) Water maceration 25ºC; G) Hot reflux mucilage; H): image of Solvent maceration; I) Mucilage from hot maceration (40ºC-2h); J): Mucilage from hot maceration (50ºC-1h); K): Mucilage from hot maceration (40ºC-1h); L): Mucilage from hot maceration (70ºC).

Comparing the roughness data for the dry mucin on mica with the hydrated mucin coat in Table 3.1 confirmed that the hydration of mucin coating was effective in providing an adhesive surface to the polymers later in the experiment. However, there was no significant difference ($p>0.05$) in surface roughness between steps 1 and 2 of the experiment, and it is believed that the water made the mucin swell and become dispersed on the mica providing a smoother surface to interact with the experimental substance (Proust *et al.*, 1984).

Table 3.1 Roughness and adhesion parameters for the blank mica-mucin in both the dried stage and hydrated step, along with the HPMC K100 LV, and Standard Pectin measurement.

Polymer	**Roughness (R_a) nm ± SD**	**Adhesion force (nN) ± SD**
Step 1 (dried mucin on mica)	29.01±12.05	0.80±0.50
Step2 (rehydration of mucin coated mica)	19.99±16.78	2.30±2.92
HPMC K100	10.28±13.80	2.36±1.30
Standard Pectin	27.67±10.42	1.39±0.64

The roughness parameter (Ra) for mucilage hot maceration 50°C-2h in Figure 3.2 was 12.41±1.4 nm which was smaller than the blank mucin coating Ra (19.60±16.7 nm). Furthermore, the adhesion force shown in Figure 3-3 for mucilage hot maceration 50°C-2hr was 1.16±1.4 nN and smaller than standard pectin measured adhesion force 1.33±0.6 nN. In contrast, mucilage extract hot maceration 40°C-2h adhesion force was 5.33 ±1.85 nN and hot maceration 40°C-1h and 50°C-1h had the same adhesion force which was 3.50±2.7nN. The hot maceration 40°C-2h mucilage showed the roughest surface in all measured extracts of Ra 65.62±23.4 nm. The increased roughness means less interaction with the surface and reduced adhesion.

The graph in Figure 3.2 showed the quantification of roughness measured as the root mean square for all the Shepherd's purse extracts compared with standard pectin and HPMC K100.

Solvent maceration mucilage had a smoother surface (Ra =17.74±8.6 nm), relatively to hot reflux mucilage Ra (25.02±3.9 nm) and standard pectin Ra (27.66±13.8 nm), but solvent maceration mucilage showed stronger adhesion (3.99±2.8 nN) than standard pectin (1.33±0.6 nN) and less force of adhesion than the hot reflux mucilage (6.77±4.8 nN).

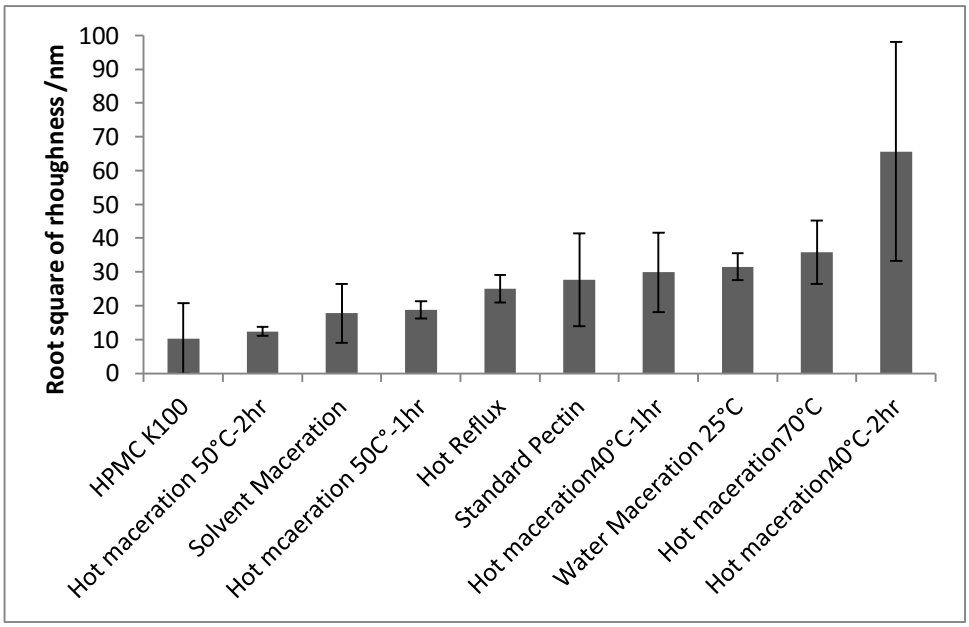

Figure 3-2 Arithmetic average roughness measurements of mucilage extracts compared with standard pectin and HPMC K100 (n=3). Each bar represents the mean of 3 readings ±SD.

The adhesion force for all extracted mucilage samples and the standards were measured using Nanoscope software and they were illustrated in Figure 3-3.

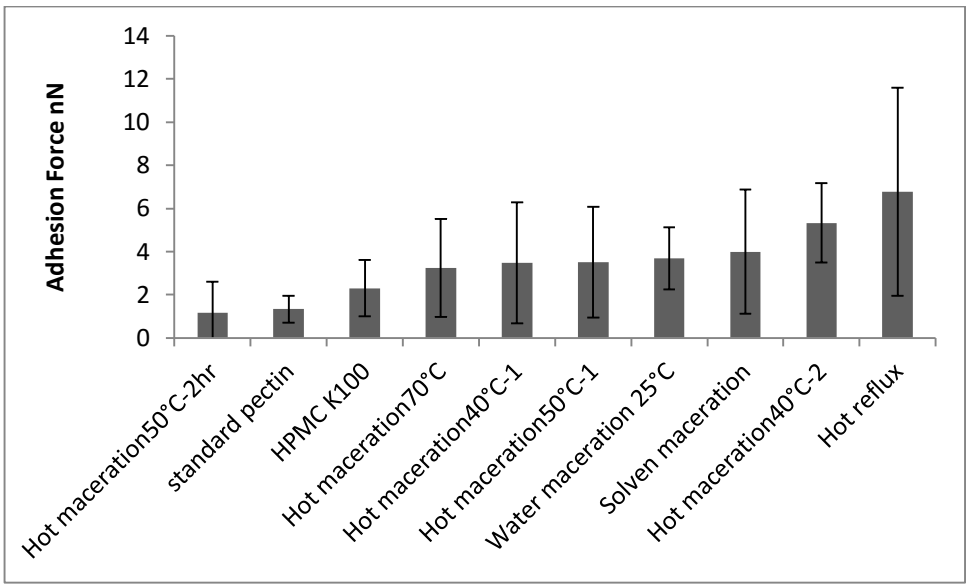

Figure 3-3 The adhesion force (nN) of different mucilage extracts, HPMC K100 and standard pectin to mucin (n=3). Each bar represents the mean of 3 readings ±SD.

The arithmetic average roughness and adhesion parameters of mucin coated mica sheet before and after hydration was measured and displayed in Table 3-1 for comparison with HPMCK100 and standard pectin data.

3.5. Discussion

Mucin mainly consists of a protein backbone and oligosaccharide side chains which makes it dispersible in aqueous medium at pH 7, while in acidic pH it forms a gel (Sriamornsak *et al.*, 2010). During preparation, mucin was dispersed in 12.5mM NaCl, which has a neutral pH, to get a mucin solution that could cover the whole mica sheet uniformly. When the freshly cleaved mica sheets were covered with mucin solution and solvent evaporated they were checked microscopically. To confirm coating was uniform, surface roughness was measured for the mucin-coated mica sheets. The step one of dried mica-mucin and step two of hydrated mucin

images showed similarity in the measured surface roughness mucin under AFM. When mucin was hydrated in step two, scattered white spots and clumps of mucin on the mica appeared ranging from 1.75μm to 4.46 μm radius. The light areas indicated more concentrated spots of mucin, while the black areas showed a thin layer of mucin. It was suggested that mucin fibres were extended filamentous molecules in dry form which when hydrated went into conformational changes and formed isotropic coils and were swollen in the water (Deacon *et al.*, 2000). Therefore, they appeared as bigger clumps under the microscope and the adhesion force of mucin coated mica increased in step 2. The rehydration step of mucin provided suitable conditions for the polymers under examination to attach to mucin.

When mucilage and HPMC K100 were applied onto the mucin-mica sheets followed by washing, scans showed large white spots of all the Shepherd's purse mucilage extracts (1.75 μm to 4.70 μm radius) compared with HPMC K100 (0.65μm to 1.70 μm radius). Shepherd's purse mucilage extracts did not spread evenly on mucin while HPMC K100 images showed small white spots scattered on a dark uniform background. The measured arithmetic roughness average in Figure 3.2 of HPMC K100 showed a smoother surface, and a thin layer of HPMC K100. The HPMC K100 did not attach strongly to the mucin and that was indicated in Figure 3.3 by the adhesion force.

According to the standard pectin on mucin AFM image, large clumps (1.20μm to 3.50μm raduis) were observed and the measured Ra of the standard pectin was higher than for HPMC K100. Additionally, Ra of the standard pectin surface was

significantly different from HPMC K100 (p=0.004). On the contrary, the adhesion force measured for HPMC K100 was not different to the adhesion force of standard pectin.

The AFM images implied differences in the adhesion properties of mucilage, standard pectin and HPMC K100 to the mucin. The Ra of samples of different Shepherd's purse mucilage extracts indicated that they resembled standard pectin when adhered to the mucin (Morris *et al.*, 2010). When all mucilage extracts spread on the mucin coated mica sheets they formed a thick layer seen as large white areas on the topography images and its measured roughness was high. The thicker the layer the brighter it appears under the microscope (Joergensen *et al.*, 2011). All mucilage extracts were similar to standard pectin with regard to their Ra. Only hot maceration 40°C-2h showed a significant difference in adhesion force and Ra compared to standard pectin (p=0.01) and HPMC K100 (p=0.008).

By and large, the statistical analysis of the measured data revealed that the measured root mean square of Ra for standard pectin was not significantly different from Shepherd's purse mucilage extracted by water maceration 25ºC, solvent maceration, hot reflux, hot maceration 70°C, hot maceration 40°C-1h and hot maceration 50°C-1h. This indicates that the surface property of these mucilage extracts resembled that of standard pectin as expected. With regard to adhesion force, only Shepherd's purse extracted by water maceration, solvent maceration (p=0.01), hot reflux (p=0.001) and hot maceration 40°C-2h (p=0.001) were significantly different than both standard pectin and HPMC K100 adhesion.

Though surface roughness of the water maceration 25ºC extract showed a relatively high surface roughness compared to HPMC K100, the water maceration extract adherence to mucin was not significantly different to HPMC K100 ($p=0.12$). On the other hand, water maceration extract surface properties were similar to standard pectin, the adhesion force to mucin was significantly different than standard pectin ($p=0.009$) which was less adherent. Therefore, Shepherd's purse mucilage extracted by water maceration interacted as standard pectin with the mucin, and it possessed the same surface properties of pectin with a stronger adhesion force than standard pectin.

It was suggested in the literature that the smoother the surface the better and stronger the adhesion (Deacon *et al.*, 2000; Joergensen *et al.*, 2011; Le *et al.*, 2013). In this study, Shepherd's purse mucilage seemed to interact with mucin, forming complexes, and possessed a stronger adhesion force; though the surface roughness measurement of most mucilage extracts showed that Shepherd's purse mucilage had a rough surface. Therefore, whenever these complexes were bigger, adhesion was stronger and this was implied when comparing the topographic images of hot reflux with its adhesion force and hot maceration 50°C-2h smooth dark image with its weak adhesion force.

Hong *et al.*, (2005) found that mucin at pH 6 consisted of long fibres while at lower pH tended to aggregate and form clusters. This condition existed during the experiments due to using NaCl as dispersion medium of mucin. It was also

concluded from literature studies that the pectin and mucin in water tend to coil as they were present in partially ionised form in addition to H-bonding of pectin branches with mucin in the aqueous medium generated by the hydration of mucin coated mica (Accili *et al.*, 2004; Hong *et al.*, 2005; Khutoryanskiy, 2007; Thirawong *et al.*, 2007). These interactions would have led to the adhesion of mucilage to the mucin (Hong *et al.*, 2005; Sriamornsak *et al.*, 2010). Extracted mucilage had a similar structure to standard pectin. The predicted structure of Shepherd's purse mucilage using NMR spectroscopy in chapter two showed hydroxyl groups in the uronolactone were able to form H-bonds with mucin. Also hydroxyl groups were present in the uronic acid units of pectin and they formed H-bonds with mucin. Though both standard pectin and Shepherd's mucilage formed H-bonds to mucin, the mucilage adhesion force was significantly stronger than standard pectin. This finding suggested that another mechanism was involved in the adhesion of Shepherd's purse mucilage with mucin. It was believed that pectin (DE<50%) could open Ca^{+2} channels and trigger gel formation as a result of an "egg-box" model formation in the nasal secretions (Morris *et al.*, 2010). Further mucoadhesion studies would reveal the full theory of adhesion adopted by Shepherd's mucilage to mucin (Morris *et al.*, 2010).

There has been some debate as to whether mucin-particle studies are the best way to study mucoadhesion due to the large particle size of pectin and the large particle distribution (Sriamornsak *et al.*, 2010). The Shepherd's purse mucilage showed ability to adhere to mucin and therefore a further drug release study is essential to find out its suitability for drug delivery system.

3.6. Conclusion

The results from this chapter suggest that surface smoothness was not correlated to the adhesion ability of the surface. The rough surfaces of Shepherd's purse mucilage were the most adherent surfaces to mucin than smooth surfaces of HPMC K100.

Extracted Shepherd's purse mucilage by different methods showed similar surface roughness as the standard pectin. It was proposed that both standard pectin and mucilage formed H-bonds with mucin due to similarity in the chemical structure.

The extracted mucilage especially by water maceration 25ºC, hot reflux, solvent maceration and HM 40°C-2h exhibited better adhesion to the mucin than the commercially available standard pectin and HPMC K100.

The adhesion force to mucin, the easy preparation and extraction, the physiochemical properties determined in chapter two, are all characteristics that allowed selection of water maceration mucilage 25ºC for the choice to be used for further studies of a mucoadhesive drug delivery system.

The results concluded the suitability of water maceration mucilage 25ºC for use in drug release studies as a best candidate because it showed higher adhesion force than standard pectin.

As synthetic mucin resembles mucin in mucosal membranes, the findings of this experiment could be related to the effectiveness of adhesion of the extracted Shepherd's purse mucilage to the mucosal membrane in the nasal cavity. These findings need confirmation with another method of studying mucoadhesion because one of the parameters which were the surface roughness was not suitable for this study.

Chapter 4 Drug delivery system formulation and drug release studies

4.1. Introduction

The development of a dosage form is not complete without drug release studies, which are essential to check the suitability of the developed dosage form for delivering drugs to their target site (Rathbone, 1996). Drug release is the process by which drug leaves the dosage form or delivery system and is available in the diffusion medium for absorption, distribution, metabolism and excretion (Fu and Kao, 2010). Trans-mucosal drug delivery is studied by a variety of methods, including Franz cells of diffusion and micro dialysis (Allen *et al.*, 2011; Leveque *et al.*, 2004). Use of Franz cells is a well-established technique for studying drug release through transdermal tissue, and they have been developed to study diffusion through mucosal membranes (Cornaz *et al.*, 1996; Khutoryanskiy, 2011).

4.2. Drug release conditions for using Franz cells of diffusion

Franz cells are mainly composed of two compartments; the lower is the receiver compartment which is filled with the diffusion media and topped with the donor compartment containing the dosage form, separated with a natural or artificial membrane that mimics the biological system (Figure 4-1) (McInnes, 2003). The whole diffusion system is surrounded by a hot water jacket maintained at 36°C through a hot water stream from a temperature controlled water bath.

Standardisation of the conditions of the experiment is needed to achieve reproducible results and to maintain sink conditions (Phillips *et al.*, 2012). There is a vast literature describing different conditions of studying the release patterns of drugs using Franz cells. Sink conditions are the state in which the drug concentration in the diffusion medium is at least 3 times less than the saturation concentration of the drug in that given medium (Fu and Kao, 2010). Sink conditions are very important when the diffusion medium is limited in volume and to ensure the drug is released continuously from the dosage form or the drug delivery system towards the diffusion medium to be available for absorption, distribution, metabolism and excretion (Ranade, 2004).

Firstly, a small volume of sample needs to be taken (0.5-1 ml) (Hagesaether, 2011; McInnes *et al.*, 2005; Na *et al.*, 2010). Secondly, sampling frequency needs to be increased when taking small sample volumes, i.e. 10-30 min and preferably every 15 min (Lafforgue *et al.*, 2011; Na *et al.*, 2010). Generally, the experiments should not be very long and preferably not in excess of seven hours for nasal delivery studies (Datta and Bandyopadhyay, 2005; Kuotsu and Bandyopadhyay, 2007). This value has been chosen from studying the clearance rate of nasal mucosa. The system needs to equilibrate to the required temperature for 15 min before starting the experiment (Leveque *et al.*, 2004) and care should be taken to avoid air bubbles in the receiver compartment as they prevent permeation and form a barrier against drug penetration. Tilting the cells forward can help in eliminating the bubbles in addition to buffer solution de-aeration (Ng *et al.*, 2010). In case of using animal membranes, pre-hydration is essential to maintain the membrane's properties (Ng *et al.*, 2010).

Lastly, a less than 10% of saturation solubility concentration of the drug should be considered essential when applying the tested formulation (Leveque *et al.*, 2004; Na *et al.*, 2010).

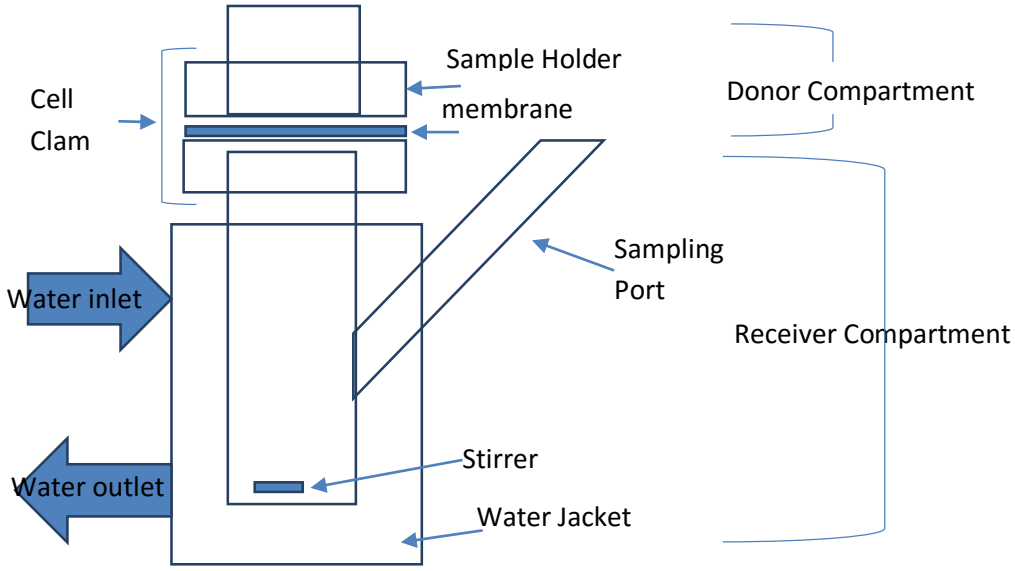

Figure 4-1 Schematic diagram of a Franz cell

The drug release profile from polymers is affected by the physicochemical properties of the drug used (Bogataj *et al.*, 1999). Water-soluble drug is released faster in aqueous medium than water insoluble drugs. Shepherd's purse polymer is believed to affect the drug release by its water sorbent and water-swellable properties and these two properties have been cited as factors that can delay drug release (Liu *et al.*, 2007; Morris *et al.*, 2010). Therefore, two different drugs were chosen for this study. Paracetamol, and amitriptyline HCl, were chosen as model drugs for their molecular weights, in addition to different solubilities where amitriptyline HCl is water soluble drug while paracetamol is sparingly soluble in water. Furthermore, they could both be detected readily using a UV spectrophotometer.

4.3. Aims and objectives

The aim of this chapter was to form different dosage forms of the extracted mucilage and to examine their efficacy in releasing drugs. From previous results identified in earlier chapters it was decided that the water mucilage extract should be studied further.

The objectives of this work were to form a disc shaped dosage form or cake using the Shepherd's purse water mucilage to enable release of the drugs when they came into contact with diffusion medium. Studying drug uptake ability of the drug delivery system, and examining the effect of extracted compounds on the mucilage on the % uptake and the release profile of the drug delivery system was also carried out. The water maceration mucilage was mixed with the model drugs in a 1:1 ratio. Different shaped drug delivery systems were formulated with varying surface areas to examine the effect of physical characteristics on the release profile.

Comparison was made with a HPMC because it has been widely studied and used for drug delivery systems. It is also widely adopted as a standard for water soluble and swellable polymer studies (Datta and Bandyopadhyay, 2006; Khutoryanskiy, 2011; Kuotsu and Bandyopadhyay, 2007)

Further comparison studies were carried out aimed at studying the formulation of drug delivery systems using higher drug:polymer weight ratios, where 1:2 and 1:3 drug:mucilage were formed and compared to each other and to 1:1 drug:mucilage systems.

Drug-mucilage discs of 17 mm and 20 mm diameter were formed using glass vials, and twelve well culture plates, respectively. Cylindrical shaped inserts, were formed using microtitre plates (96-well, flat bottom) with 6.4 mm diameter wells. Different drug:mucilage ratio (1:2, and 1:3) discs were formed using 12 well culture plates and compared.

4.4. Materials and Methods

4.4.1. Equipment and Materials

- Hydroxypropyl methylcellulose (HPMC)[2] powder K100 LV grade (lot number KK08012N21) was obtained from Dow Chemicals, USA.
- Amitriptyline HCl (lot number BCBC4769V), paracetamol (lot number 078K0032), mannitol 1% (w/w) lot number 125K009, sodium chloride (lot number 038K0020), 3-glycidoxypropyltrimethoxysilane (lot number STBC1856V) and pectin from apple (meets USP xxiii requirements, lot number 67H16351) were all procured from Sigma-Aldrich.
- Whatman cellulose nitrate membranes of three different pore diameters (0.45µm; 12 µm); potassium chloride (lot number 0444678); hypodermic syringes without needles 1ml luer lock clear polycarbonate barrel concentric and latex free; needles 19G*203mm length all were procured from Fisher Scientific.

[2] The letter K represents a hydroxypropyl molar substitution of 0.21 and a methoxyl degree of substitution of 1.4. The number 100 indicates the viscosity in millipascal-seconds of 2% aqueous solution at 20ºC. The suffix LV refers to special low viscosity product.

- Calcium chloride dehydrate (lot number132450250307P81) was procured from Fluka, UK.
- Glycerol B.P was sourced from J.V. Loveridge Ltd. (UK).
- Multi-point agitation plate (Thermo Fisher Scientific Inc, USA).
- Digital calibre (Parkside, Germany).
- UV-Visible spectroscopy was carried out on a Varian Carey 50 Bio UV-visible spectrometer, equipped with Carey WinUV software.
- Customised borosilicate glass Franz cells (PermeGear V6A-O2, PA, USA) were used consisting of a 20 ml receptor with a custom flow porting, and 25mm in diameter flat ground joint donor, stirred using a V6A stirring unit.

4.4.2. Preparation of dosage forms for diffusion studies

A 1:1 drug and mucilage mixture was prepared by dissolving 500 mg of mucilage in 30 ml distilled water, then adding 500 mg paracetamol. The solution (1.66% w/w) was stirred overnight on a multi-point agitation plate to allow polymer hydration. Similarly 500 mg of HPMC K100 and 500 mg of paracetamol was dissolved in 30 ml distilled water and stirred overnight. Different moulds as described below were filled with 294 µl of the drug-polymer solution to produce dosage forms with different surface areas.

4.4.2.1. Silanisation of culture plates

Aliquots of 3-glycidoxypropyltrimethoxysilane (100 µl/well) were added to 96 well culture plates, 12 well culture plates and glass vials as moulds which were used later to form the discs and inserts. The solution was aspirated and the moulds were

allowed to dry at room temperature under a hood for 8 h to allow evaporation of residual silane solution. This step was used to reduce interactions of the polymer matrix with the culture plate material (Phaner-Goutorbe *et al.*, 2011).

4.4.2.2. Formation of discs

In order to form discs of different surface area, glass vials of 17mm inner diameter and culture plates of 20 mm well diameter were prepared and silanised prior to use as described in section 4.4.2.1. Aliquots of 294 µl of drug solution containing 5 mg of drug were placed into clear glass vials of 5 ml volume and 40 x 20 mm dimensions to obtain disc-shaped cakes. The vials were sealed with parafilm and the contents freeze dried as described in section 2.4.2.2.

Twelve-well culture plates (20 mm well diameter) were used as a mould to lyophilise the polymer solution to increase the size of the formed discs. Aliqouts equivalent to 5 mg of the drug were pipetted from the drug-polymer solution and placed in the wells of the plates which were sealed with parafilm and lyophilised as described in section 2.4.2.2.

4.4.2.3. Formation of nasal inserts

To produce cylindrical shaped inserts, microtitre plates (96-well, flat bottom) were used: 6.4 mm diameter wells, external dimensions 128 x 86 mm. Aliquots from the drug-polymer solution equivalent to 5 mg of the drug were placed in the wells of the plates which were silanised in advance, sealed with parafilm and freeze dried as described in section 2.4.2.2.

4.4.2.4. The use of plasticisers

McInness and colleagues described the use of mannitol to increase the mechanical strength of dosage forms (McInnes *et al.*, 2005). It involved dissolving 0.5 g of mannitol and paracetamol of 5 mg in one third of required amount of distilled water that was previously used to form the drug delivery systems described in section 4.4.2. Then the specified amount of polymer to make 2% w/v was added to the one third of distilled water with continuous stirring until a thick gel formed. Then the remaining volume of distilled water was added and left in the fridge overnight to allow polymer expansion. The next day, aliquots (250µl) of the solution containing 5 mg of the drug were placed in the prepared culture plates and lyophilised according to the method described in section 2.4.2.2.

Glycerol is commonly used as a plasticiser in film formation (Boateng, 2005). It was used as a second choice of plasticiser. The method was adopted from Boateng (2005) in which 2.5g glycerine was mixed with 50 ml water and heated above 90°C with vigorous stirring, then dry polymer (0.5 g of mucilage or HPMC K100) was added and vortexed vigorously in hot distilled water. Stirring carried on until a uniform mixture was obtained. Finally the mixture was left to stand for 5-10 min before pipetting 1 ml into the wells of the culture plates and lyophilised following the process described in section 2.4.2.2.

4.4.3. Formation of 1:2 and 1:3 drug: polymer ratio discs

The drug : mucilage ratios of 1:2 and 1:3 were prepared for comparison with the 1:1 ratio. Standard polymer HPMC K100 LV samples were prepared in the same ratios. Then all samples were lyophilised as described in section 2.4.2.2.

4.4.4. *In vitro* release studies using Franz cells of diffusion

Franz cells of diffusion were used for studying drug release (Figure 4-2). Simulated nasal electrolyte solution (SNES) was prepared by dissolving NaCl (7.45g), KCl (1.29g), $CaCl_2$. $2H_2O$ (0.32g) in 1L of distilled water. This solution was filtered under vacuum through a Whatman filter membrane (0.45µm). Each solution was analysed with a pH/ion analyser to make sure that the pH was within a range of 5.5-6. Fresh solution was prepared prior to each diffusion study.

Figure 4.2 Franz cells and the stirring unit.

The receptor compartment was filled with 20ml SNES and maintained at 37°C with a hot water jacket under continuous stirring. A Whatman cellulose nitrate filter membrane (12 µm pore size) was mounted on top of the receptor compartment, and the donor compartment was fitted on top with clamps. The drug-polymer disc or nasal insert was then placed on the filter membrane through the donor. To prevent evaporation and temperature drops during the experiments, the donor compartments and sampling ports were occluded using parafilm and aluminium foil. Sample volumes (1ml) were taken at frequent intervals (1, 2, 3, 4, 5h) from the receptor compartment and replaced with an equal volume of fresh SNES.

A positive control was also set up using drug solution. Five ml of a drug solution (1 mg/ml) was added to each Franz cell on the donor compartment. Samples of 1 ml were taken at 1, 2, 3, 4, 5 h intervals from the diffusion medium in Franz cells. The drugs were prepared and dissolved in SNES for the study.

4.4.4.1. Testing the effect of plasticiser on drug release properties

Drug-polymer discs containing plasticisers were tested for the effect of plasticiser on drug release properties using Franz cells of diffusion.

4.4.4.2. Studying the effect of surface area on the release properties of drug

Drug release from nasal inserts and from discs were studied using Franz cells. Nasal inserts had a smaller contact surface area compared with the nasal discs.

4.4.4.3. Analysis of samples from release studies

All samples were analysed spectrophotometrically using a UV single beam spectrophotometer. Paracetamol and amitriptyline standard calibration curves were prepared to extract the calculation equation. Paracetamol stock solution (1 mg/ml) was prepared and dilution of 1, 2, 4, 10, 15, 20 µg/ml were prepared and their absorption was plotted against concentration. Amitriptyline Stock solution of 1mg/ml was prepared and dilution of 20, 40, 80, 100 µg/ml were measured for absorption and calibration curve equation was extracted.

Paracetamol absorbance was measured at 249nm, while amitriptyline was measured at 239nm. The similarity factor was used to calculate the similarity of release profiles of the tested sample compared with a reference as follows (Stevens *et al.*, 2015) :

$$\text{Similarity factor} = 50+\log [((1+(Rt-Tt)*1/n))-0.5]$$

Where Rt is % release of the reference, Tt is % release of test, n is number of samples

4.4.5. Statistical analysis

All data from release studies were analysed statistically using one-way analysis of variance (ANOVA) to compare data within replicates. A two-sample T-test was used to compare different polymers, membranes, and the effect of a plasticiser.

4.5. Results

4.5.1. Preparation of dosage form

4.5.1.1. Formation of discs

Discs prepared using glass vials used a minimum amount of water and resulted in formation of mechanically robust discs of amitriptyline with both polymers, and paracetamol with HPMC, which could be handled without damage (Figures 4-3 c and d). However, the paracetamol-mucilage combination resulted in discs that were fluffy, which could still be handled, but with caution (Figure 4-3a and b). This characteristic caused some of the mucilage discs to deform when being lifted from the glass vials and it was difficult to measure the actual size accurately.

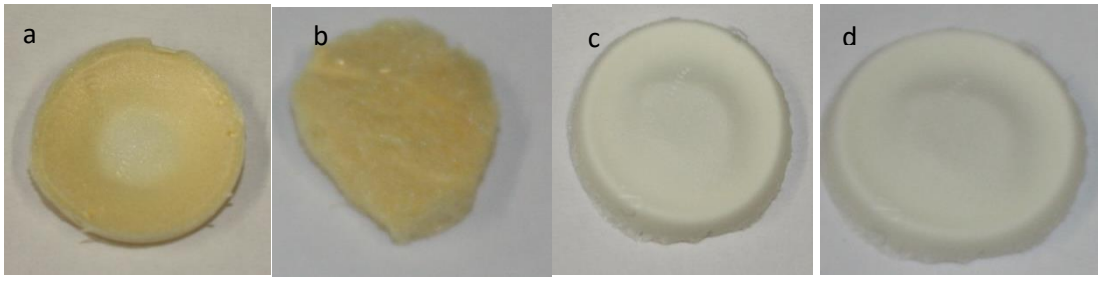

Figure 4-3 Images of discs (a) Amitriptyline loaded mucilage (1:1), (b) Paracetamol loaded mucilage (1:1); (c) Amitriptyline loaded HPMC K100 (1:1), (d) Paracetamol loaded HPMC K100 (1:1).

Discs formed using the 12 well plates are shown in Figure 4-4.

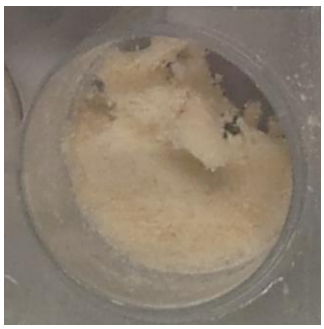

Figure 4-4 Image of paracetamol-mucilage disc into the 20mm culture plate.

4.5.1.1.1. Drug content measurement in the discs

In order to assess whether each disc contained 5 mg of drug, 10 randomly chosen discs were measured for drug content (Table 4.1).

Due to the fragility of the paracetamol-mucilage discs, it was impossible to measure any intact disc diameters. Therefore, comparing mucilage and HMPCK100 paracetamol discs was not accomplished and only amitriptyline measurements are displayed in Table 4.1. Measurements of amitriptyline discs (Table 4-1) revealed that both mucilage and HPMC K100 were similar in diameter and drug content.

Table 4.1 Measurement of mean amitriptyline disc diameter and drug content with different polymers (n=10).

Polymer Type	**Mean disc diameter (mm) ± SD**	**Mean drug content (mg) ± SD**
Mucilage	16.25±0.06	4.69±0.207
HPMC K100	16.86± 0.42	3.96±0.286

4.5.1.2. Formation of nasal inserts

When the formation of discs using the culture plate gave negative results, smaller size moulds were investigated to assess the effect of the mould size on the use of mucilage to make sturdier drug delivery systems. The inserts were made using microplates of small diameter (6.4 mm); these resulted in rod-shaped drug loaded inserts (Figures 4-5). The inserts were sturdy and strong enough to be handled.

Mucilage inserts, showed in Figure 4-5 a and b, were less strong and hollow compared with HPMC K100 (Figure 4-5 c and d).

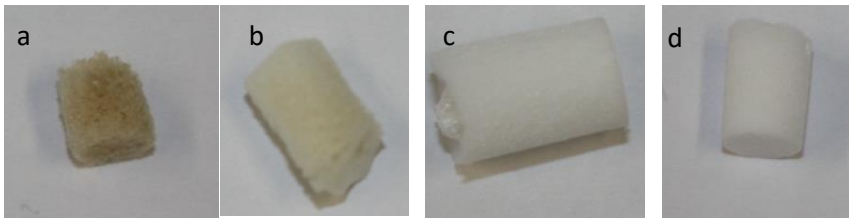

Figure 4-5 Images of inserts of (a) amitriptyline-mucilage (1:1), (b) Paracetamol-mucilage nasal inserts (1:1), (c) Amitrityline-HPMCK100 (1:1), (d) paracetamol-HPMCK100 (1:1) nasal inserts.

4.5.1.2.1. Drug content measurements

Measurements of dimensions and surface area of produced inserts were performed using an electronic calliper (Tables 4-2).

From the results displayed in Table 4-2, the insert shaped drug delivery systems using Shepherd's purse mucilage could not take up drug to reach 5 mg in each insert.

Shepherd's purse mucilage showed less amount of drug uptake, compared with HPMC K100. The amitriptyline-mucilage and paracetamol-mucilage showed less drug content compared to other inserts made with HPMC K100. Only amitriptyline-mucilage insert showed different measured surface area.

Table 4.2 – Mean amitriptyline HCl and paracetamol content and diameter in different polymer inserts (n=10).

Drug-Polymer Type	**Mean insert surface area (mm^2) ± SD**	**Mean insert diameter (mm) ± SD**	**Mean drug content (mg) ± SD**
Amitriptyline-Mucilage	164.00±29.07	5.57±0.62	0.846±0.02
Paracetamol-Mucilage	240.82±26.62	6.07±0.54	0.85±0.02
Amitriptyline-HPMC K100	247.59±11.53	6.32±0.076	4.29±0.02
Paracetamol-HPMC K100	252.68±21.85	6.35±0.29	3.96±0.28

4.5.1.3. The effect of plasticiser on drug release

Since the mucilage discs were not strong enough to handle, mannitol was used to increase the disc strength. The mucilage discs formed with mannitol were still found to be fragile, soft and weak on handling after (Figure 4-6). The mucilage discs with mannitol were stronger than discs formed without mannitol though the measurements were difficult to obtain comparatively to HPMC K100 discs (Figure 4-6).

Paracetamol was chosen as the model drug because the paracetamol-mucilage discs formed in section 4.5.1.1 were strong and could be held.

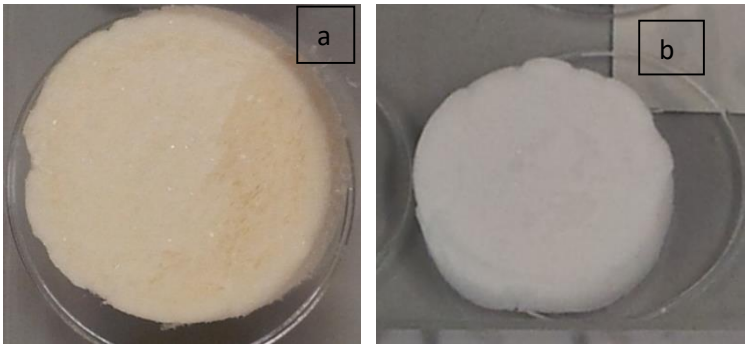

Figure 4-6 image of discs of (a) paracetamol-mucilage disc containing mannitol; (b) paracetamol-HPMC K100 disc with mannitol

Glycerol was assessed for its suitability as a plasticiser using a method adopted for film formation (Boateng, 2005). Unfortunately it did not give the strength sought. The discs of either mucilage and HPMC K100 were very elastic, sagging and the glycerol was easily squeezed out (Figure 4-7). No further experiments were carried out using glycerol.

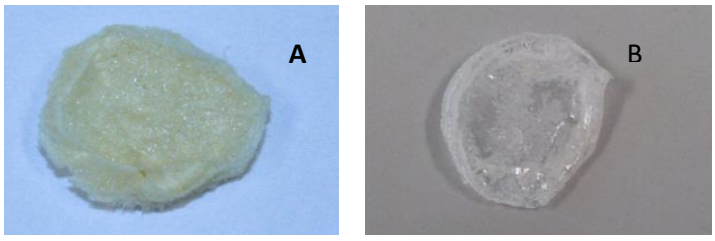

Figure 4-7 Images of disc prepared with glycerol (a) blank mucilage disc; (b) blank HPMC K100 disc with glycerol.

4.5.1.3.1. Drug content measurments for mannitol-containing discs

Size measurments were conducted using an electronic caliper and the results displayed in Table 4.3

Table 4.3- Measurement of drug discs contained mannitol (n=6)

Polymer type	**Mean disc diamter (mm) ± SD**	**Mean disc weight (mg) ± SD**	**Mean drug content (mg) ± SD**
Paracetamol-mucilage	2.5±0.34	11.7±1.60	5.0±0.60
Amitriptylin-mucilage	19.71±0.24	12.23±1.18	5.69±1.56
Paracetamol-HPMC K100	2.5±0.30	13.4±1.20	4.9±0.45
Amitriptylin-HPMC K100	20.10±0.25	12.10±0.60	5.15±1.52

Discs of both mucilage and HPMC K100 were similar and showed no differences

4.5.1.4. Formation of 1:2, and 1:3 ratio discs

Increasing the ratio of mucilage to the drug was studied to assess the ability of increased mucilage on the strength of the discs.

Paracetamol-mucilage (1:2) discs were formulated and found to be, fragile, shiny, fluffy (Figure 4-8), and could not withstand handling for measurements to be taken. Use of mannitol resulted in discs that were less fluffy than the drug-polymer alone, but they were still fragile upon handling (Figure 4-8). The fragilty of the discs increased with increasing the ratio of paracetamol-mucilage to 1:3 (Figure 4-9).

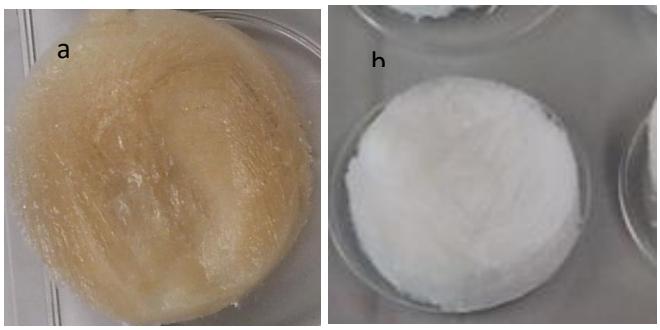

Figure 4-8 Image of discs of (a) paracetamol-mucilage disc(1:2); (b) paracetamol-HPMC K100 discs (1:2).

In contrast, the HPMC K100 formed dics were slightly rigid which could be handled. Addition of mannitol to HPMC K100 further increased strength of the discs (Figures 4-8 and 4-9).

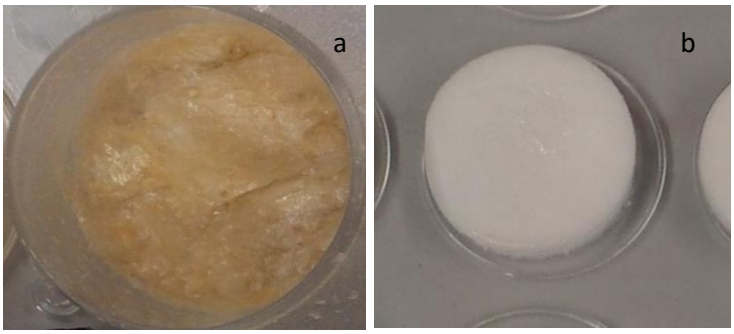

Figure 4-9 Images of (a) of culture plate containing paracetamol-mucilage (1:3) disc, (b) of paracetamol-HPMC K100 disc (1:3).

The formed discs from 1:2 and 1:3 ratios of drug:mucilage, were not strong enough to allow size measurements.

4.5.2. *In vitro* release studies using Franz cells of diffusion

Typical calibration curves for paracetamol and amitriptyline HCl are shown in Figures 4-10 and 4-11.

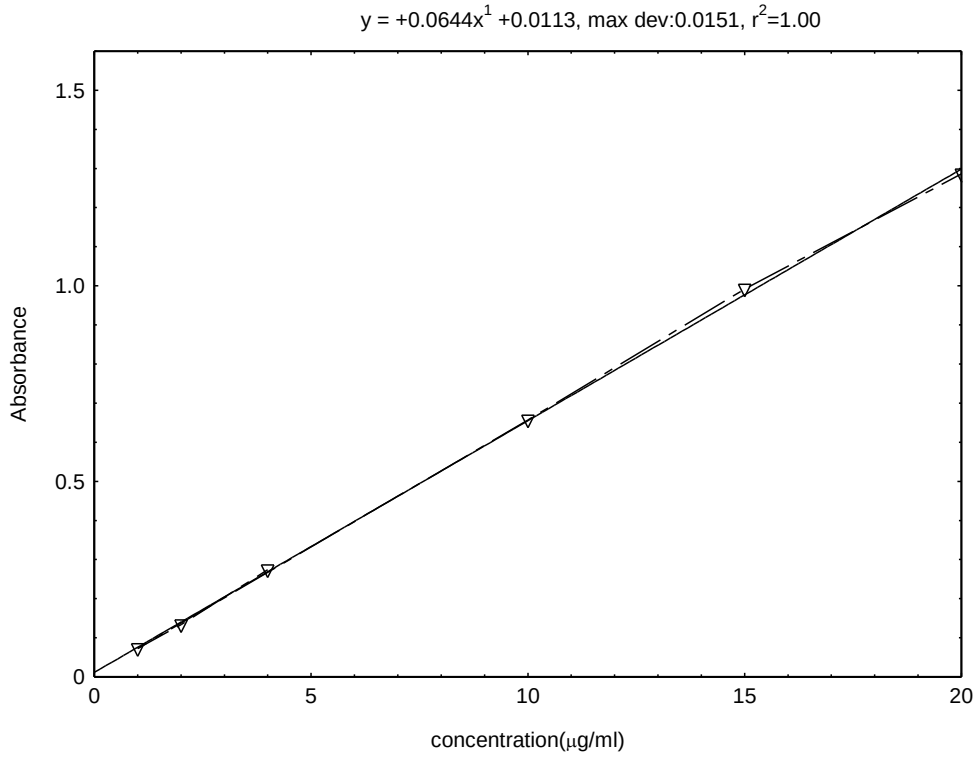

Figure 4-10 Paracetamol calibration curve (n=3)

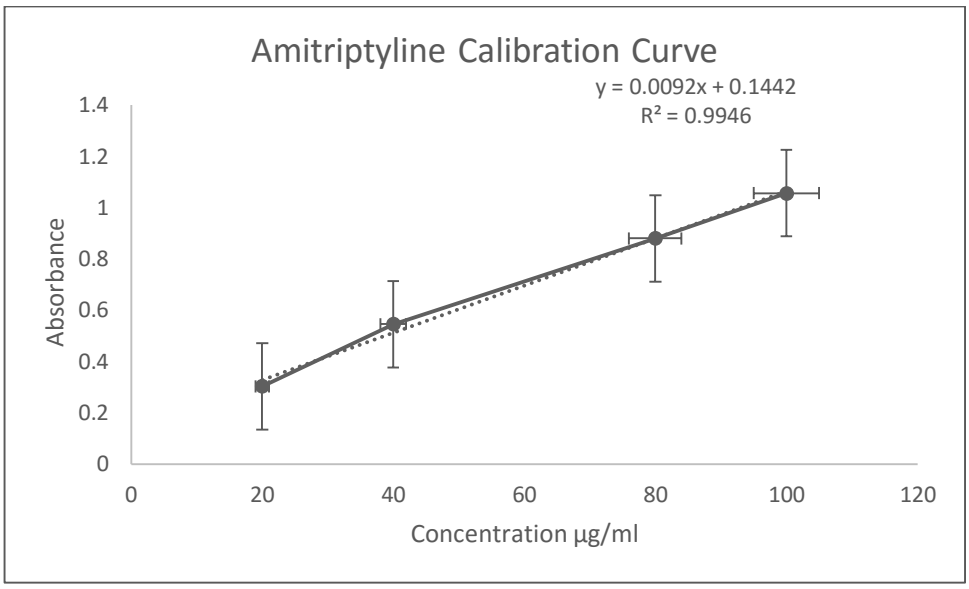

Figure 4-11 Amitriptyline HCl calibration curve (n=3)

Positive controls were conducted for both drugs (paracetamol and amitriptyline) in order to compare the effect of mucilage and HPMC K100 on the release of these drugs. Paracetamol solution of 1 mg/ml was used for a positive control. Figure 4-12 shows that the maximum release reached was 40% after 5 h then it started to decline.

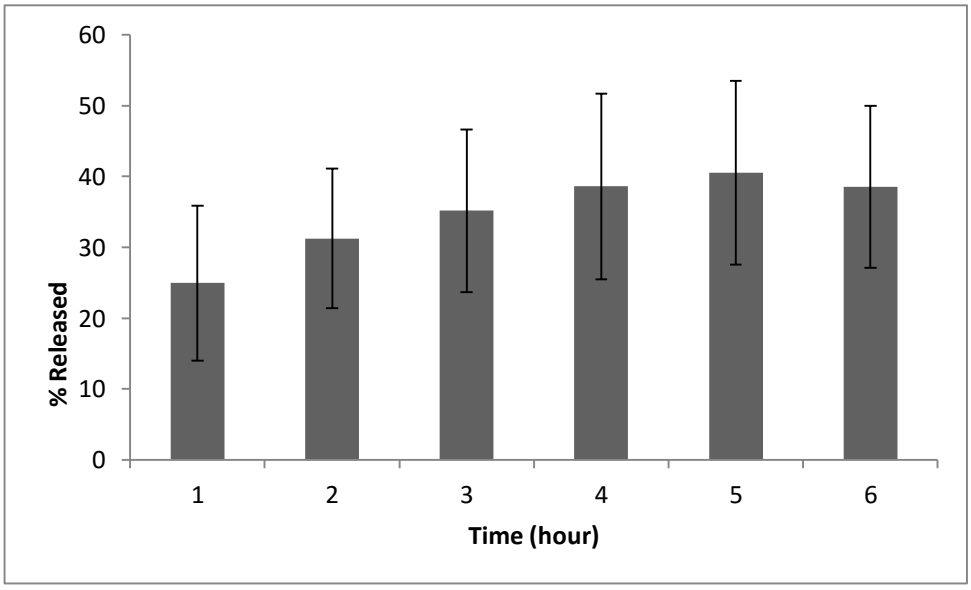

Figure 4-12 Percentage paracetamol released using a paracetamol positive control (n=3).

Amitriptyline HCl % released in the positive control experiment is shown in Figure 4-13. The % release reached its maximum of 43% after three hours.

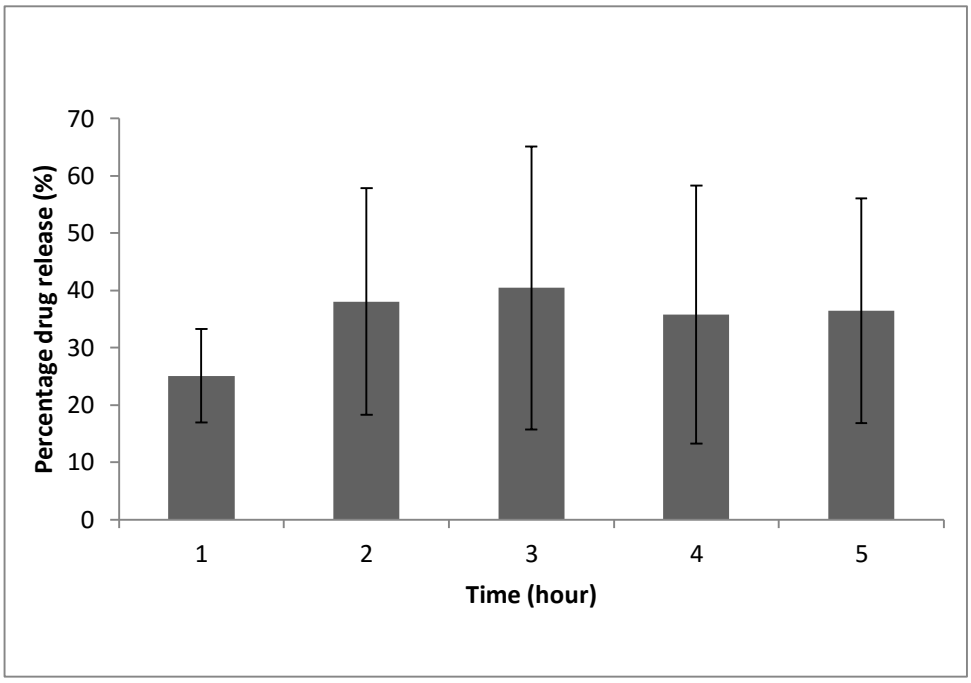

Figure 4-13 Percentage released from Amitriptyline HCl positive control (n=3).

4.5.2.1. The release profile of paracetamol from nasal inserts

The maximum % release of paracetamol in Figure 4-14 was nearly 50% from the mucilage after 4 h, and almost 60% from HPMC K100 after 3 h.

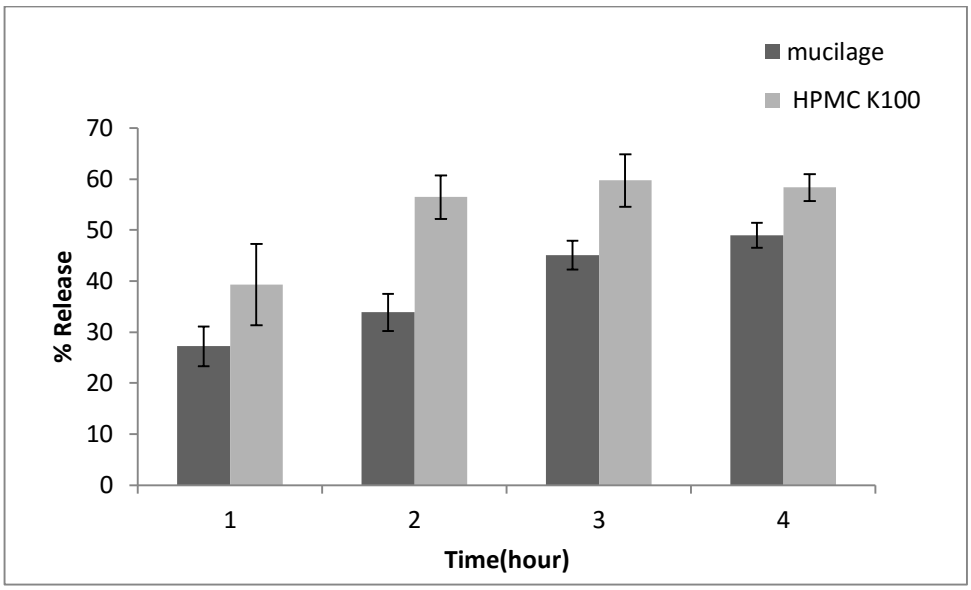

Figure 4-14. The percentage release of paracetamol from the nasal inserts of different polymers (Shepherd's purse seed mucilage and HPMC) after 4h incubation (n=3)

The calculated similarity factor of paracetamol from the nasal inserts of different polymers was 43.3 comparing the release from mucilage to release from HMPC K100.

4.5.2.2. Amitriptyline release from nasal inserts and nasal discs

The percentage released from amitriptyline nasal inserts was calculated and illustrated in Figure 4-15. The highest % amitriptyline released from mucilage nasal inserts 12% after 3 h, though the maximum amitriptyline released from HPMC K100 was 9% after 3 h.

The amitriptyline release from mucilage discs of and from HPMC K100 discs displayed in Figure 4-15. It showed that the % drug released from mucilage was 59%

after 3 h and % release of the drug from HPMC K100 reached 75% after 2 h from the start of the experiment.

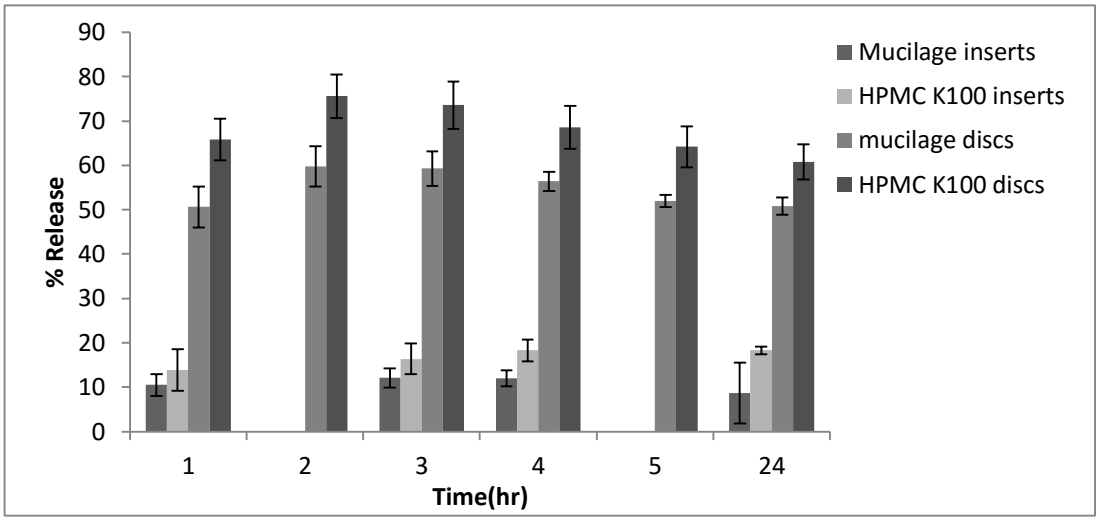

Figure 4-15. The percentage released of amitriptyline from mucilage and HPMC K100 nasal disc and nasal inserts.

The calculated similarity factor of the release profile of amitriptyline from mucilage nasal insert and HPMC K100 nasal insert was 43.5. The similarity factor of amitriptyline release from nasal discs of mucilage and HPMC K100 was 59.6.

4.5.2.3. Study the effect of mannitol on the drug release profile

The addition of mannitol on the release properties of paracetamol and amitriptyline was studied using Franz cells. The release profile of amitriptyline from mucilage in Figure 4-16 showed that the maximum % released was almost 10% after 2 h.

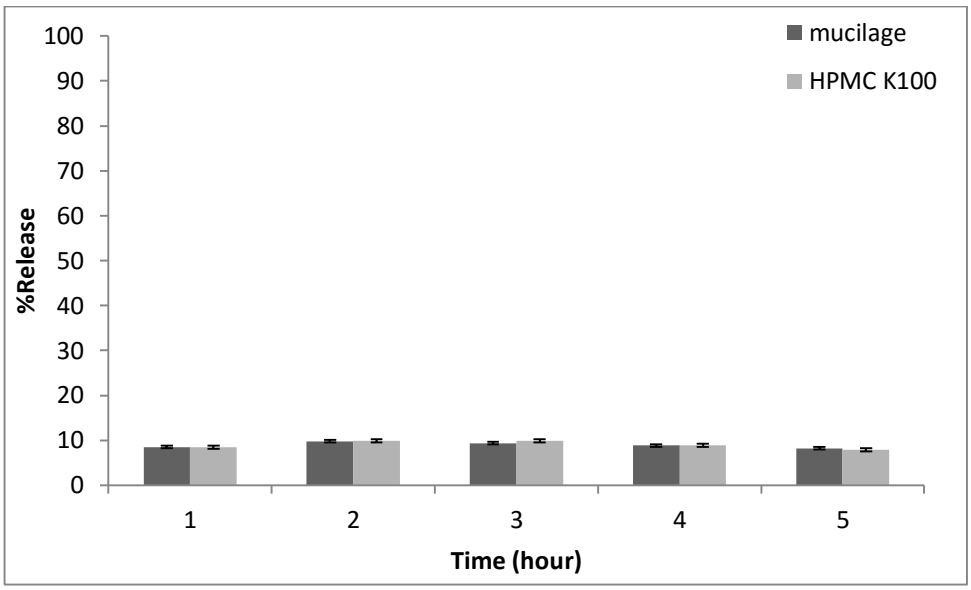

Figure 4-16. The Percentage released of amitriptyline from mannitol containing discs.

The similarity factor of amitriptyline from mucilage discs contain mannitol was 99.3 to HPMC K100 discs containing mannitol which indicated a similarity of release profile of both polymers. The paracetamol released from mucilage discs with mannitol (Figure 4-17) showed % release that reached was over 40% at 4 h, while the HPMC K100 mannitol discs showed a higher % release of the drug and reached the highest which is 45% at 5 h. The similarity factor of paracetamol-mucilage discs containing mannitol was 59.08 to paracetamol-HPMC K100 discs with mannitol that was an indication of no difference between both polymers.

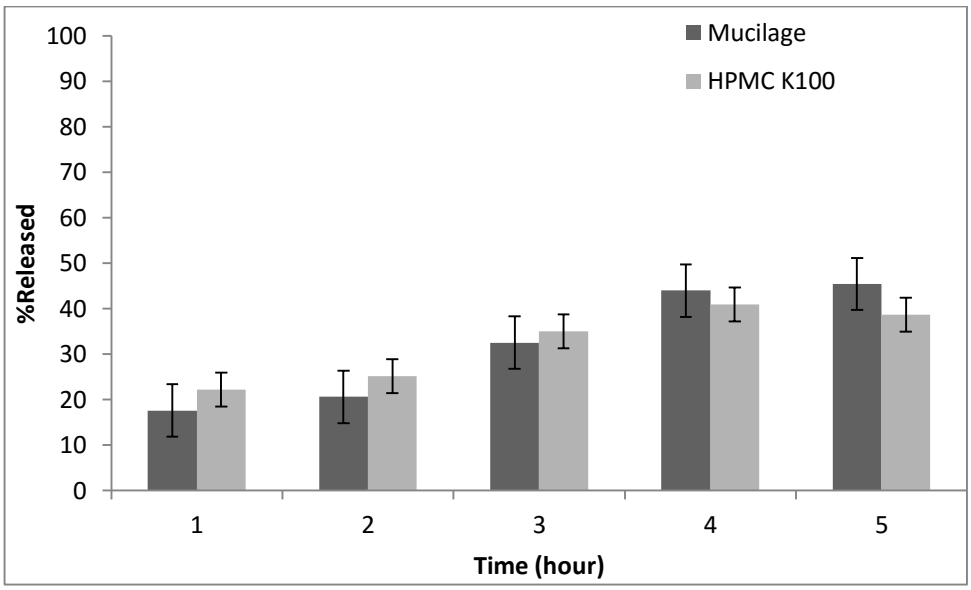

Figure 4-17. The percentage of paracetamol released from discs containing mannitol over different incubation times

4.6. Discussion

Making the drug into a disc shape to study drug release using Franz cells of diffusion was a challenging task. The water solubility of the drug was an important factor to be considered when forming the discs as well the polymer properties. The properties of extracted mucilage led to the formation of very fragile discs for either drug irrespective to their properties. This was attributed to the nature of the mucilage polymer and the presence of fibres, which caused the discs to be brittle upon lifting from the culture plates. HPMC K100 discs were strong enough to be measured with digital calliper to determine their diameter and thickness. In contrast, mucilage discs formed in 20 mm culture plates were impossible to be lifted out of the plates intact. They had a soft touch like cotton, very thin, fluffy (straw like). The mucilage discs formed in the culture plates could not be prepared using the same volume of samples used in glass vials. It was thought that the mucilage fibres swelled upon addition of

water and relaxed forming coil shaped fibres; this was concluded from the mucoadhesion study using AFM. These fibres could not shrink back to their original size again when freeze dried and instead they were moulded to the size and shape of culture plate. Therefore, it was believed that the drug mucilage sample did not contain enough mucilage to be moulded into the wells of the culture plate.

These findings were similar to the research carried out using Shepherd's purse mucilage with Ibuprofen (Chander, 2012). Chander (2012) used Shepherd's purse mucilage extracted by water maceration and mixed it in different ratios with different polymers such as HPMC K100 and carbapol 980 in order to form discs for Ibuprofen drug delivery systems. He found that the commercial polymers formed strong discs without the mucilage. While when these polymers were mixed with Shepherd's purse mucilage, the discs were fragile and soft and fluffy. His results were similar to the results of this research, in that the mucilage could not make strong discs alone.

The mucilage discs with mannitol were stronger than discs formed without mannitol though the measurements were difficult to obtain comparatively to HPMC K100 discs. Mannitol added strength to mucilage structures made it them though the added strength was not enough.

During discs and inserts preparation, mucilage was dissolved in solution with the drug. It is believed that the amount of water used to form a 2% solution allowed the mucilage polymer matrix to expand to a high degree that made it difficult to shrink again to the original size before the expansion, and resulted in softer fluffy discs. As

the mucilage was previously described as water absorbent, the amount of water used to dissolve the mucilage was just enough to suspend it in the water and enable mixing it with the drug. Adding higher quantities of the mucilage did not help in making the discs stronger, and it was clear when 1:2 and 1:3 drug: mucilage ratio was prepared, it only increased the disc fragility and fluffy texture and made wafer like discs which were impossible to handle intact.

With regard to the drug content and dimensional measurements of produced discs and inserts, the amitriptyline-mucilage discs and amitriptyline-HPMC K100 discs were similar in the amount of drug taken into the discs and the discs dimensions. However, the amitriptyline-mucilage inserts and paracetamol-mucilage inserts showed less amount of drug content than amitriptyline-HPMC K100 inserts and paracetamol-HPMC K100 inserts. It was believed that this reduced amount of drug content in mucilage inserts because of the physical characteristics of mucilage inserts themselves, i.e, the fluffy texture and the fragility led to damaged parts of the inserts during measurements and that may resulted in changes of the amount of drug and insert dimensions.

The mannitol containing discs showed that mannitol did not affect the drug uptake by mucilage or HPMC K100. Therefore, paracetamol-mucilage discs, amitriptyline-mucilage, paracetamol-HPMC K100 and amitriptyline-HPMC K100 were all similar in drug content and disc diameter.

The Franz cell system was not a perfect system in these studies. Once an air bubble became entrapped underneath the filter membrane during sample withdrawal, it caused a failure of the system and stopped drug release through the membrane to the diffusion medium. Once the air was freed through the sampling port by the replacement medium, the diffusion resumed.

The positive controls % release for paracetamol was just above 50% at 5 h; amitriptyline reached its maximum of 43% at 3 h. Therefore, amitriptyline was faster to diffuse through the cellulose membranes compared to paracetamol. The physicochemical properties would be the reason and especially water solubility of amitriptyline. Water soluble drugs are generally released faster in aqueous medium than water insoluble drugs (Bogataj *et al.*, 1999).

For the comparison of the drug release profile from mucilage with that from HPMC K100, the similarity factor (f_2) which was used in the modified release dosage forms to compare the drug dissolution of tested system with a reference was employed in this study (Stevens *et al.*, 2015). For two products to be different, their similarity factor needed to be below 40. On the other hand when f_2 was above 50 the products were considered to be the same.

Comparing paracetamol release profile from mucilage with that from HPMC K100 showed that paracetamol release from mucilage inserts was not different from paracetamol release from HPMC K100 nasal inserts. Furthermore, comparing drug release profile of the amitriptyline-mucilage inserts with amitriptyline-HPMC K100

inserts did not show any difference between both. The calculated f_2 for paracetamol inserts was 43.3, and the calculated f_2 for amitriptyline nasal inserts was 43.5. Even the amitriptyline-mucilage discs did not show any difference in their % release from amitriptyline-HPMC K100 nasal discs and f_2 was 59.6 which showed similarity.

On the other hand, studying the effect of surface area on the % release of amitriptyline diffusion from inserts made by mucilage and comparing it to the discs made by mucilage, showed that the nasal inserts released only a maximum 12% of its drug content after 3 h while amitriptyline discs reached its maximum of 59% at the same time. The difference in % released of the drug was because the surface area of the insert that in contact with the diffusion medium was smaller than that area from the discs in contact with the diffusion medium (SNES) when placed on the cellulose nitrated membrane. The nasal insert was cylindrical shape with a measured diameter 5mm compared with the disc diameter of around 16 mm. Furthermore, as previously found that mucilage was a huge water sorbent and able to adsorb 50-70% of its weight and able to bind 50% of this adsorbed water, during disc preparation the amount of amitriptyline was dissolved in water which carried amitriptyline into the mucilage and 50% of the dissolved quantity was incorporated inside the mucilage particles and the rest was adsorbed on the surface of mucilage particles. The discs had a larger surface area contacting the SNES and therefore more of the drug was available to diffuse through the cellulose membrane. Moreover, the mucilage discs rapidly swelled when placed in the donor compartments of Franz cells due to absorbing SNES through the membrane. The absorbed SNES would dissolve more of amitriptyline from inside the particles. Then amitriptyline diffused out of the

mucilage particles through SNES and then diffused through the cellulose membrane to the receiver compartment of Franz cells. While the nasal inserts took longer to swell on the cellulose membrane and therefore less % of drug was dissolved and diffused at the same time.

Amitriptyline release from mucilage inserts reached the highest after 3 h while paracetamol % released from mucilage inserts reached the highest after 4 h. Furthermore, amitriptyline % released from HPMC K100 reached the maximum after 2 h while paracetamol-HPMC K100 reached its maximum % release after 3 h.

Generally mucilage drug release profile was not different from HPMC K100 drug release profile when comparing inserts with discs and when comparing paracetamol with amitriptyline.

Amitriptyline release from mannitol-mucilage discs was not different from its release from mannitol-HPMC K100 discs and, f_2 almost identical release profile of amitriptyline from mucilage and HPMC K100 contained mannitol. However, mannitol decreased the % release of amitriptyline from mucilage discs significantly from 59% for mucilage alone discs to almost 10% for mannitol contained discs. Also amitriptyline % released from HPMC K100 disc reduced from 75% for HPMC K100 alone discs to almost 10% for HPMC K100 discs contained mannitol. It seemed as mannitol prevented amitriptyline release from the discs equally and this caused the f_2 showed similarity.

The paracetamol released from mannitol contained mucilage discs showed a release that reached just over 40% at 4 h, while the HPMC K100 mannitol discs showed % release of the drug and reached the highest which is 45% at 5 h; however f_2 calculations revealed that mucilage-mannitol and HPMC K100-mannitol discs were not different in their drug release profile.

The overall % release was reduced when mannitol was incorporated to form the discs with amitriptyline. Mannitol had affected the properties of the polymer and reduced the % drug released from mucilage and HPMC K100.

Generally mucilage was only developed into drug delivery system by the addition of a plasticiser. The mucilage drug delivery system was able to take up the drugs from the solution and to incorporate it into the structure of the mucilage and release it later. Moreover, the highest % drug release from mucilage was 59% at 3 h.

Though the development of a drug delivery system using Shepherd's purse mucilage was successful, the physical strength of the mucilage system was very weak compared to HPMC K100 system. Furthermore, the drug release profile of mucilage system resembled that of HPMC. The developed drug delivery system was similar to the drug delivery system of HPMC in its drug release properties.

The drug delivery systems formed from mucilage was able to release at a slow rate. The rate of drug release from the system relied on the surface area, rate of water absorption into mucilage and swelling rate of the mucilage. Changing the surface

area of the system in contact with site of drug absorption would affect the drug release rate by changing the rate of water absorption and rate of swelling.

4.7. Conclusion

Shepherd's purse mucilage could not form a drug delivery systems compared with HPMC K100, without the addition of mannitol. Mucilage discs were easily deformed and broken when handled reducing the drug content in the discs, however the plasticiser improved the physical strength of the mucilage developed system. Mannitol served its job as expected and improved mucilage disc strength and shape while glycerol was not a suitable plasticiser for disc formation.

The mucilage drug delivery systems showed no difference from HPMC K100 in drug content and were able to take up similar amounts of the drug from solutions. The Shepherd's purse had an advantage over HPMC K100 for drug delivery system and it was the strong mucoadhesion property, therefore mucilage would suit nasal delivery better than HPMC K100. Drug delivery system using Shepherd's purse mucilage could also act as sustained release system for nasal drug delivery.

The surface area of the mucilage that was exposed to diffusion medium affected the % drug released and the rate. So the larger the surface area in contact with the diffusion medium, the better the drug release from the mucilage. Since the large surface area of the mucilage systems allowed the mucilage swelled faster and released its drug content into the diffusion medium, the ability of the developed

mucilage systems to release the drug into the medium depended upon its water absorption and swelling rate.

The drug release from mucilage discs was similar to the drug release from HPMC K100 discs. Also drug release from mucilage inserts did not show any difference from that of HPMC K100 inserts.

To sum up, the development of a drug delivery system using Shepherd's mucilage was successful by the addition of mannitol. Moreover, the extracted mucilage behaved the same way as HPMC K100 in their drug release profiles. The drug release profile for both mucilage drug delivery system and HPMC K100 drug delivery system showed similarity. The drug delivery systems developed from Shepherd's purse can be used for drug delivery.

It was believed that the drug delivery system developed using Shepherds' purse mucilage would absorb water from the nasal mucosa and swell; therefore the viscosity and rheological properties needed to be examined to scrutinise the behaviour of swollen polymer into the nasal cavity.

Chapter 5 Rheological behaviour and viscosity measurements

5.1. Introduction

Rheology is the science of flow of material and originates from the Greek word (*rheo*) to flow. The term rheology describes the science of deformation of solids and the flow of the liquids when a force is applied (Mezger, 2006).

Characterising the rheological properties of a polymer with mucoadhesive potential plays an important role in understanding the behaviour of these polymers with mucosal membranes (Madsen *et al.*, 1998b). Examining the rheological properties of dosage forms and drug delivery systems and their relationship to the site of administration especially if it is a mucosal membrane is very important because several parameters like apparent viscosity, complex viscosity, storage modulus, loss modulus, critical oscillatory stress for the dosage form and drug delivery system are affected by the mucus viscosity, body temperature and clearance rate (Madsen *et al.*, 1998a; Sriamornsak and Wattanakorn, 2008).

The rheological behaviour of fluids can be either, Newtonian, or non-Newtonian. Newtonian polymers are fluids with a viscosity that does not change with shear rate changes as shown in figure 5.1. However, non-Newtonian fluid viscosity changes upon exposure to shear rate and either the viscosity is reduced and is called shear thinning fluid or the viscosity is increased and is called shear thickening fluid (Mezger, 2006).

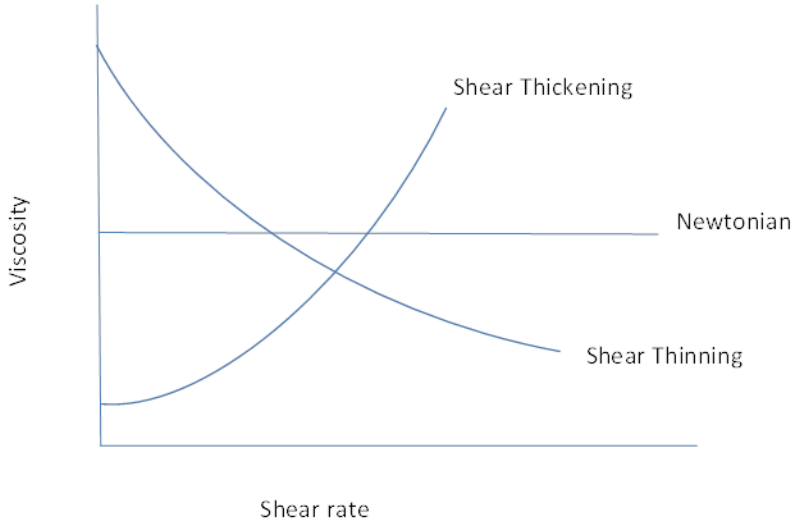

Figure 5-1 Viscosity behaviour as a function of shear rate change (Lee *et al.*, 2009).

The rheological behaviour of *Capsella bursa-pastoris* seed mucilage was studied by Deng *et.al*, (2013) through oscillatory rheological measurements on freshly secreted mucilage. They studied mucilage behaviour at different strengths ranging from 1% (w/v) to 7% (w/v) solutions, and found the storage modulus and loss modulus at low shear stress were the same. They also found that the mucilage had viscoelastic behaviour at low shear stress and it was frequency dependent at different shear stresses. Viscoelastic fluids change in shape when a stress is applied and retain their shape when the stress is removed.

5.2. Aims and Objective

The aim of this chapter was the study of the rheological behaviour and viscosity of the drug delivery system that was formed in section 4.4.2 using Shepherd's purse mucilage extracted by water maceration when contacting the nasal mucosal membrane.

The main objectives were to measure the apparent viscosity of 1%, 2% and 10% of Shepherd's purse mucilage solutions. The mucilage extracted by water maceration which was used in drug delivery study was used in this study and compared with HPMC K100.

Rheological behaviour of a polymer is best examined by oscillatory rheology testing. Since the extracted mucilage was found from chapter two to be a complex polysaccharide polymer, further viscosity changes were studied as a function of change in shear rate, and shear stress. In addition to viscosity ($\eta*$), both storage modulus (G'), and loss modulus (G") were measured by oscillatory rheology measurements. Understanding the rheology of extracted mucilage applying shear stress to the drug delivery systems formed in section 4.4.2.2 would help to understand the behaviour of the extracted mucilage in the nose especially that the mucilage showed strong mucoadhesion force.

5.3. Materials and Methods

5.3.1. Materials and Equipment

- Shepherd's purse mucilage extracted using methods described in section 2.4.2.1.
- Hydroxypropyl methylcellulose (HPMC)[3] powder K100 LV grade (lot number KK08012N21) was obtained from Dow Chemicals, USA.

[3] The letter K represents a hydroxypropyl molar substitution of 0.21 and a methoxyl degree of substitution of 1.4. The number 100 indicates the viscosity in millipascal-seconds of 2% aqueous solution at 20ºC. The suffix LV refers to special low viscosity product.

- Calcium chloride dihydrate (lot number 132450450307P81) was procured from Fulka, UK.
- Sodium chloride (analytical reagent grade, lot number 10370), D-mannitol (lot number125K009) , pectin from apple (meets USP xxiii requirements, lot number 67H16351) were all procured from Sigma-Aldrich
- Potassium chloride(lot number 0444678); procured from Fisher Scientific
- Multi-point agitation plate (Thermo Fisher Scientific Inc, USA).
- Brookfield DV-II viscometer mounted on the Helipath drive motor and a T-bar spindle
- Water bath
- Carri-Med CSL2 100 rheometer (TA Instruments, Surrey, UK) with 50 mm stainless steel plate geometry.

5.3.2. Methods

5.3.2.1. Apparent Viscosity measurement using viscometer

Solutions of 1%, 2% and 10% mucilage were prepared as well as 1%, 2% and 10% of HPMC. Apparent viscosity was measured using a Brookfield DV-II viscometer. The range of spindles were coded S91 for spindle A; S92 for spindle B; S93 for spindle C; S94 for spindle D; S95 for spindle E; and S96 for spindle F. Spindle A was usually recommended as first choice to start with, in case % torque reading was either below 2% or over 99% then the spindle needs to be changed to a smaller one. The speed was chosen 5 RPM for this experiment and the temperature was 25°C.

5.3.2.2. Rheological behaviour

Formulation containing 2% (w/w) polymer and 1% (w/w) mannitol in simulated nasal electrolyte solution (SNES) was prepared as described in section 4.4.4. The mucilage concentration used was the same concentration used to form mucilage discs and inserts used for drug delivery and release assessment (section 4.4.2.). Water maceration freeze dried mucilage was used

Viscosity was measured by flow rheometry in stepped-Ramp with a shear rate 1-100 s^{-1} at 37°C. The oscillatory measurements were tested by oscillation sweep test in different amplitude stress sweeps where the minimum stress was 1 Pa and maximum stress was 100 Pa at a constant frequency of 10 rad s−1 and constant temperature of 37°C. Also viscosity was measured by frequency sweeps in which frequency changed from 0.1 to 100 rad s−1 at 37°C.

Each sample was assessed and measured on a Carri-Med CSL2 100 rheometer in the flow mode with parallel plate geometry, with a fixed gap (1mm) showed in Figure 5.1. A 1g sample was placed on the rheometer plate and left for 180 seconds at 37°C to equilibrate.

Figure 5-2 Carri-Med CSL-200 Rheometer apparatus.

5.3.3. Statistical analysis

The collected data was analysed statistically using Minitab17 to assess any differences in the viscosity and rheological data.

5.4. Results

5.4.1. Apparent viscosity measurement using viscometer

Solutions of mucilage of 1% and 2% (w/w) strengths were very thin to detect their viscosity using Brookfield viscometer. Hence, they were not compared with the same strength HPMC K100.

However, increased mucilage solution strength to 10% (w/w) showed apparent viscosity (2072±143.36 mPa.s) lower than that of HPMC K100 (10% w/w) as shown in Table 5.1.

Table 5-1 shows the viscosity reading of 10% w/w solution. These values are mean ± SD (n=10)

	Apparent Viscosity (mPa.s)	**% Torque**	**Spindle**
Mucilage-paracetamol (1:1)	2072± 143.36	2.59± 0.18	B
HPMC K100-paracetamol (1:1)	36640± 4635	9.16± 1.16	C

5.4.2. Rheological study

Flow rheology measured the viscosity as shear rate changed for of water maceration mucilage extract was displayed in Figure 5-3.

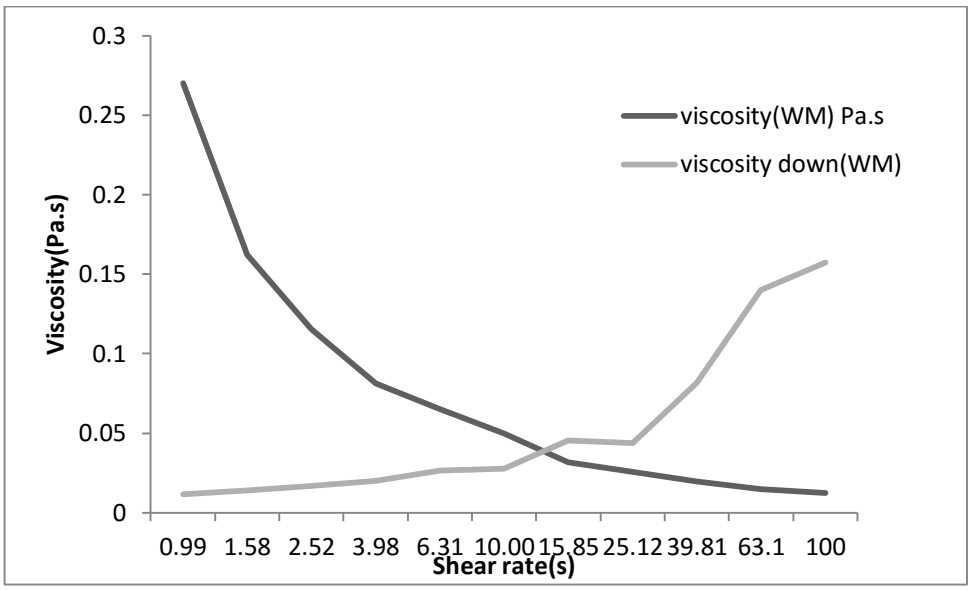

Figure 5.3 The flow rheology measurements of viscosity behaviour with shear stress changes for mucilage extracted by water maceration (WM) (n=3).

The findings for the water maceration mucilage showed that the G' and G" did not change a lot and the storage and loss modulus showed the same behaviour in Figure 5.4.

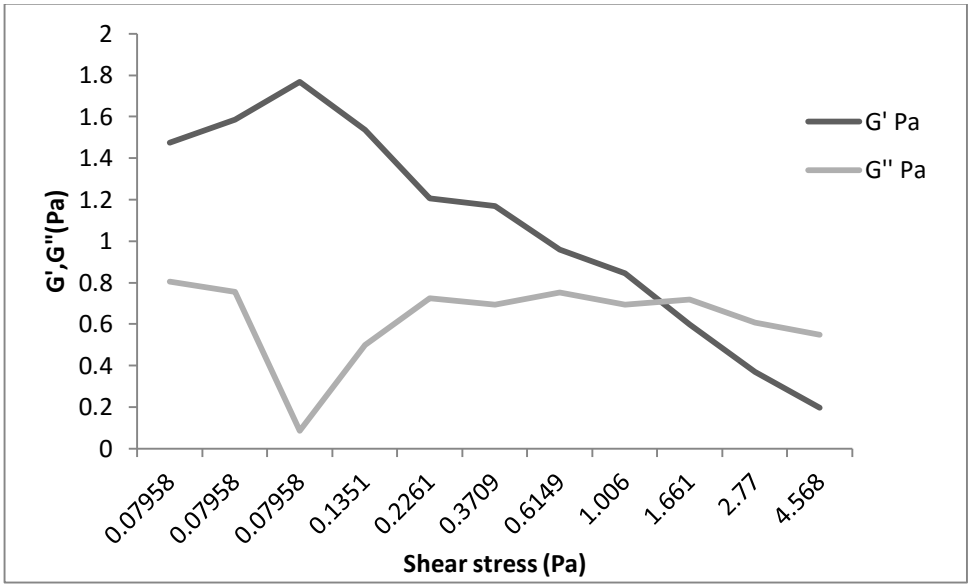

Figure 5.4 Oscillatory rheology measurements with amplitude stepped-Ramp stress for water maceration mucilage.

However, the two mucilage extracts under assessment did not show any frequency dependent changes in G' and G" moduli as shown in Figure 5.5

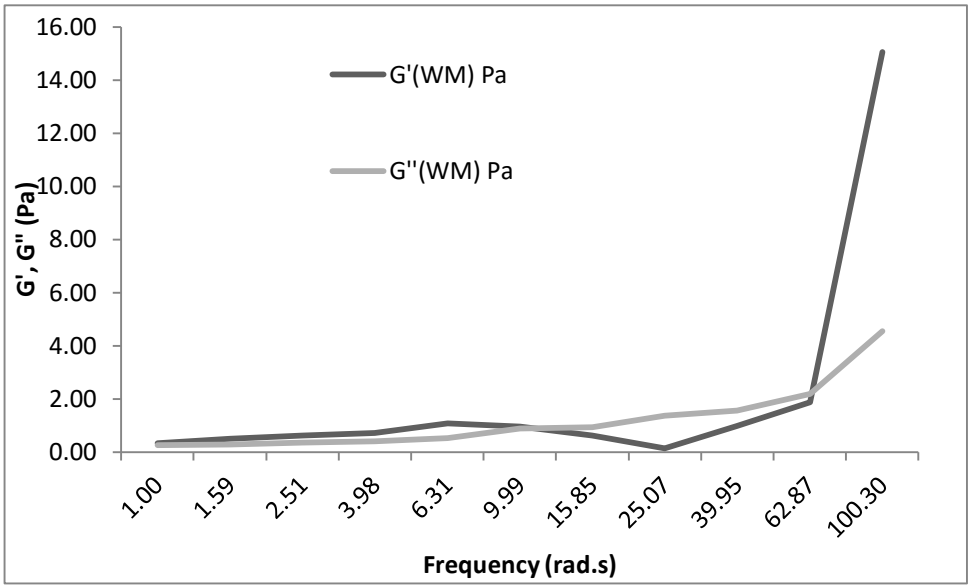

Figure 5.5 The Oscillatory rheology with frequency sweep for water maceration mucilage (WM).

5.5. Discussion

The apparent viscosity of 1% and 2% mucilage solutions could not be measured using a Brookfield viscometer, probably because the solution was very weak and during the experiment as the spindle of the viscometer turned the solution the viscosity was reduced and could not be detected by the instrument, while increasing the concentration of the mucilage up to 10% enabled detection of changes of viscosity that could be picked by the viscometer. The data showed that mucilage viscosity was less than that of HPMC K100. Additionally the measured viscosity with rheometer displayed that mucilage was decreased as a function of shear stress. The viscosity was reduced as shear rate increased, while when the shear rate reduced

the viscosity sarted to pick up and this was shown in by the viscosity down in Figure 5.3 the mucilage extract solution was shear thining.

The water maceration mucilage viscosity showed the same behaviour when the shear rate increased. The viscosity reduced as the shear rate increased and when the shear rate reduced the viscosity increased again.

Deng *et al*., (2011) studied the viscosity of 7% solution of Shepherd's purse mucilage and found it to be viscoelastic. The findings were similar to the observations of this study. Therefore, the developed drug delivery system would behave inside the nose as pseudoelastic with viscoelastic solution. The flow rheology results in this thesis confirmed that the mucilage was shear thinning, which indicated that its flow increased with the applied shear stress. The applied shear stress could result from applied forces during mixing, dosage form administration (Fennema, 1996).

To mimic the conditions in the nose, SNES was used to dissolve mucilage for the study. It was important to note that the mucilage concentration used to prepare the sample for the rheometry was the same as that used to prepare the drug delivery systems in chapter 4.

The rheology study indicated that the mucilage used to develop the drug delivery system showed pseudoelastic behaviour when in solution form. Moreover, it was assumed the developed drug delivery system from mucilage would absorb huge

amounts of water from the nasal mucosa as DVS data showed that, and form a solution with relatively lower concentration than the one used to prepare the system. As the mucilage solution in the nose would be a very low concentration, no difference in its rheology would be expected from what was examined in this study. The mucilage behaved as pectin with regard its rheological properties (Liu *et al.*, 2007). It was cited that pectin formed a viscoelastic gel, and the viscosity was affected by the DE. In other words, pectin with high DE (>50%) gelled at low pH in presence of sugar and formed weak gels. Pectin with low DE (<50%) formed strong gel with or without sugar and in presence of Ca^{+2} (Morris *et al.*, 2010). Furthermore polygalacturonic acid required a large amount of sugar at low pH (equal 3) to induce gelling (Park *et al.*, 2011).

This property was a disadvantage for the mucilage because it would be easy to clear the developed mucilage-drug system from the nose by the mucociliary movement, causing the mucilage system to be removed via the nasopharynx. However, it was assumed that mucilage systems would adhere to the mucosal membrane and prolong the residence time of the drug delivery system. In fact it was found that the mucilage drug delivery system would clear from the nose by the fast mucociliary movement before the drug release reached its target because the mucilage was pseudoplastic solution which would make the drug delivery system flow down the nose faster than needed and reduce its residence time.

5.6. Conclusion

Apparent viscosity of Shepherd's purse mucilage was very low compared with HPMC K100.

The Shepherd's purse mucilage was a shear thinning fluid and exhibited viscoelastic properties. As shear stress increased the viscosity decreased, but when the stress was removed the mucilage structure regained its shape and structure and its viscosity resumed to increase. The rheology parameter G' and G" did not change as a function of change in frequency.

These results concluded that the solution used for developing drug delivery systems from Shepherd's purse seeds was a pseudoplastic solution with viscoelastic properties. Additionally the extracted mucilage would act as pseudoplastic when dissolved inside the nose, and its viscosity would reduce the residence time with the mucociliary clearance, and the mucilage would be cleared from the nose.

Chapter 6 General conclusion and Future work

6.1. General Conclusion

The myxospermous seeds are manifested by the secretion of mucilage around the seed during germination. *Arabidopsis A.* was studied extensively as a model plant for myxospermous mucilage. This thesis studied extracted *Capsella bursa-pastoris* mucilage and how it can be employed into developing a drug delivery system targeting the nasal cavity.

Primarily, different extraction methods were used in order to extract the polysaccharide polymer from the Shepherd's purse seed without other ingredients present in the seed coat such as the fatty acids and proteins. Pure polysaccharide polymer was targeted because other ingredients in the seed coat may affect the physical and chemical properties of the polymer or may affect the mucilage behaviour with drugs.

The first extraction method was simple method and used only water at room temperature under continuous stirring. The other method was solvent maceration primarily used hexane to extract all the fatty acids in the seed coat followed by macerating the seeds with water. Furthermore, hot maceration was believed to inactivate any enzyme secreted during extraction and the seeds were extracted by water. Because it was known that heat could affect pectin different temperature (40°C, C50°C, 70°C) were used to examine the mucilage and any possible effect the temperature would make. Furthermore, the combined effect of different solvents with

temperature was examined through the hot reflux, where the seeds compounds were extracted by hexane followed by ethyl acetate, then methanol before methanol-water and finally water at 40°C. All final water extracts were collected and freeze dried. The dried mucilage was later underwent extensive studies of the physical and chemical characteristics to compare them and finding the ideal extraction method that give the polysaccharide polymer from the seed without being accompanied with other seeds compounds. The comparison study of different extracts properties showed that all the extracts showed the same property and there was no difference between the mucilage extracted with water only and solvent extracted mucilage, also when heat was involved it did not affect the properties of the mucilage. Therefore, a summarised conclusion of all physicochemical properties of the mucilage was mentioned this this part of the thesis.

The colorimetric identification of mucilage components found rhamnose and uronic acid were the major components and indicative of pectic type polymers extracted. Comparison of different extracts showed that all extraction method were successful in extracting the polysaccharide polymer.

Examining the FTIR spectra obtained from different samples of mucilage for the ester carboxyl group in the region of 1800cm^{-1} -1700cm^{-1} revealed that none of the extracts possessed peaks in that region. And it was suggested that the mucilage could be a polygalacuturonic acid. These findings were supported by NMR findings which showed facilitated the prediction intramolecular esterification lead the uronic acid to form a lactone ring through intramolecular linkage of uronic acid carboxylic group in

carbon 6 with same molecule carbon 3. And this esterification could not be detected in the same FTRI region of esterified carboxylic acid.

The vapour sorption ability of mucilage measured by DVS was found huge and capable of adsorbing 50-70% of its weight. Mucilage was able to adsorb moisture from atmosphere effectively and could be described as a sponge. However this vapour adsorption would be accompanied with crystallisation assessed by DCS at temperature below room temperature (17°C) and relative humidity as low as 10%. Mucilage was thermal unstable and lost its adsorbed moisture at 40°C when was heated in TGA.

Because the mucilage drug delivery system were targeting the nasal cavity, the mucoadhesion property was essential .it was conducted by AFM to show that the mucoadhesion power of extracted mucilage to mucin was higher than that of standard pectin and HPMC K100. These findings implicated from the measured force of adhesion of mucilage to the mucin coated mica sheets. It seemed that mucilage would be a better candidate for drug delivery system to the nasal cavity for its mucoadhesive property. It was assumed that the drug delivery system would strongly adhere to the nasal mucosal membrane and release the drug content into the nasal membrane.

Considering the properties of water sorption ability, and chemical composition, and the adhesion force, mucilage from water maceration was chosen for the development of drug delivery system and to assess its suitability for drug delivery to the nose.

The drug delivery system formed using Shepherd's purse mucilage was compared to drug delivery system using HPMC K100 for the physical properties and drug release profile. The study found that mucilage drug delivery systems succeeded only by the effect of a plasticiser which increased the strength of the mucilage system to stand handling. Additionally, mucilage drug delivery system was able to take up drugs into the developed drug delivery system as equal as HPMC K100 and to release the drug to diffuse through the cellulose membrane into the diffusion medium in the same drug release profile as HPMC K100. Therefore the developed drug delivery system using mucilage succeeded in delivering the drugs to diffusion and would be able to deliver drugs for absorption into the nasal cavity.

Moreover the drug release profile from mucilage drug delivery system can be modified by changing the surface the area of the system in contact with absorption site which was cellulose nitrate membrane in the *in vitro* study, and thereby changing the swelling rate of mucilage drug delivery system.

On the other hand, the rheological properties found that the drug delivery system developed from Shepherd's purse mucilage when dissolved in simulated nasal electrolyte solution to mimic the condition in the nasal cavity was pseudoplastic solution. As the mucociliary clearance rate of the nose was considered fast by the action of mucociliary movement, it was assumed that the drug delivery system using Shepherd's purse mucilage would be cleared out of the nose shortly after administration by the action of mucociliary movement into the nasopharynx. In the contrary, the mucilage exhibited strong mucoadhesion power to the mucin and was

believed that the drug delivery systems would adhere to the nasal mucosa stronger than HPMC K100.

In order to understand if the drug delivery system could adhere strong enough to the nasal mucosa to be able to deliver the required amount of the drug when administered into the nasal cavity before it could be washed out, needs *in vivo* study to be carried out in further work to assess the developed drug delivery system from Shepherd's purse seeds' mucilage. Further study of comparing of combined effect of mucoadhesion power and the effect of pseudoplastic property on the ability of mucilage system to adhere to the nasal mucosa and to deliver its drug content before being washed away is needed. The study can involve assessing the strength of mucoadhesion power to nasal relatively to the effect of shear stress on mucilage viscosity to reveal which effect would be stronger when the mucilage drug delivery system administered into the nasal cavity.

Finally the thesis described many of the physicochemical properties of the Shepherd's purse seeds' mucilage towards understanding the nature and behaviour of the extracted mucilage and its components. And a predicted structure of the major compound of the mucilage was reached.

The Shepherd's purse mucilage successfully formed drug delivery system able to deliver drugs to the site of administration. The developed drug delivery system was able to adhere to the nasal mucosa stronger than HPMC K100 and commercial available standard pectin; however the pseudoplastic behaviour of the mucilage used

to develop the system would lead to the system being washed out of the nasal cavity before delivering its drug content.

Therefore, more experiments were found essential to understand the *in vivo* behaviour of the drug delivery system using Shepherd's purse seeds' mucilage and they are suggested in the next part.

6.2.Future work

This thesis has helped understand many of the behaviours of *Capsella bursa-pastoris* seed mucilage. However, the outcome of some experiments were either not optimistic or were not clear; further experiments would clarify some of the ambiguity connected with the results due to the presence of a mixture of compounds in the extract. The findings of this research will light the way for next steps in understanding the adhesive property of Shepherd's purse mucilage. Some suggested experiments are discussed below.

For further characterisation of the Shepherd's seeds mucilage, it is essential to identify the different components of the extracted polymer. The identification of the components will need the polymers to be isolated from other seed components released in the mucilage. Chromatography is a suitable method to separate and isolate mixtures. Chiral column chromatography suits mixtures of compounds of different chirality and this is the expected case with a pectic polysaccharide extract (Souter, 1985). Gel permeation chromatography is suggested for separating mixtures of compounds based on their molecular weights (Anger and Berth, 1986). These two

chromatographic techniques are useful to separate different carbohydrates and widely used for pectin separation.

After the polysaccharide polymer is isolated, fractionation of the polymer to its composing units prior to further NMR studies will help to identify each fraction and assign chemical shift of atoms and their linking bonds efficiently. COSY LR NMR is suggested as previous work showed some compounds had a small *J* value along with ^{13}C J-mode NMR, ^{1}H NMR, 2D HMBC, 2D TOCSY and 2D NOESY. Further spectroscopy to reveal the molecular size of the polymer by use of Mass Spectroscopy will be useful in understanding mucilage interaction with other chemicals (Zhu *et al.*, 2014).

Further rheological studies of the extracted mucilage in mucilage-mucin mixture to examine the rheological behaviour of the mixture in the nasal cavity will enable understanding of residence time of drug delivery system using Shepherd's purse seed mucilage.

Finally *in vivo* studies of the drug delivery system using Shepherd's purse seed mucilage will reveal if the strength of the adhesion force in attaching the developing system relatively to the mucociliary clearance rate will hold the drug delivery system on the mucosa for the required time to deliver its drug content.

Lastly, the thesis concludes that Shepherds' purse seeds secreted mucilage that contains a polysaccharide polymer. It was found that this polymer was not pectin but

instead it was polygalact/glucuronic acid with a tendency to form galact/glucurononlactone. This polymer resembled polygatacturonic acid described in the literature (Liu *et al.*, 2007; Morris *et al.*, 2010; Park *et al.*, 2011); however the mucilage was different from standard pectin in many properties like mucoadhesion. The use of natural polymers is widely studied for drug delivery and any decision of suitability of this mucilage for drug delivery system would need careful isolation and would depend on the outcomes of *in vivo* studies which will illustrate the behaviour of mucilage inside the nasal cavity.

References

ACCILI, D., MENGHI, G., BONACUCINA, G., MARTINO, P. D. & PALMIERI, G. F. (2004). Mucoadhesion Dependence of Pharmaceutical Polymers on Mucosa Characteristics. *European Journal of Pharmaceutical Sciences,* 22**,** 225-234.

ACTON, Q. A. (2012). *Advances in Imaging Technology Research and Application: 2012 Edition,* ScholarlyEditions.

AGRAWAL, A. M., MANEK, R. V., KOLLING, W. M. & NEAU, S. H. (2004). Water Distribution Studies within Microcrystalline Cellulose and Chitosan Using Differential Scanning Calorimetry and Dynamic Vapor Sorption Analysis. *Journal of Pharmaceutical Sciences,* 93**,** 1766-1779.

AKSOY, A., DIXON, J. M. & HALE, W. H. G. (1998). Capsella Bursa-Pastoris (L.) Medikus (Thlaspi Bursa-Pastoris L., Bursa Bursa-Pastoris (L.) Shull, Bursa Pastoris (L.) Weber) *Journal of Ecology,* 86 pp. 171-18.

AKSOY, A., HALE, W. H. G. & DIXON, J. M. (1999). Capsella Bursa-Pastoris (L.) Medic. As a Biomonitor of Heavy Metals. *The Science of The Total Environment,* 226**,** 177-186.

ALHALAWEH, A., ANDERSSON, S. & VELAGA, S. P. (2009). Preparation of Zolmitriptan–Chitosan Microparticles by Spray Drying for Nasal Delivery. *European Journal of Pharmaceutical Sciences,* 38**,** 206-214.

ALLEN, L. V., POPOVICH, N. & ANSEL, H. C. (2011). *Ansel's Pharmaceutical Dosage Forms and Drug Delivery Systems* Baltimore, Lippincott Williams &Wiilkins, a Wolters Kluwer business.

ANDREASEN, C. & SKOVGAARD, I. M. (2009). Crop and Soil Factors of Importance for the Distribution of Plant Species on Arable Fields in Denmark. *Agriculture, Ecosystems & Environment,* 133**,** 61-67.

ANGER, H. & BERTH, G. (1986). Gel Permeation Chromatography and the Mark-Houwink Relation for Pectins with Different Degrees of Esterification. *Carbohydrate Polymers,* 6**,** 193-202.

BARROS, A. S., MAFRA, I., FERREIRA, D., CARDOSO, S., REIS, A., LOPES DA SILVA, J. A., DELGADILLO, I., RUTLEDGE, D. N. & COIMBRA, M. A. (2002). Determination of the Degree of Methylesterification of Pectic

Polysaccharides by Ft-Ir Using an Outer Product Pls1 Regression. *Carbohydrate Polymers,* 50**,** 85-94.

BASU, S., CHAKRABATPRTY, S. & BANDYOPADHYAY, A. K. (2009). Development and Evaluation of a Mucoadhesive Nasal Gel of Midazolam Prepared with Linum Usitatissimum L. Seed Mucilage. *Scientia Phamaceutica,* 77**,** 899-910.

BERGER, W. E., JACOBS, R. L., AMAR, N. J., TANTRY, S. K., LI, J. & SMALL, C. J. (2015). Efficacy and Safety of Beclomethasone Dipropionate Nasal Aerosol in Children with Perennial Allergic Rhinitis. *Annals of Allergy, Asthma & Immunology,* 115**,** 130-136.

BNF 2015. (Fluticasone Propionate). *British Natioanl Formulary.* BMJ Group and the Royal Pharmaceutical Society of Great Britain

BOATENG, J. S. (2005). *Development of Formulations for Delivery of Drugs to Wounds* Ph. D., University of Strathclyde.

BOGATAJ, M., MRHAR, A. & KOROÅ¡EC, L. (1999). Influence of Physicochemical and Biological Parameters on Drug Release from Microspheres Adhered on Vesical and Intestinal Mucosa. *International Journal of Pharmaceutics,* 177**,** 211-220.

BRAR, V. & KAUR, G. (2014). Biopolymers as Carriers for Nasal Drug Delivery. *Polymer-Plastics Technology and Engineering,* 53**,** 1518-1531.

BROWNE, C. A. (1912). *A Handbook of Sugar Analysis: A Practical and Descriptive Treatise for Use in Research, Technical and Control Laboratories* New York, John Wiley & Sons.

BROWNE, C. A. & ZERBAN, F. W. (1941). *Physical and Chemical Methods of Sugar Analysis: A Practical and Descriptive Treatise for Use in Research, Technical and Control Laboratories,* New York, Jonh Wiley & Sons.

BYFIELD, A. J. W., P. J. 2005. (Important Arable Plant Areas: Identifying Priority Sites for Arable Plant Conservation in the United Kingdom.). *In:* INTERNATIONAL, P. (ed.). Salisbury, UK.

CAFFALL, K. H., PATTATHIL, S., PHILLIPS, S. E., HAHN, M. G. & MOHNEN, D. (2009). Arabidopsis Thaliana T-DNA Mutants Implicate Gaut Genes in

the Biosynthesis of Pectin and Xylan in Cell Walls and Seed Testa. *Molecular Plant,* 2**,** 1000-1014.

CHANDER, V. (2012). *Assessment of Drug Delivery Potential of a Natural Fibre.* MSc, Strathclyde University.

CHATJIGAKIS, A. K., PAPPAS, C., N.PROXENIA, O.KALANTZI, P.RODIS & POLISSIOU, M. (1998). Ft-Ir Spectroscopic Determination of the Degree of Esterification of Cell Wall Pectins from Stored Peaches and Correlation to Textural Changes. *Carbohydrate Polymers,* 37**,** 395-408.

CHUGH, Y., KAPOOR, P. & KAPOOR, A. (2009). Intranasal Drug Delivery: A Novel Approach. *Indian Journal of Otolaryngology and Head & Neck Surgery,* 61**,** 90-94.

CLEMENTS, D. R., DITOMMASO, A., JORDAN, N., BOOTH, B. D., CARDINA, J., DOOHAN, D., MOHLER, C. L., MURPHY, S. D. & SWANTON, C. J. (2004). Adaptability of Plants Invading North American Cropland. *Agriculture, Ecosystems & Environment,* 104**,** 379-398.

CORNAZ, A. L., DE ASCENTIS, A., COLOMBO, P. & BURI, P. (1996). In Vitro Characteristics of Nicotine Microspheres for Transnasal Delivery. *International Journal of Pharmaceutics,* 129**,** 175-183.

DATTA, R. & BANDYOPADHYAY, A. K. (2005). Development of a New Nasal Drug Delivery System of Diazepam with Natural Mucoadhesive Agent from *Trigonella Foenum-Graecum* L. *Journal of Scientific and Industrial Research,* 64**,** 973-977.

DATTA, R. & BANDYOPADHYAY, A. K. (2006). A New Drug Delivery System for Diazepam Using Natural Mucoadhesive Polysaccharide Obtained from Tamarid Seeds. *Saudi Pharmaceutical Journal,* 14**,** 115-119.

DEACON, M. P., MCGURK, S., ROBERTS, C. J., WILLIAMS, P. M., TENDLER, S. J., DAVIES, M. C., DAVIS, S. S. & HARDING, S. E. (2000). Atomic Force Microscopy of Gastric Mucin and Chitosan Mucoadhesive Systems. *Biochem J.,* 348**,** 557-563. .

DENG, W., HALLETT, P. D., JENG, D. S., SQUIRE, G. R., TOOROP, P. E. & IANNETTA, P. P. (2015). The Effect of Natural Seed Coatings of Capsella

Bursa-Pastoris L. Medik.(Shepherd's Purse) on Soil-Water Retention, Stability and Hydraulic Conductivity. *Plant and Soil,* 387**,** 167-176.

DENG, W., JENG, D.-S., TOOROP, P. E., SQUIRE, G. R. & IANNETTA, P. P. M. (2012). A Mathematical Model of Mucilage Expansion in Myxospermous Seeds of Capsella Bursa-Pastoris (Shepherd's Purse). *Annals of Botany,* 109**,** 419-427.

DJUPESLAND, P. G. (2013). Nasal Drug Delivery Devices: Characteristics and Performance in a Clinical Perspective—a Review. *Drug Delivery and Translational Research,* 3**,** 42-62.

DONOVAN, M. D. & HUANG, Y. (1998). Large Molecule and Particulate Uptake in the Nasal Cavity: The Effect of Size on Nasal Absorption. *Advanced Drug Delivery Reviews,* 29**,** 147-155.

DUBOLAZOV, A. V., NURKEEVA, Z. S., MUN, G. A. & KHUTORYANSKIY, V. V. (2006). Design of Mucoadhesive Polymeric Films Based on Blends of Poly(Acrylic Acid) and (Hydroxypropyl)Cellulose. *Biomacromolecules,* 7**,** 1637-1643.

DUCHÊNE, D. & PONCHEL, G. (1997). Bioadhesion of Solid Oral Dosage Forms, Why and How? *European Journal of Pharmaceutics and Biopharmaceutics,* 44**,** 15-23.

EINHORN-STOLL, U., KUNZEK, H. & DONGOWSKI, G. (2007). Thermal Analysis of Chemically and Mechanically Modified Pectins. *Food Hydrocolloids,* 21**,** 1101-1112.

FDA 2002. (Guidance for Industry – Nasal Spray and Inhalation Solution, Suspension, and Spray Drug Products – Chemistry, Manufacturing, and Controls Documentation). *In:* FDA (ed.). Center for Drug Evaluation and Research.

FENNEMA, O. R. (1996). *Food Chemistry, Third Edition*, Taylor & Francis.

FILISETTI-COZZI, T. M. C. C. & CARPITA, N. C. (1991). Measurement of Uronic Acids without Interference from Neutral Sugars. *Analytical Biochemistry,* 197**,** 157-162.

FORD, J. L. (1999). Thermal Analysis of Hydroxypropylmethylcellulose and Methylcellulose: Powders, Gels and Matrix Tablets. *International Journal of Pharmaceutics,* 179**,** 209-228.

FRANCOZ, E., RANOCHA, P., BURLAT, V. & DUNAND, C. (2015). Arabidopsis Seed Mucilage Secretory Cells: Regulation and Dynamics. *Trends in Plant Science,* 20**,** 515-524.

FU, Y. & KAO, W. J. (2010). Drug Release Kinetics and Transport Mechanisms of Non-Degradable and Degradable Polymeric Delivery Systems. *Expert Opinion on Drug Delivery,* 7**,** 429-444.

GABA, P., SINGH, S., GABA, M. & GUPTA, G. D. (2011). Galactomannan Gum Coated Mucoadhesive Microspheres of Glipizide for Treatment of Type 2 Diabetes Mellitus: In Vitro and in Vivo Evaluation. *Saudi Pharmaceutical Journal,* 19**,** 143-152.

GNANASAMBANDAM, R. & PROCTOR, A. (2000). Determination of Pectin Degree of Esterification by Diffuse Reflectance Fourier Transform Infrared Spectroscopy. *Food Chemistry,* 68**,** 327-332.

GONDA, I. (1998). Mathematical Modeling of Deposition and Disposition of Drugs Administered Via the Nose. *Advanced Drug Delivery Reviews,* 29**,** 179-184.

GRUBERT, M. (1974). Studies on the Distribution of Myxospermy among Seeds and Fruits of Angiospermae and Its Ecological Importance. *Acta Biol, Venez,* 8**,** 315-551.

GUO, R., DU, X., ZHANG, R., DENG, L., DONG, A. & ZHANG, J. (2011). Bioadhesive Film Formed from a Novel Organic–Inorganic Hybrid Gel for Transdermal Drug Delivery System. *European Journal of Pharmaceutics and Biopharmaceutics,* 79**,** 574-583.

GURNY, R. & LENAERTS, V. (1990). *Bioadhesive Drug Delivery Systems* Boca Raton, Fla., CRC Press.

HAGESAETHER, E. (2011). Permeation Modulating Properties of Natural Polymers – Effect of Molecular Weight and Mucus. *International Journal of Pharmaceutics,* 409**,** 150-155.

HAMMER, A. 2010. (Thermal Analysis of Polymers.Part 1: Dsc of Thermoplastics). *Thermal analysis of users. Usercom 31.* Mettelr Toledo.

HAMMER, A. 2011. (Thermal Analysis of Polymers. Part 3: Dsc of Thermosets). *Mettler Toledo information for users. Usercom 33.*: Mettler Toledo.

HAMMER, A., FEDELICH, N., GIANI, S., HEMPEL, E., JING, N., NIJMAN, M., RIESEN, R., SCHAWE, J. & SCHUBNELL, M. 2013. (Thermal Analysis of Polymers-Selected Applications). Mettler Toledo.

HARHOLT, J., SUTTANGKAKUL, A. & VIBE SCHELLER, H. (2010). Biosynthesis of Pectin. *Plant Physiology,* 153**,** 384-395.

HARRIS, A. S., NILSSON, I. M., G-.WAGNER, Z. & ALKNER, U. (1986). Intranasal Administration of Peptides: Nasal Deposition, Biological Response, and Absorption of Desmopressin. *Journal of Pharmaceutical Sciences,* 75**,** 1085-1088.

HAUGHN, G. & CHAUDHURY, A. (2005). Genetic Analysis of Seed Coat Development in Arabidopsis. *Trends in Plant Science,* 10**,** 472-477.

HAWES, C., BEGG, G. S., SQUIRE, G. R. & IANNETTA, P. P. M. (2005). Individuals as the Basic Accounting Unit in Studies of Ecosystem Function: Functional Diversity in Shepherd's Purse, Capsella. *Oikos,* 109**,** 521-534.

HINTZ, M., BARTHOLMES C., NUTT P., ZIERMAN J., HAMEISTER S., NEUFFER B. & G., T. (2006). Catching a 'Hopeful Monster': Shepherd's Purse (Capsella Bursa-Pastoris) as a Model System to Study the Evolution of Flower Development. . *Journal of Experimental Botany* 57**,** pp 3531-3542.

HMPC 2010. (Assessment Report on Capsella Bursa-Pastoris (L.) Medikus, Herba). *In:* (HMPC), C. O. H. M. P. (ed.). London European Medicines Agency.

HONG, Z., CHASAN, B., BANSIL, R., TURNER, B. S., BHASKAR, K. R. & AFDHAL, N. H. (2005). Atomic Force Microscopy Reveals Aggregation of Gastric Mucin at Low Ph. *Biomacromolecules,* 6**,** 3458-3466.

HURKA, H., BLEEKER, W. & NEUFFER, B. (2003). Evolutionary Processes Associated with Biological Invasions in the Brassicaceae. *Biological Invasions,* 5**,** 281-292.

HURKA, H. & NEUFFER, B. (1997). Evolutionary Processes in the Genus Capsella (Brassicaceae). *Plant Systematics and Evolution,* 206**,** 295-316.

HUSSAIN, A. A., BAWARSHI-NASSAR, R. & HUANG, C. H. (1985). Physicochemical Consideration in Intranasal Drug Adminstration. *In:*

CHIEN, Y. W. (ed.) *Transnasal Systemic Medications.* Amesterdam: Elsiever.

IANNETTA, P., BEGG, G., HAWES, C., YOUNG, M., RUSSELL, J. & SQUIRE, G. (2007a). Variation in Capsella (Shepherd's Purse): An Example of Intraspecific Functional Diversity. *Physiologia Plantarum,* 129**,** 542-554.

IANNETTA, P., VALENTINE, T., HOLMAN, T., WELLS, D., DOBSON, G., SHEPHERD, T., DENG, W., JENG, D.-S., CARRERA, L., WISHART, J., SQUIRE, G. & TOOROP, P. 2010. (Mucilage Expansion on the Testa Surface of Myxospermous Seeds from Capsella Bursa Pastoris L. Medic (Shepherd's Purse): A Novel Plant Fibre Motor.). *New Phytologist.*

IANNETTA, P. M. (2011). Capsella. *In:* KOLE, C. (ed.) *Wild Crop Relatives: Genomic and Breeding Resources.* Springer Berlin Heidelberg.

IANNETTA, P. P. M., BEGG, G., HAWES, C., YOUNG, M., RUSSELL, J. & SQUIRE, G. R. (2007b). Variation in Capsella (Shepherd's Purse): An Example of Intraspecific Functional Diversity. *Physiologia Plantarum* 129**,** 542-554.

ILLUM, L. (2003). Nasal Drug Delivery—Possibilities, Problems and Solutions. *Journal of Controlled Release,* 87**,** 187-198.

JAAFARI, M. R., TAFAGHODIA, M. & TABASSI, S. A. (2005). Evaluation of the Clearance Characteristics of Liposomes in the Human Nose by Gamma-Scintigraphy. *Iranian Journal of pharmaceutical research,* 4**,** 3-11.

JOERGENSEN, L., KLOSGEN, B., SIMONSEN, A. C., BORCH, J. & HAGESAETHER, E. (2011). New Insights into the Mucoadhesion of Pectins by Afm Roughness Parameters in Combination with Spr. *International Journal of Pharmaceutics,* 411**,** 162-168.

JÖRIMANN, U., BENZLER, B., DEBUHR, J., RIESEN, R. & WIDMANN, G. 1996. (Investigating Unknown Samples). *Information for users of METTLER-TOLEDO thermal analysis systems.User Com 3.*: Mettler Toldeo.

KAČURÁKOVÁ, M., CAPEK, P., SASINKOVÁ, V., WELLNER, N. & EBRINGEROVÁ, A. (2000). Ft-Ir Study of Plant Cell Wall Model Compounds: Pectic Polysaccharides and Hemicelluloses. *Carbohydrate Polymers,* 43**,** 195-203.

KAČURÁKOVÁ, M. & WILSON, R. H. (2001). Developments in Mid-Infrared Ft-Ir Spectroscopy of Selected Carbohydrates. *Carbohydrate Polymers,* 44**,** 291-303.

KADAJJI, V. G. & BETAGERI, G. V. (2011). Water Soluble Polymers for Pharmaceutical Applications. *Polymers,* 3.

KAHUTHIA-GATHU, R., LOHR, B., POEHLING, H. M. & MBUGUA, P. K. (2009). Diversity, Distribution and Role of Wild Crucifers in Major Cabbage and Kale Growing Areas of Kenya. *Bulletin of Entomological Research,* 99**,** 287-297.

KARLEY, A. J., HAWES, C., IANNETTA, P. P. M. & SQUIRE, G. R. (2008). Intraspecific Variation in Capsella Bursa-Pastoris in Plant Quality Traits for Insect Herbivores. *Weed Research,* 48**,** 147-156.

KHARENKO, E., LARIONOVA, N. & DEMINA, N. (2008). Mucoadhesive Drug Delivery Systems: Quantitative Assessment of Interaction between Synthetic and Natural Polymer Films and Mucosa. *Pharmaceutical Chemistry Journal,* 42**,** 392-399.

KHUTORYANSKAYA, O. V., POTGIETER, M. & KHUTORYANSKIY, V. V. (2010). Multilayered Hydrogel Coatings Covalently-Linked to Glass Surfaces Showing a Potential to Mimic Mucosal Tissues. *Soft Matter,* 6**,** 551-557.

KHUTORYANSKIY, V. V. (2007). Hydrogen-Bonded Interpolymer Complexes as Materials for Pharmaceutical Applications. *International Journal of Pharmaceutics,* 334**,** 15-26.

KHUTORYANSKIY, V. V. (2011). Advances in Mucoadhesion and Mucoadhesive Polymers. *Macromolecular Bioscience,* 11**,** 748-764.

KIMURA, R., MIWA, M., KATO, Y., SATO, M. & YAMADA, S. (1991). Relationship between Nasal Absorption and Physicochemical Properties of Quaternary Ammonium Compounds. *Archives internationales de pharmacodynamie et de therapie,* 310**,** 13-21.

KNEZEVIC, S. Z., DATTA, A., SCOTT, J. & CHARVAT, L. D. (2010). Application Timing and Adjuvant Type Affected Saflufenacil Efficacy on Selected Broadleaf Weeds. *Crop Protection,* 29**,** 94-99.

KUBLIK, H. & VIDGREN, M. T. (1998). Nasal Delivery Systems and Their Effect on Deposition and Absorption. *Advanced Drug Delivery Reviews,* 29**,** 157-177.

KUOTSU, K. & BANDYOPADHYAY, A. K. (2007). Development of Oxytocin Nasal Gel Using Natural Mucoadhesive Agent Obtained from the Fruits of Dellinia Indica. L. *ScienceAsia* 33**,** 57-60.

KUSHWAHA, S. K. S., KESHARI, R. K. & RAI, A. K. (2011). Advances in Nasal Trans-Mucosal Drug Delivery. *Journal of Applied Pharamceutical Science,* 01 21-28.

LABIRIS, N. R. & DOLOVICH, M. B. (2003). Pulmonary Drug Delivery. Part I: Physiological Factors Affecting Therapeutic Effectiveness of Aerosolized Medications. *British Journal of Clinical Pharmacology,* 56**,** 588-599.

LAFFORGUE, C., MARTY, J., FENINA, N. & MUSTAPHA, R. (2011). Influence of Drug Concentration on the Diffusion Parameters of Caffeine. *Indian Journal of Pharmacology,* 43**,** 157-162.

LAMPMAN, G. M. (2010). *Spectroscopy,* Australia ; United States : Brooks/Cole Cengage Learning.

LE, D. T. L., TRAN, T.-L., DUVIAU, M.-P., MEYRAND, M., GUÉRARDEL, Y., CASTELAIN, M., LOUBIÈRE, P., CHAPOT-CHARTIER, M.-P., DAGUE, E. & MERCIER-BONIN, M. (2013). Unraveling the Role of Surface Mucus-Binding Protein and Pili in Muco-Adhesion of *Lactococcus Lactis*. *PLoS One,* 8**,** e79850.

LEE, C. H., MOTURI, V. & LEE, Y. (2009). Thixotropic Property in Pharmaceutical Formulations. *Journal of Controlled Release,* 136**,** 88-98.

LEVEQUE, N., MAKKI, S., HADGRAFT, J. & HUMBERT, P. (2004). Comparison of Franz Cells and Microdialysis for Assessing Salicylic Acid Penetration through Human Skin. *International Journal of Pharmaceutics,* 269**,** 323-328.

LINDBERG, S. (1994). Morphological and Functional Studies of the Mucociliary System During Infections in the Upper Airways. *Acta Oto-laryngologica,* 114**,** 22-25.

LIU, L., FISHMAN, M. & HICKS, K. (2007). Pectin in Controlled Drug Delivery – a Review. *Cellulose,* 14**,** 15-24.

MACQUET, A., RALET, M.-C., KRONENBERGER, J., MARION-POLL, A. & NORTH, H. M. (2007). In Situ, Chemical and Macromolecular Study of the Composition of Arabidopsis Thaliana Seed Coat Mucilage. *Plant and Cell Physiology,* 48**,** 984-999.

MADSEN, F., EBERTH, K. & SMART, J. D. (1998a). A Rheological Assessment of the Nature of Interactions between Mucoadhesive Polymers and a Homogenised Mucus Gel. *Biomaterials,* 19**,** 1083-1092.

MADSEN, F., EBERTH, K. & SMART, J. D. (1998b). A Rheological Examination of the Mucoadhesive/Mucus Interaction: The Effect of Mucoadhesive Type and Concentration. *Journal of Controlled Release,* 50**,** 167-178.

MAHAJAN, H. S., SHAH, S. K. & SURANA, S. J. (2011). Nasal in Situ Gel Containing Hydroxy Propyl B-Cyclodextrin Inclusion Complex of Artemether: Development and in Vitro Evaluation. *J Incl Phenom Macrocycl Chem,* 70**,** 49-58.

MALVIYA, R., SRIVASTAVA, P. & KULKARNI, G. T. (2011). Applications of Mucilages in Drug Delivery - a Review. *Advances in Biological Research,* 5**,** 01-07.

MANRIQUE, G. D. & LAJOLO, F. M. (2002). Ft-Ir Spectroscopy as a Tool for Measuring Degree of Methyl Esterification in Pectins Isolated from Ripening Papaya Fruit. *Postharvest Biology and Technology,* 25**,** 99-107.

MARIEB, E. (2003). *Essential of Human Anatomy and Physiology*, San Francisco, Benjamin Cummings.

MARTTIN, E., SCHIPPER, N. G. M., VERHOEF, J. C. & MERKUS, F. W. H. M. (1998). Nasal Mucociliary Clearance as a Factor in Nasal Drug Delivery. *Advanced Drug Delivery Reviews,* 29**,** 13-38.

MCCANN, M. C., SHI, J., ROBERTS, K. & CARPITA, N. C. (1994). Changes in Pectin Structure and Localization During the Growth of Unadapted and Naci-Adapted Tobacco Cells. *The Plant Journal* 5**,** 773-785.

MCFEETERS, R. F. 1985. (Changes in Pectin and Cellulose During Processing). *Chemical changes in food during processing.*

MCINNES, F. (2003). *In - Vitro and in - Vivo Properties of a Lyophilised Nasal Dosage System.* Ph. D, University of Strathclyde

MCINNES, F., BAILLIE, A. J. & STEVENS, H. N. E. (2007). The Use of Simple Dynamic Mucosal Models and Confocal Microscopy for the Evaluation of Lyophilised Nasal Formulations. *Journal of Pharmacy and Pharmacology,* 59**,** 759-767.

MCINNES, F. J., THAPA, P., BAILLIE, A. J., WELLING, P. G., WATSON, D. G., GIBSON, I., NOLAN, A. & STEVENS, H. N. E. (2005). In Vivo Evaluation of Nicotine Lyophilised Nasal Insert in Sheep. *International Journal of Pharmaceutics,* 304**,** 72-82.

MEDLINEPLUS. (2010). *Cyanocobalamin Nasal* [Online]. American Society of Health-System Pharmacists, Inc. Available: https://www.nlm.nih.gov/medlineplus/druginfo/meds/a604029.html.

MEZGER, T. G. (2006). *The Rheology Handbook: For Users of Rotational and Oscillatory Rheometers,* Vincentz Network.

MONSOOR, M. A., KALAPATHY, U. & PROCTOR, A. (2001). Determination of Polygalacturonic Acid Content in Pectin Extracts by Diffuse Reflectance Fourier Transform Infrared Spectroscopy. *Food Chemistry,* 74**,** 233-238.

MORRIS, G. A., FOSTER, T. J. & HARDING, S. E. (2000). The Effect of the Degree of Esterification on the Hydrodynamic Properties of Citrus Pectin. *Food Hydrocolloids,* 14**,** 227-235.

MORRIS, G. A., KOK, M. S., HARDING, S. E. & ADAMS, G. G. (2010). Polysaccharide Drug Delivery Systems Based on Pectin and Chitosan. *Biotechnology and Genetic Engineering Reviews, Vol 27.* Loughborough: Nottingham University Press.

MOSER, B. R., WINKLER-MOSER, J. K., SHAH, S. N. & VAUGHN, S. F. (2010). Composition and Physical Properties of Arugula, Shepherd's Purse, and Upland Cress Oils. *European Journal of Lipid Science and Technology,* 112**,** 734-740.

MUKHERJEE, K., KIEWITT, I. & HURKA, H. (1984). Lipid Content and Fatty Acid Composition of Seeds of Capsella Species from Different Geographical Locations. *Phytochemistry,* 23**,** 117-119.

NA, L., MAO, S., WANG, J. & SUN, W. (2010). Comparison of Different Absorption Enhancers on the Intranasal Absorption of Isosorbide Dinitrate in Rats. *International Journal of Pharmaceutics,* 397**,** 59-66.

NAVARRO, T., EL OUALIDI, J., TALEB, M. S., PASCUAL, V. & CABEZUDO, B. (2009). Dispersal Traits and Dispersal Patterns in an Oro-Mediterranean Thorn Cushion Plant Formation of the Eastern High Atlas, Morocco. *Flora - Morphology, Distribution, Functional Ecology of Plants,* 204**,** 658-672.

NEWALL, C. A., ANDERSON, L. A. & PHILLIPSON, J. D. (1996). *Herbal Medicines: A Guide for Health- Care Professionals,* London, The Pharmaceutical Press.

NG, S.-F., ROUSE, J., SANDERSON, F., MEIDAN, V. & ECCLESTON, G. (2010). Validation of a Static Franz Diffusion Cell System for ≪I≫in Vitro≪/I≫ Permeation Studies. *AAPS PharmSciTech,* 11**,** 1432-1441.

NGWULUKA, N. C., OCHEKPE, N. A. & ARUOMA, O. I. (2014). Naturapolyceutics: The Science of Utilizing Natural Polymers for Drug Delivery. *Polymers,* 6**,** 1312-1332.

NING, Y.-C. (2011). *Interpretation of Organic Spectra,* Hoboken, NJ : Wiley.

NOKHODCHI, A., FORD, J. L. & RUBINSTEIN, M. H. (1997). Studies on the Interaction between Water and (Hydroxypropyl)Methylcellulose. *Journal of Pharmaceutical Sciences,* 86**,** 608-615.

NORTH, H., BAUD, S., DEBEAUJON, I., DUBOS, C., DUBREUCQ, B., GRAPPIN, P., JULLIEN, M., LEPINIEC, L., MARION-POLL, A., MIQUEL, M., RAJJOU, L., ROUTABOUL, J.-M. & CABOCHE, M. (2010). Arabidopsis Seed Secrets Unravelled after a Decade of Genetic and Omics-Driven Research. *The Plant Journal,* 61**,** 971-981.

NORTH, H. M., BERGER, A., SAEZ-AGUAYO, S. & RALET, M.-C. (2014). Understanding Polysaccharide Production and Properties Using Seed Coat Mutants: Future Perspectives for the Exploitation of Natural Variants. *Annals of Botany,* 114**,** 1251-1263.

NOVOSEL'SKAYA, I. L., VOROPAEVA, N. L., SEMENOVA, L. N. & RASHIDOVA, S. S. (2000). Trends in the Science and Applications of Pectins. *Chemistry of Natural Compounds,* 36**,** 1-10.

O'NEILL, M. A., ISHII, T., ALBERSHEIM, P. & DARVILL, A. G. (2004). Rhamnogalacturonan Ii: Structure and Function of a Borate Cross-Linked Cell Wall Pectic Polysaccharide. *Annual Review of Plant Biology,* 55**,** 109-139.

OMICRON. (2014). *D-[1-13c]Galactose* [Online]. Omicron Biochemicals, Inc. Available: http://www.omicronbio.com/obdata.html 2015].

ORAHILLY, R., MULLER, F., CARPENTER, S. & SWENSON, R. (2008). The Nose and Paranasal Sinuses. *In:* SWENSON, R. (ed.) *Basic Human Anatomy.*: Dartmouth Medical School.

OZSOY, Y., GUNGOR, S. & CEVHER, E. (2009). Nasal Delivery of High Molecular Weight Drugs. *Molecules* 14.

PARK, H., PARK, K. & SHALABY, W. S. W. (2011). *Biodegradable Hydrogels for Drug Delivery*, Taylor & Francis.

PATIL, S. B. & SAWANT, K. K. (2011). Chitosan Microspheres as a Delivery System for Nasal Insufflation. *Colloids and Surfaces B: Biointerfaces,* 84**,** 384-389.

PDR 1987. (Physicians Desk Reference). 41st ed ed. Oradell, N.J: Medical Economics Company.

PENFIELD, S., MEISSNER, R. C., SHOUE, D. A., CARPITA, N. C. & BEVAN, M. W. (2001). Myb61 Is Required for Mucilage Deposition and Extrusion in the Arabidopsis Seed Coat. *The Plant Cell,* 13**,** 2777-2791.

PHANER-GOUTORBE, M., DUGAS, V., CHEVOLOT, Y. & SOUTEYRAND, E. (2011). Silanization of Silica and Glass Slides for DNA Microarrays by Impregnation and Gas Phase Protocols: A Comparative Study. *Materials Science and Engineering: C,* 31**,** 384-390.

PHILLIPS, D. J., PYGALL, S. R., COOPER, V. B. & MANN, J. C. (2012). Overcoming Sink Limitations in Dissolution Testing: A Review of Traditional Methods and the Potential Utility of Biphasic Systems. *Journal of Pharmacy and Pharmacology,* 64**,** 1549-1559.

PILLAI, O. & PANCHAGNULA, R. (2001). Polymers in Drug Delivery. *Current Opinion in Chemical Biology,* 5**,** 447-451.

PIRES, A., FORTUNA, A., ALVES, G. & FALCÃO, A. (2009). Intranasal Drug Delivery: How, Why and What For? *J Pharm Pharmaceut Sci,* 12**,** 288-311.

PONCHEL, G., TOUCHARD, F., WOUESSIDJEWE, D., DUCHÊNE, D. & PEPPAS, N. A. (1987). Bioadhesive Analysis of Controlled-Release Systems. Iii. Bioadhesive and Release Behavior of Metronidazole-Containing Poly(Acrylic Acid)-Hydroxypropyl Methylcellulose Systems. *International Journal of Pharmaceutics,* 38**,** 65-70.

PROUST, J. E., BASZKIN, A., PEREZ, E. & BOISSONNADE, M. M. (1984). Bovine Submaxillary Mucin (Bsm) Adsorption at Solid/ Liquid Interfaces and Surface Forces. *Colloids and Surfaces,* 10**,** 43-52.

RAMOS, M. L. D., CALDEIRA, M. M., M. & GIL, V. M. S. (1996). Nmr Study of Uronic Acids and Their Complexation with Molybdenum(Vi) and Tungsten(Vi) Oxoions. *Carbohydrate Research,* 286**,** 1-15.

RANADE, V. V. (2004). *Drug Delivery Systems,* Boca Raton : CRC Press.

RATHBONE, M. J. (1996). *Oral Mucosal Drug Delivery,* New York, M. Dekker

RIESEN, R. 2008. (Heat Capacity Determination at High Temperatures by Tga/Dsc. Part1: Dsc Standard Procedures). *Thermal anaylsis information for users* Mettler Toledo.

RIGHTON, L. (2011). Bringing the Patient's Voice to Nasal Drug Delivery. *Pulmonary & Nasal Drug Delivery: Could Inhalable Delivery Be Appropriate for Your Small Molecule of Biotherapeutic ?***,** 4-7.

ROSLUND, M. U., TÄHTINEN, P., NIEMITZ, M. & SJÖHOLM, R. (2008). Complete Assignments of the (1)H and (13)C Chemical Shifts and J(H,H) Coupling Constants in Nmr Spectra of D-Glucopyranose and All D-Glucopyranosyl-D-Glucopyranosides. *Carbohydrate Research,* 343**,** 101-112.

ROY, S. K. & PRABHAKAR, B. (2010). Bioadhesive Polymeric Platforms for Transmucosal Drug Delivery Systems - a Review. *Tropical Journal of Pharmaceutical Research,* 9**,** 91-104.

SCHAWE, J., REISEN, R., WIDMANN, J., SCHUBNELL, M. & JORIMANN, U. 1999. (The Glass Transition Form the Point of View of Dsc Measurments). *UserCome 10.*

SCHAWE, J., RIESEN, R., WIDMANN, J., SCHUBNELL, M. & JÖRIMANN, U. 2000. (Interpreting Dsc Curves Part 1: Dynamic Measurements). *Metteler Toledo information user. Usercom 11*. Schwerzenbach, Schweiz: METTLER TOLEDO GmbH, Analytical.

SCHUBNELL, M. 2005. (Method Development in Thermal Analysis. Part 1:). *Information for users of METTLER TOLEDO thermal analysis systems. Usecom 21*. Mettler Toledo.

SEBHATU, T., AHLNECK, C. & ALDERBORN, G. (1997). The Effect of Moisture Content on the Compression and Bond-Formation Properties of Amorphous Lactose Particles. *International Journal of Pharmaceutics,* 146**,** 101-114.

SHAJI, J., PODDAR, A. & IYER, S. (2009). Brain-Targeted Nasal Clonazepam Microspheres. *Indian Journal of Pharmaceutical Sciences,* 71**,** 715-718.

SLOTTE, T., HOLM, K., MCINTYRE, L. M., LAGERCRANTZ, U. & LASCOUX, M. (2007). Differential Expression of Genes Important for Adaptation in Capsella Bursa-Pastoris (Brassicaceae). *Plant Physiology,* 145**,** 160-173.

SONG, N. X., W. GUAN,H. LIU ,X. WANG,Y. NIE,X. (2007). Several Flavonoids from Capsella Bursa-Pastoris (L.) Medic. *Asian Journal of Traditional Medicines,,* 2 PP 218-222.

SOUTER, R. W. (1985). *Chromatographic Separations of Stereoisomers*, Taylor & Francis.

SRIAMORNSAK, P. (2003). Chemistry of Pectin and Its Pharmaceutica Uses : A Review. *SILPAKORN UNIVERSITY JOURNAL OF SOCIAL SCIENCES, HUMANITIES, AND ARTS,* 3**,** 206-228.

SRIAMORNSAK, P. & WATTANAKORN, N. (2008). Rheological Synergy in Aqueous Mixtures of Pectin and Mucin. *Carbohydrate Polymers,* 74**,** 474-481.

SRIAMORNSAK, P., WATTANAKORN, N. & TAKEUCHI, H. (2010). Study on the Mucoadhesion Mechanism of Pectin by Atomic Force Microscopy and Mucin-Particle Method. *Carbohydrate Polymers,* 79**,** 54-59.

STEVENS, R. E., GRAY, V., DORANTES, A., GOLD, L. & PHAM, L. (2015). Scientific and Regulatory Standards for Assessing Product Performance Using the Similarity Factor, F2. *The AAPS Journal,* 17**,** 301-306.

STEWART, D. & MORRISON, I. M. (1992). Ft-Ir Spectroscopy as a Tool for the Study of Biological and Chemical Treatments of Barley Straw. *Journal of the Science of Food and Agriculture,* 60**,** 431-436.

TAMBURIC, S. & CRAIG, D. Q. M. (1997). A Comparison of Different in Vitro Methods for Measuring Mucoadhesive Performance. *European Journal of Pharmaceutics and Biopharmaceutics,* 44**,** 159-167.

THIRAWONG, N., NUNTHANID, J., PUTTIPIPATKHACHORN, S. & SRIAMORNSAK, P. (2007). Mucoadhesive Properties of Various Pectins on Gastrointestinal Mucosa: An in Vitro Evaluation Using Texture Analyzer. *European Journal of Pharmaceutics and Biopharmaceutics,* 67**,** 132-140.

TOOROP, P. E., CAMPOS CUERVA, R., BEGG, G. S., LOCARDI, B., SQUIRE, G. R. & IANNETTA, P. P. M. (2012). Co-Adaptation of Seed Dormancy and Flowering Time in the Arable Weed Capsella Bursa-Pastoris (Shepherd's Purse). *Annals of Botany,* 109**,** 481-489.

TÜRKER, S., ONUR, E. & ÓZER, Y. (2004). Nasal Route and Drug Delivery Systems. *Pharmacy World and Science,* 26**,** 137-142.

URIAS-ORONA, V., RASCÓN-CHU, A., LIZARDI-MENDOZA, J., CARVAJAL-MILLÁN, E., GARDEA, A. A. & RAMÍREZ-WONG, B. (2010). A Novel Pectin Material: Extraction, Characterization and Gelling Properties. *International Journal of Molecular Sciences,* 11**,** 3686-3695.

USDA, N. 2010. (The Plants Database:Plants Profile (Capsella Bursa-Pastoris (L.) Medik. Shepherd's Purse)). National Plant Data Center.

VASIR, J. K., TAMBWEKAR, K. & GARG, S. (2003). Bioadhesive Microspheres as a Controlled Drug Delivery System. *International Journal of Pharmaceutics,* 255**,** 13-32.

VAUGHAN, J. G. (1955). The Morphology and Growth of the Vegetative and Reproductive Apices of Arabidopsis Thaliana (L.) Heynh., Capsella Bursa-Pastoris (L.) Medic. And Anagallis Arvensis L. *Journal of the Linnean Society of London, Botany,* 55**,** 279-301.

VERHERTBRUGGEN, Y., MARCUS, S. E., HAEGER, A., ORDAZ-ORTIZ, J. J. & KNOX, J. P. (2009). An Extended Set of Monoclonal Antibodies to Pectic Homogalacturonan. *Carbohydrate Research,* 344**,** 1858-1862.

VORAGEN, A. J., COENEN, G.-J., VERHOEF, R. & SCHOLS, H. (2009). Pectin, a Versatile Polysaccharide Present in Plant Cell Walls. *Structural Chemistry,* 20**,** 263-275.

WADELL, C. (2002). *Nasal Drug Delivery - in Vitro Studies on Factors Influencing Permeability and Implications on Absorption.* Degree of Doctor of Philosophy, Uppsala University.

WALTER, R. H. & TAYLOR, S. (2012). *The Chemistry and Technology of Pectin*, Elsevier Science.

WATTS, P. J. & SMITH, A. (2011). Re-Formulating Drugs and Vaccines for Intranasal Delivery: Maximum Benefits for Minimum Risks? *Drug Discovery Today,* 16**,** 4-7.

WESTERN, T. L., BURN, J., TAN, W. L., SKINNER, D. J., MARTIN-MCCAFFREY, L., MOFFATT, B. A. & HAUGHN, G. W. (2001). Isolation and Characterization of Mutants Defective in Seed Coat Mucilage Secretory Cell Development in Arabidopsis. *Plant Physiology,* 127**,** 998-1011.

WESTERN, T. L., SKINNER, D. J. & HAUGHN, G. W. (2000). Differentiation of Mucilage Secretory Cells of the Arabidopsis Seed Coat. *Plant Physiology,* 122**,** pp. 345-355.

WICHTL, M. & BISSET, N. G. (2001). *Herbal Drugs and Phytopharmaceuticals : A Handbook for Practice on a Scientific Basis* Stuttgart; Boca Raton., Medpharm ;CRC Press

WIDMANN, G. 2001. (Interepreting Tga Curves). *UserCom 1/2001.Information for users of Mettler Toledo thermal analysis systems.* Switzerland: Mettler Toledo.

WILLATS, W. G. T., MCCARTNEY, L. & KNOX, J. P. (2001). In-Situ Analysis of Pectic Polysaccharides in Seed Mucilage and at the Root Surface of *Arabidopsis Thaliana*. *Planta,* 213**,** 37-44.

WINDSOR, J. B., SYMONDS, V. V., MENDENHALL, J. & LLOYD, A. M. (2000). Arabidopsis Seed Coat Development: Morphological Differentiation of the Outer Integument. *The Plant Journal,* 22**,** 483-493.

WONDIMU, A., MOLLA, F., CHANDRA DINDA, S., GEBRE-SAMUEL, N. & TADESE, E. (2014). Literature Review on Enset Starch:Physico-Chemcial

Proerties and Pharmacetical Applications *Journal of Drug Delivery & Therapeutics,* 4**,** 1-6.

ZHANG, P.-J., SHU, J.-P. & FU, C.-X. (2008). Trade-Offs between Constitutive and Induced Resistance in Wild Crucifers Shown by a Natural, but Not an Artificial, Elicitor. *Oecologia,* 157**,** 83-92.

ZHU, X., LIU, B., ZHENG, S. & GAO, Y. (2014). Quantitative and Structure Analysis of Pectin in Tobacco by 13c Cp/Mas Nmr Spectroscopy. *Analytical Methods,* 6**,** 6407-6413.

APPENDIX A

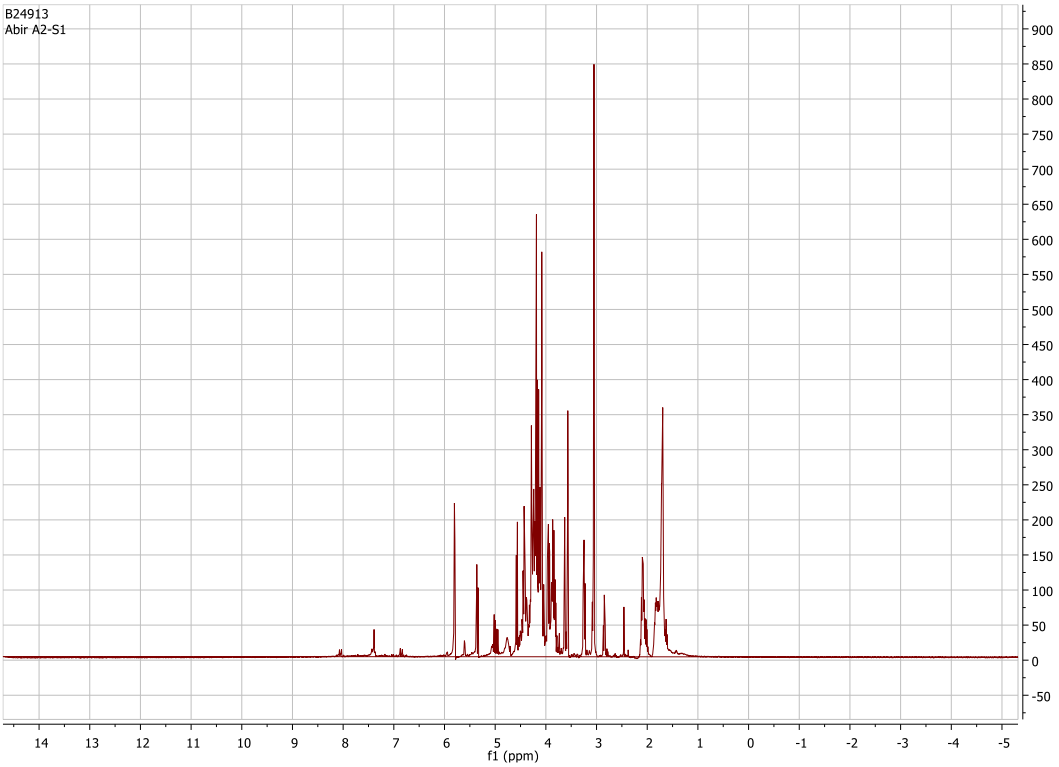

Figure A1-^{1}H NMR spectrum of Shepherd's purse mucilage hot reflux extract in D_2O at 400MHz with water suppression at 4.8 ppm.

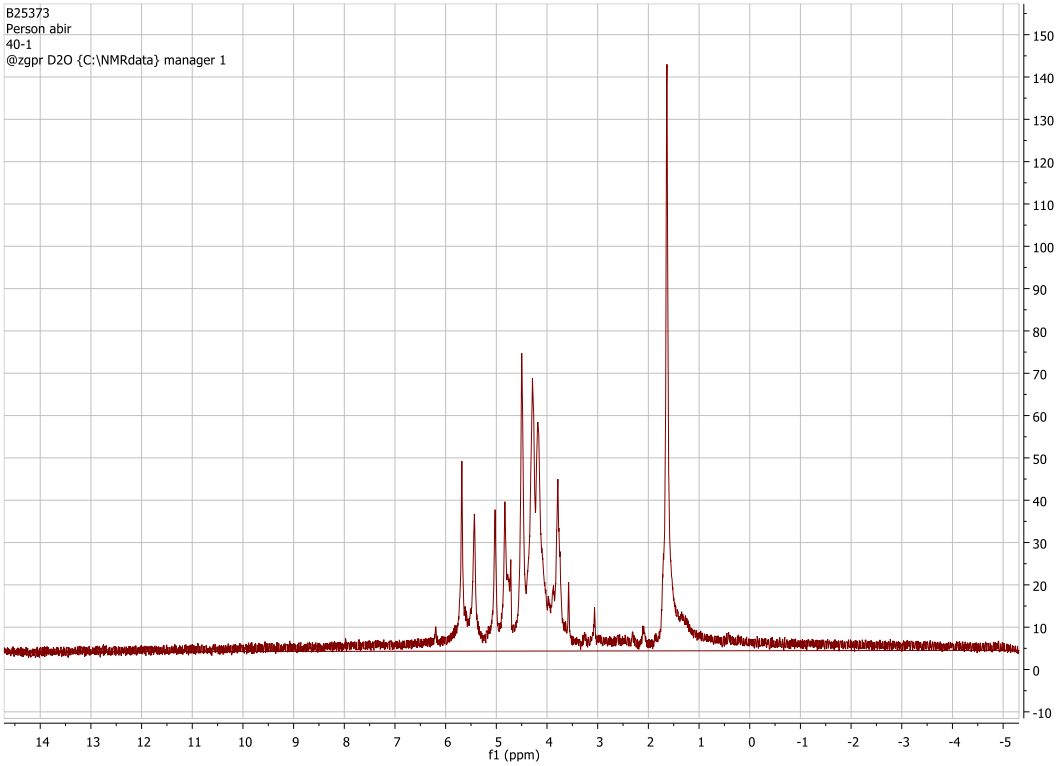

Figure A2-^{1}H NMR spectrum of Shepherd's purse mucilage extract 40°C-1h in D_2O at 400MHz with water suppression at 4.8 ppm.

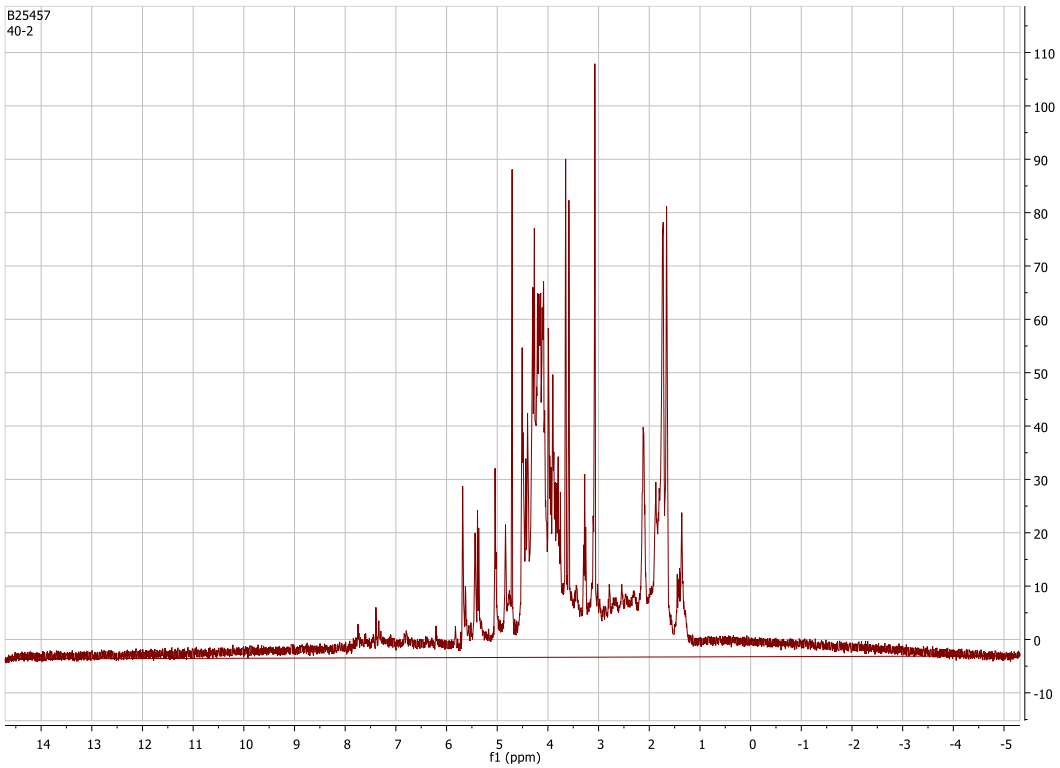

Figure A3-^{1}H NMR spectrum of Shepherd's purse mucilage extract 40°C-2h in D_2O at 400MHz with water suppression at 4.8 ppm.

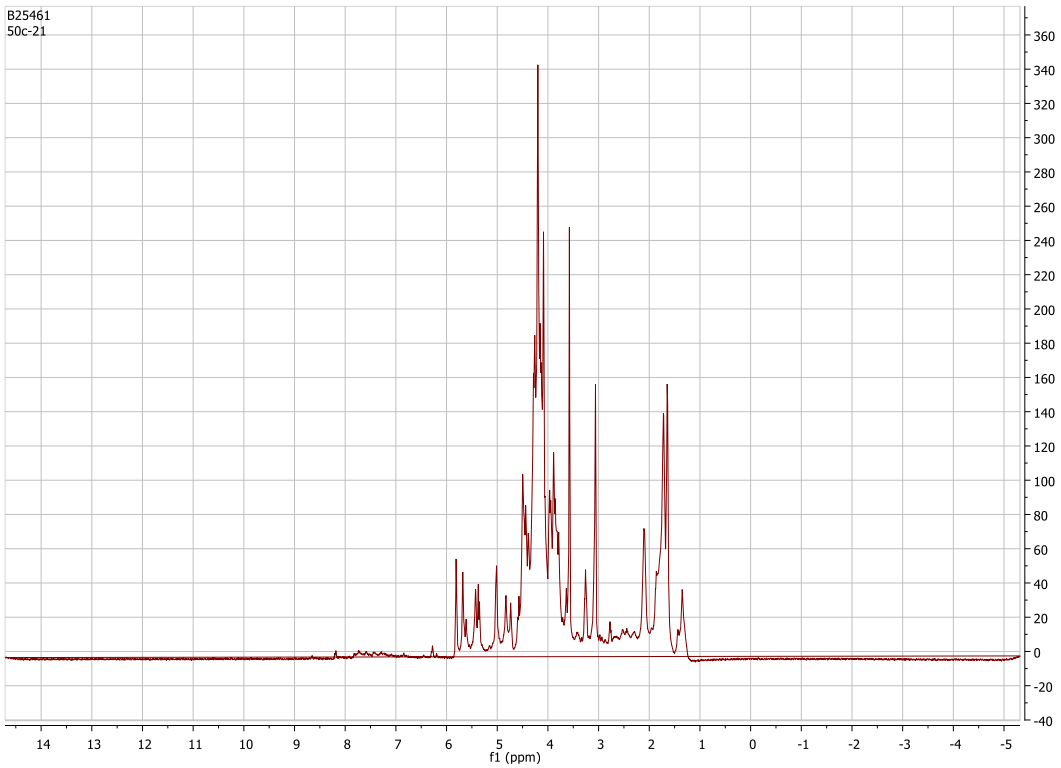

Figure A4-^{1}H NMR spectrum of Shepherd's purse mucilage extract 50°C-2h in D_2O at 400MHz with water suppression at 4.8 ppm.

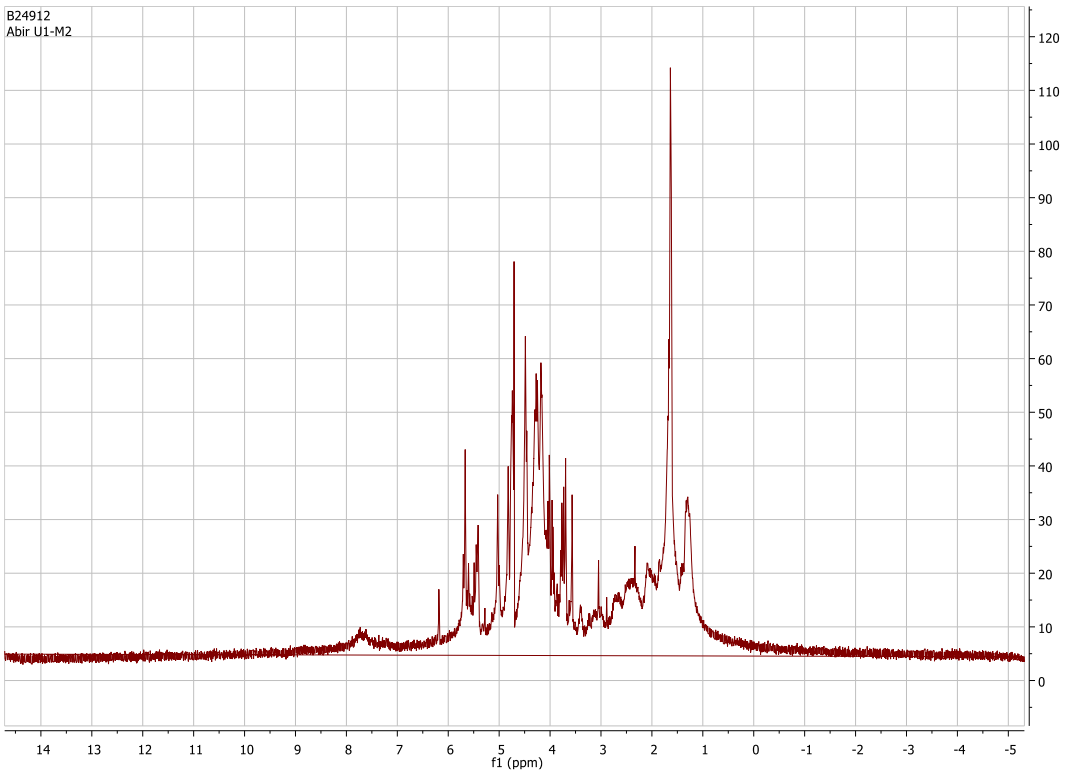

Figure A5-^{1}H NMR spectrum of Shepherd's purse mucilage extract from hot maceration in D_2O at 400MHz with water suppression at 4.8 ppm.

APPENDIX B

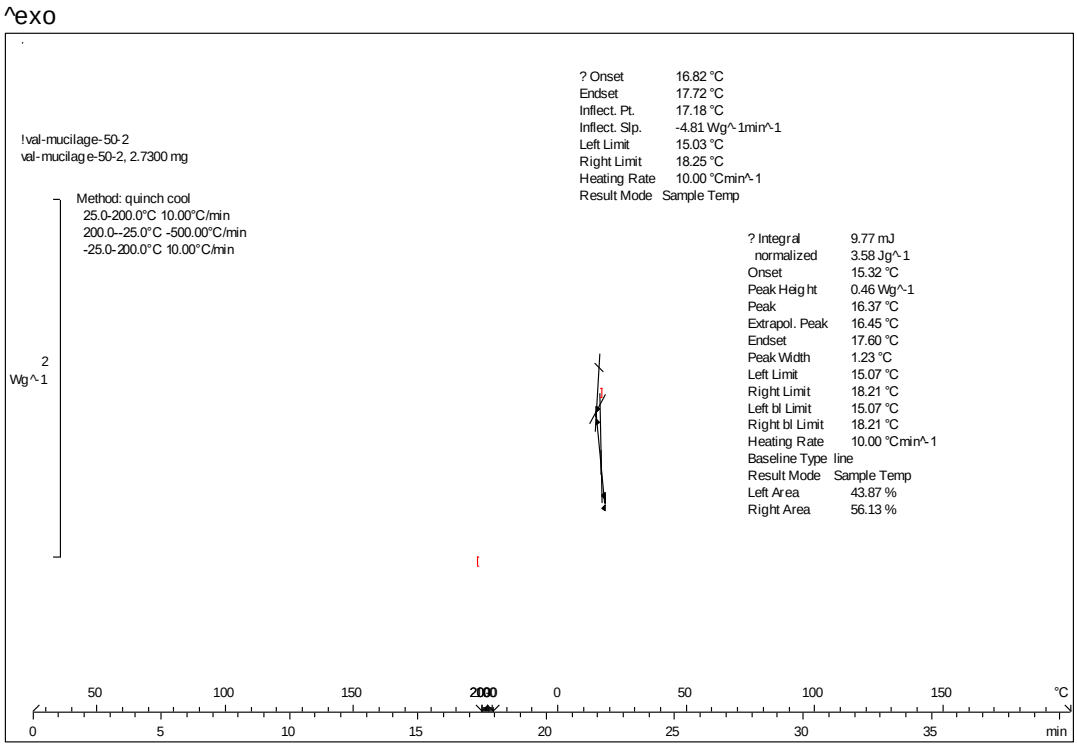

Figure B1-DSC thermogram of water maceration 50º C mucilage by the quench-cool method.

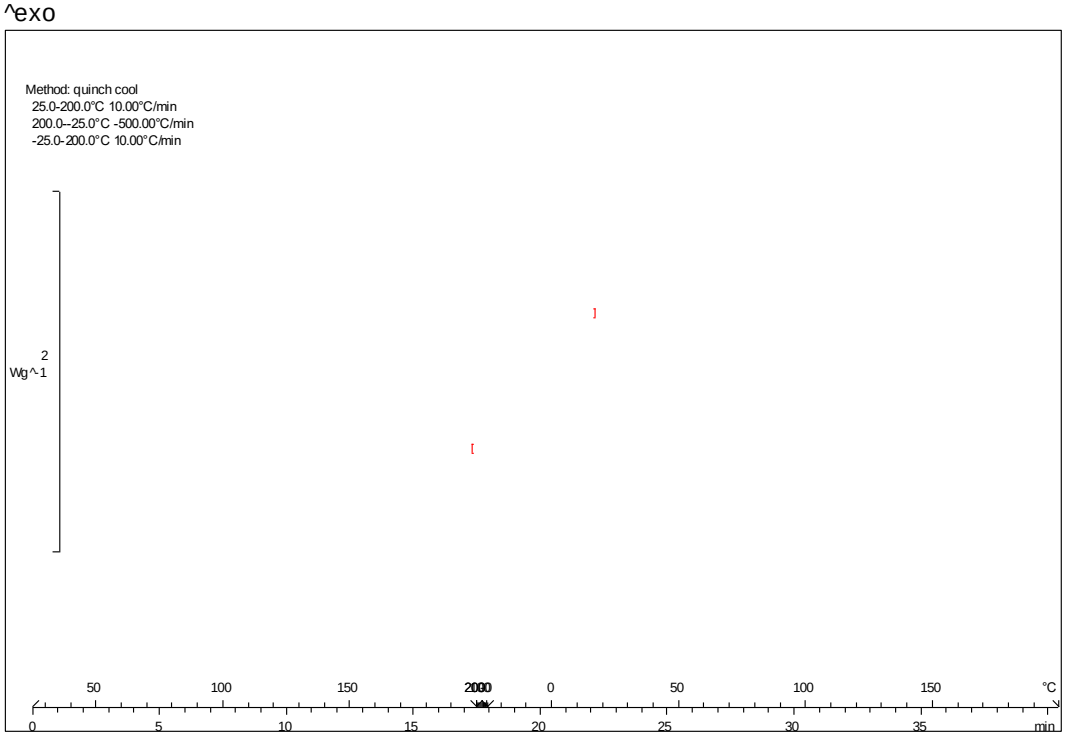

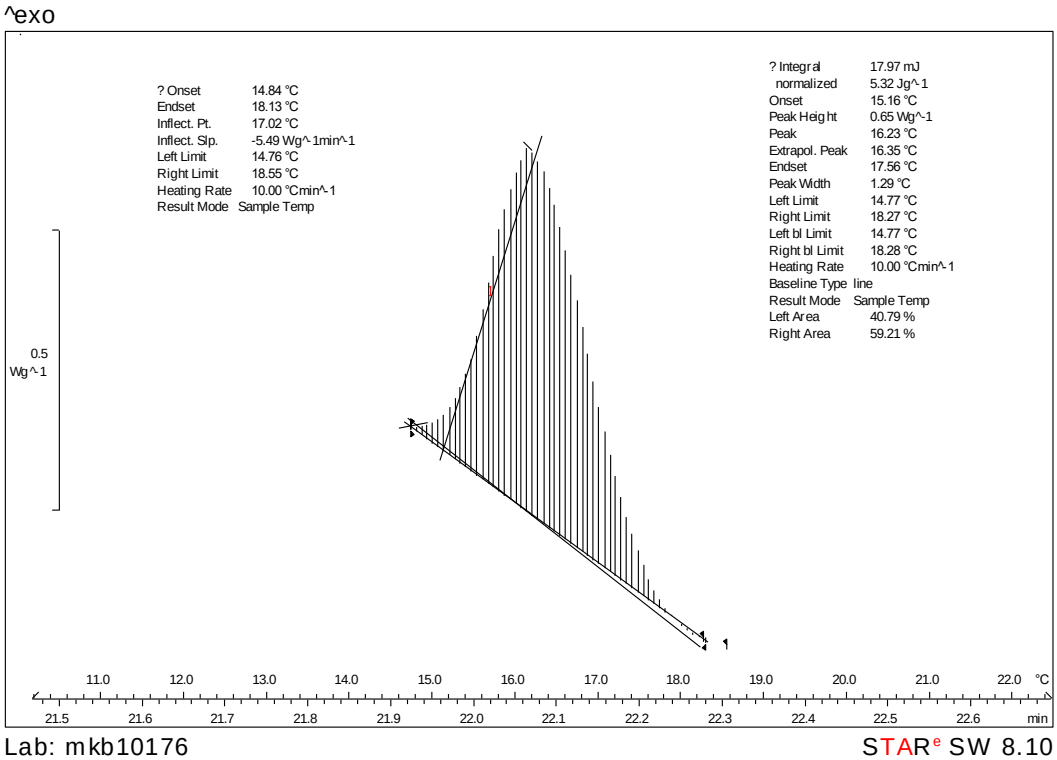

Figure B2-DSC thermogram of hot maceration 40º C mucilage by the quench-cool method.

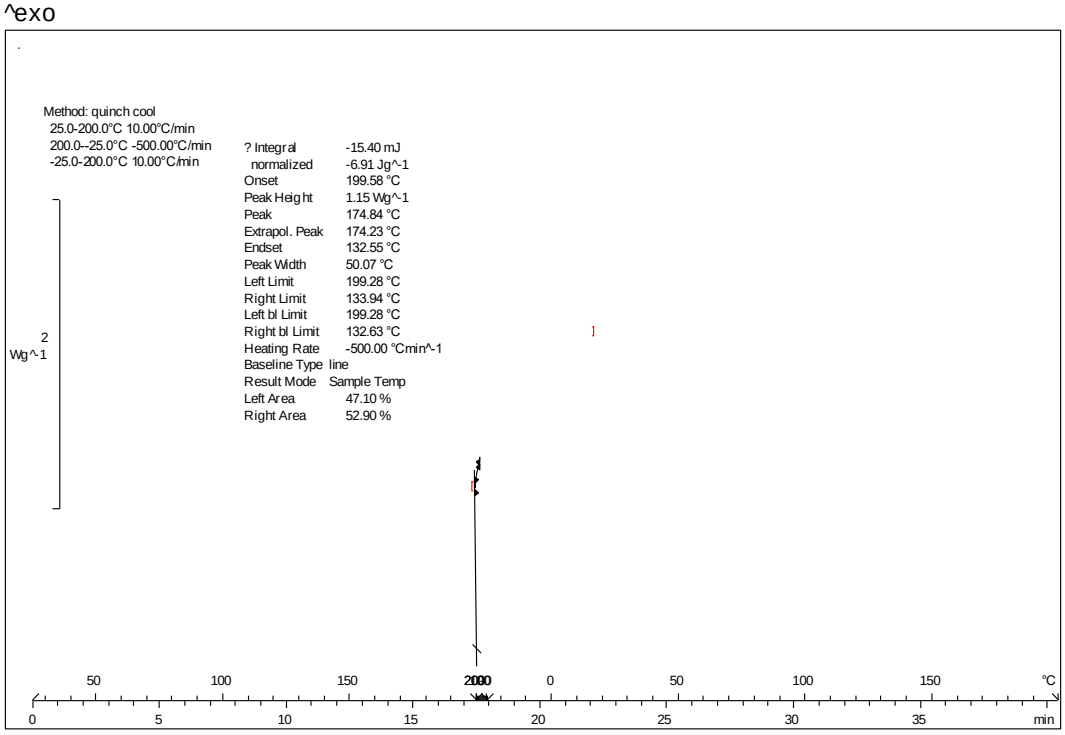

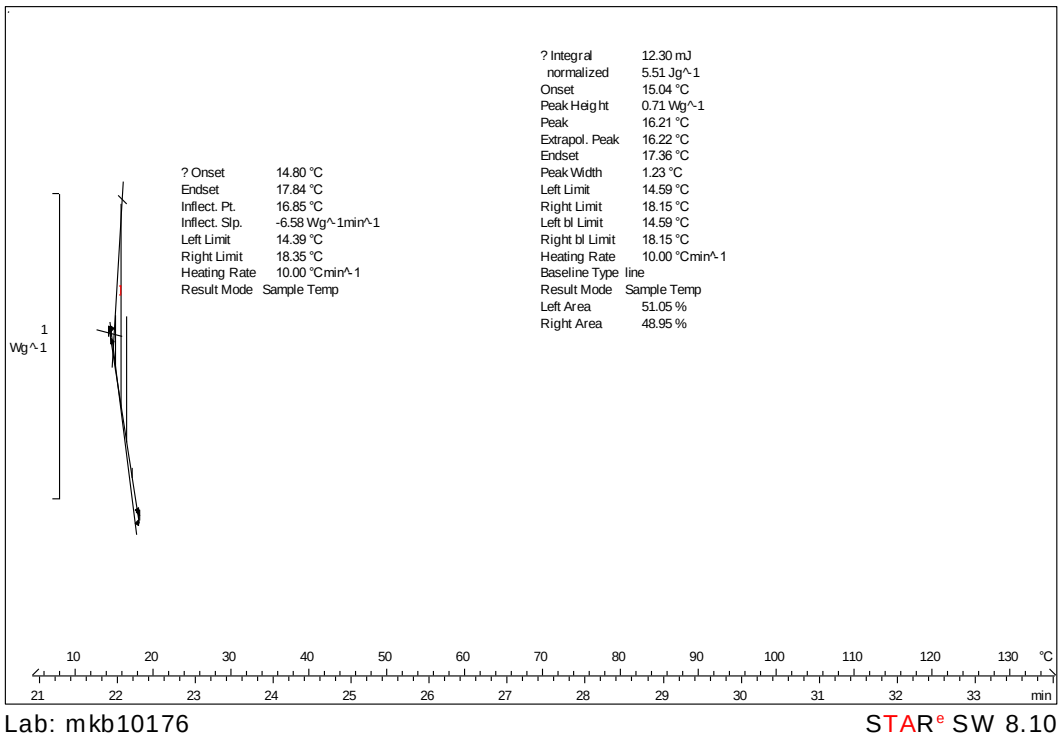

Figure B3- DSC thermogram of solvent maceration 25º C mucilage by the quench-cool method.

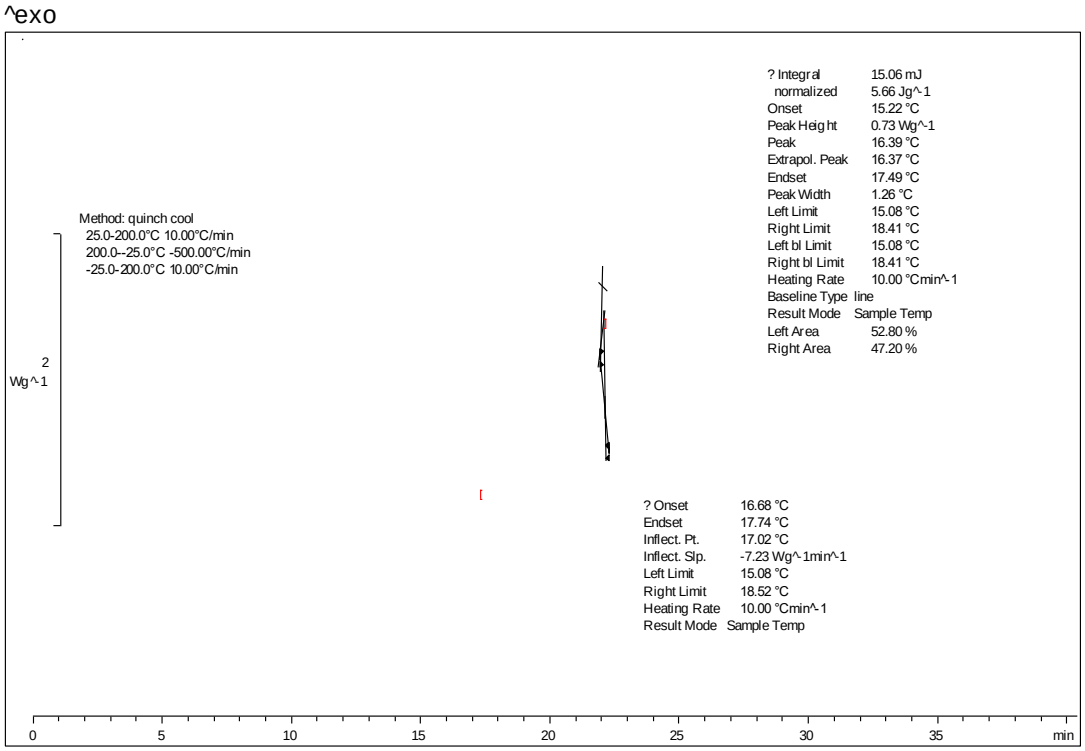

Figure B4- DSC thermogram of water maceration 70º C mucilage by the quench-cool method.

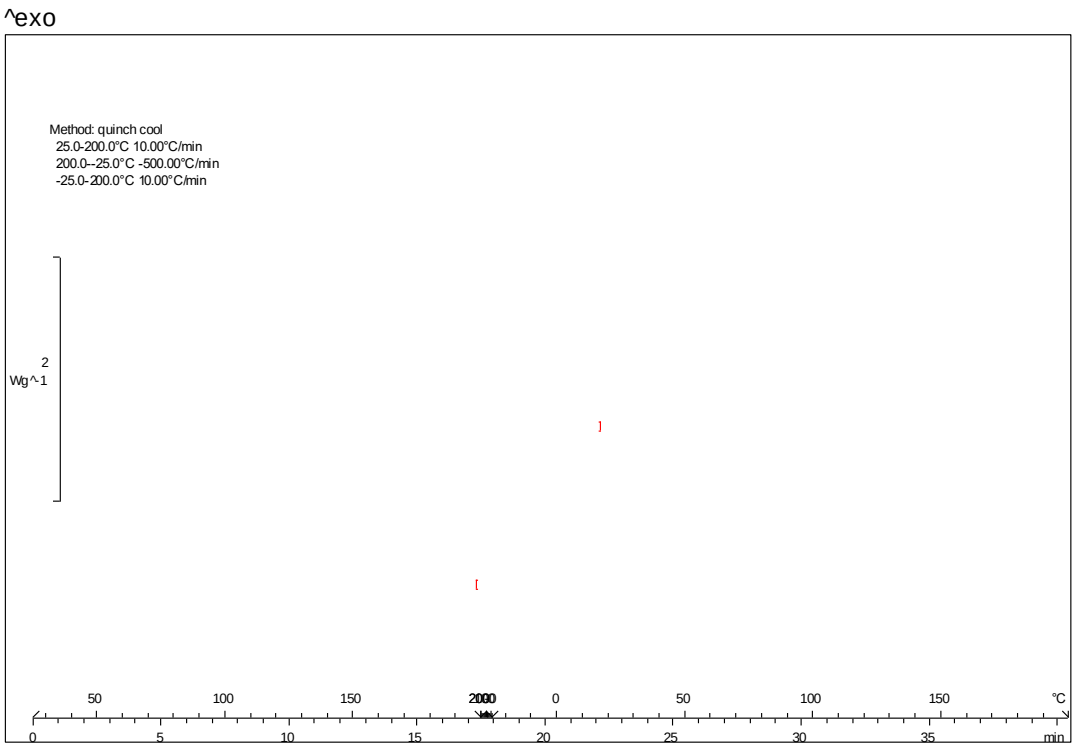

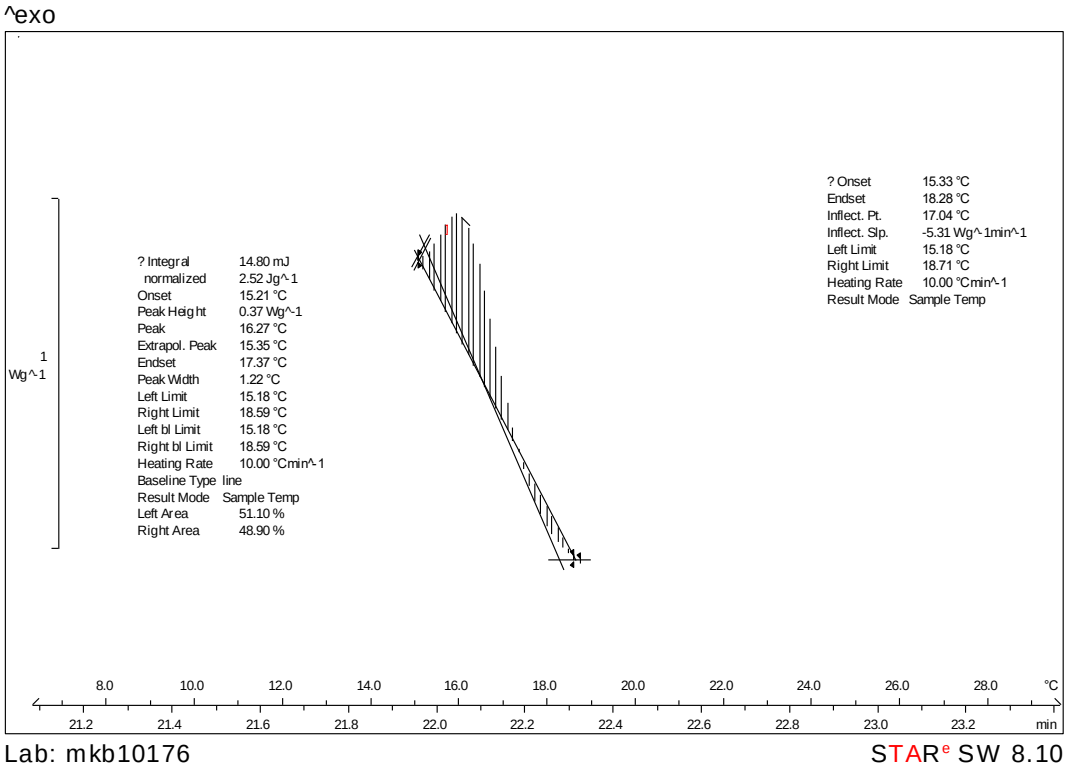

Figure B5-DSC thermogram of hot reflux mucilage by the quench-cool method.